Journal Pre-proof

A Review on Friction Stir Butt Welding of Aluminum with Magnesium: A New Insight on Joining Mechanisms by Interfacial Enhancement

Usman Abdul Khaliq, Mohd Ridha Muhamad, Farazila Yusof, Suriani Ibrahim, Mohammad Syahid Mohd Isa, Zhan Chen, Gürel Çam

PII: S2238-7854(23)02608-X

DOI: https://doi.org/10.1016/j.jmrt.2023.10.158

Reference: JMRTEC 8889

To appear in: *Journal of Materials Research and Technology*

Received Date: 28 August 2023

Revised Date: 5 October 2023

Accepted Date: 16 October 2023

Please cite this article as: Abdul Khaliq U, Muhamad MR, Yusof F, Ibrahim S, Mohd Isa MS, Chen Z, Çam G, A Review on Friction Stir Butt Welding of Aluminum with Magnesium: A New Insight on Joining Mechanisms by Interfacial Enhancement, *Journal of Materials Research and Technology*, https://doi.org/10.1016/j.jmrt.2023.10.158.

A ~~Comprehensive~~ Review on Friction Stir Butt Welding of Aluminum with Magnesium: A New Insight on Joining Mechanisms by Interfacial Enhancement

Usman Abdul Khaliq
Department of Mechanical Engineering, Faculty of Engineering, University of Malaya, 50603, Kuala Lumpur, Malaysia.
e-mail: mani2263@hotmail.com

Mohd Ridha Muhamad*
Department of Mechanical Engineering, Faculty of Engineering, University of Malaya, 50603, Kuala Lumpur, Malaysia.
Centre of Advanced Manufacturing and Material Processing (AMMP Centre), University of Malaya, 50603, Kuala Lumpur, Malaysia.
e-mail: ridha@um.edu.my

Farazila Yusof
Department of Mechanical Engineering, Faculty of Engineering, University of Malaya, 50603, Kuala Lumpur, Malaysia.
Centre of Advanced Manufacturing and Material Processing (AMMP Centre), University of Malaya, 50603, Kuala Lumpur, Malaysia.
e-mail: farazila@um.edu.my

Suriani Ibrahim
Department of Mechanical Engineering, Faculty of Engineering, University of Malaya, 50603, Kuala Lumpur, Malaysia.
Centre of Advanced Manufacturing and Material Processing (AMMP Centre), University of Malaya, 50603, Kuala Lumpur, Malaysia.
e-mail: sue_83@um.edu.my

Mohammad Syahid Mohd Isa
Department of Mechanical Engineering, Faculty of Engineering, University of Malaya, 50603, Kuala Lumpur, Malaysia.
e-mail: syahidisa@um.edu.my

Zhan Chen
Department of Mechanical Engineering, School of Engineering, Computer & Mathematical Sciences, Auckland University of Technology, Auckland 1010, New Zealand
email: zhan.chen@aut.ac.nz

Gürel Çam
Department of Mechanical Engineering, Faculty of Engineering and Natural Sciences, Iskenderun Technical University, 31200 Iskenderun-Hatay, Turkey.
e-mail: gurel.cam@iste.edu.tr

* Corresponding author.

Abstract

The growing demand for lightweight materials in the automotive and aerospace industries has driven research on joining dissimilar lightweight alloys, particularly Al and Mg alloys (Al/Mg). Friction stir welding (FSW) is a promising technique for joining Al/Mg alloys, as it works below the base metal's melting temperature, leading to refined microstructures, reduced porosity, and enhanced productivity. The strength of Al/Mg friction stir weldment depends on the evolved interface, which is primarily characterized by micromechanical interlocks, type, and intermetallic compounds (IMCs) distribution. Different interfaces for butt joints have been discussed in the literature. However, the mechanism of interfacial interaction together with the ways to enhance the interface have not been reviewed yet. This review article fills the gap by analyzing the retrospective data for process parameters and mechanical properties. Joining mechanisms and the evolution of different interfaces at the microstructural level have been discussed. Lastly, ways to enhance the interface for improved mechanical properties are explained. By offering essential insights into FSW techniques and Al/Mg weld interfaces, this review article paves the way for developing FSW procedures for Al/Mg butt welds aiming for enhanced strength and performance. This review article is expected to be of interest to researchers and engineers working in the field of FSW, particularly for Al/Mg lightweight applications. It provides an overview of the current state of knowledge and identifies key areas for future research.

Keywords: Friction stir welding, Dissimilar Metal, Mechanical interlocking, Intermetallic compounds, Joining mechanisms, Interface.

1. Introduction

1.1. Background

The world population has grown significantly from 2.5 billion in 1950 to 8 billion in 2020 [1], prompting many countries to explore non-renewable energy resources for sustaining economic growth. However, this pursuit of sustainability has led to increased global warming due to higher CO_2 emissions [2]. Legislations are now in place to compel vehicle manufacturers to meet fuel efficiency targets, with the United States aiming to reduce CO_2 emissions by 40% in 2025 compared to 2015. To achieve this, approaches like transitioning to electric vehicles, improving engine efficiency, and weight reduction are being pursued, with a particular focus on weight-saving strategies [3,4]. ~~Among these, manufacturing functionally graded multi-material structures [5] through the exploration of dissimilar alloy welding is a prominent area garnering significant attention.~~

Iron, aluminum, magnesium, and their alloys stand as the most prevalent structural metallic materials (hereafter, aluminum and magnesium will encompass both the parent metals and their respective alloys). In numerous applications, aluminum or steel-aluminum hybrid structures have replaced steel. Current endeavors focus on joining aluminum and magnesium to further reduce weight, replacing Al with Mg, given Al's density of 2.7 g/cm^3 and Mg's 1.7 g/cm^3, while maintaining acceptable joint

efficiency. From 1999 to 2019, world steel, aluminum, and magnesium production have impressively increased by 140% [6], 180% [7], and 300% [8], respectively [9]. The escalated production of aluminum and magnesium in comparison to iron/steel over the same period signifies a burgeoning trend towards utilizing these lightweight metals to conserve structural weight. ~~Moreover, the steady surge in publications from 2012 to 2022 highlights the growing research interest in the Al-Mg dissimilar friction stir welding domain (refer to Figure 1).~~

Choosing materials for different applications is a complex task. Lightweight materials often have lesser strength. The pursuit of superior materials persists due to the demand for energy-efficient, durable, and cost-effective vehicles. Finding one material with all the necessary properties for engineering is nearly impossible. Therefore, materials are often combined, like alloys or composites, to leverage their distinct properties [10,11]. Another approach is manufacturing multi-material structures by joining dissimilar metals to reduce component weight without sacrificing specific required properties [5].

Welding is a popular technique for joining metallic materials, offering advantages over other methods like adhesive and mechanical fasteners. Recent research focuses on advanced welding methods, including friction stir welding (FSW) [12], laser and electron beam welding [13], and laser-arc hybrid welding [14], to improve joint quality. However, welding dissimilar metal combinations poses challenges due to the difference in physical properties like melting point, coefficient of thermal expansion, and thermal conductivity. Despite this, dissimilar welding has benefits such as lower costs, greater energy efficiency, and material optimization, applied in various industrial settings [15]. ~~Joining aluminum and magnesium alloys (Al/Mg), widely used in the auto and aerospace sectors, is an area where demand for dissimilar welding is growing.~~

Fusion welding has some intrinsic difficulties in joining Al-alloys such as porosity formation in the fusion zone and intolerable strength loss in the weld region of particularly high-strength precipitation-hardened Al-alloys [16–18]. The fusion welding of dissimilar aluminum and magnesium pairs (Al/Mg) is even more challenging. In fusion welding, the temperature easily surpasses the melting points of aluminum and magnesium, causing the materials at the interface to melt [17–20]. Upon solidification, this results in a cast structure characterized by poor mechanical properties, porosity, and the formation of intermetallic compounds (IMCs) [21–25].

FSW is classified as a solid-state joining process, as it operates below the melting point of base metals. This characteristic makes FSW the most promising technique for welding both similar and dissimilar alloys. By avoiding the melting of base metals, it eliminates defects like porosity which are commonly found in fusion welded joints. Additionally, the process involves severe plastic deformation (SPD), resulting in superior strength compared to cast structures. FSW has found applications in a wide range of materials including aluminum [26–29], magnesium, steel [30,31], copper [32,33], and lead [34], both in metallic and alloy forms. Beyond metals, FSW has also proven successful in joining polymers [35–38]. Moreover, FSW has been utilized for welding dissimilar materials. Various dissimilar material combinations include steel/steel [39,40], aluminum/aluminum [41,42], magnesium/magnesium [43,44], aluminum/titanium (Al/Ti) [45,46], aluminum/copper (Al/Cu) [10,47], aluminum/steel (Al/Fe) [48,49], and polymer/metal [50,51]. The steady surge in publications from 2012 to 2022 highlights the growing research interest in the Al/Mg

FSW (refer to Figure 1). FSW finds applications in both butt and lap joint configurations. When it comes to endeavors focused on reducing structural weight, the Al/Mg butt joint configuration stands out as the more widely adopted choice.

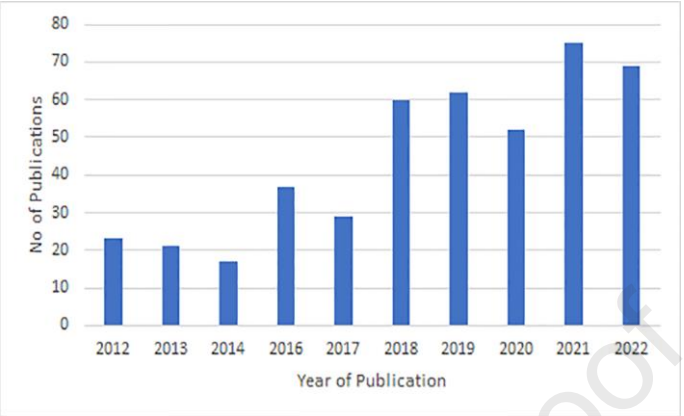

Figure 1: Number of publications in aluminum-magnesium dissimilar FSW for the past 10 years (WoS).

~~In contrast, solid-state FSW can be successfully used for joining low melting temperature structural alloys such as Al-, Mg- and Cu-alloys and it has also the potential to be used in joining high melting temperature structural alloys such as steels and stainless steels~~ [20,26–34,39,52–54]~~. This technique has also been successful in Al/Mg dissimilar welding as well as other different structural material combinations, with joint strength depending on mechanical mixing and IMC properties.~~

The strength of an Al/Mg friction stir butt weld depends on the interface, characterized by mechanical interlocking and IMCs. These features, along with potential defects, are contingent on the selection of process parameters for FSW. The subsequent section will introduce the FSW process, its associated parameters, and possible defects.

1.2. Overview of friction stir welding

In FSW, a non-consumable tool, rotating around its axis, is inserted into the joint to facilitate the joining of workpieces (Figure 2-a). The friction between the tool and workpiece generates heat, causing the base materials to transition into a semi-solid state. In the plastic state, the material behaves akin to non-Newtonian fluid. Subsequently, the tool advances along the joint line moving the material from the tool's leading edge is forced into the joint region, effectively filling the wake of the tool. This enables material flow, fine recrystallized grain formation, and substantial plastic deformation at approximately 80% of the material's melting point [55,56].

The FSW tool (Figure 2-b) consists of two main components: the pin and the shoulder. The dimensions of these parts are carefully selected so that the pin length is slightly less than the thickness of the base metal. When inserted into the base metal, it ensures proper contact of the shoulder with the base metal surface [57].

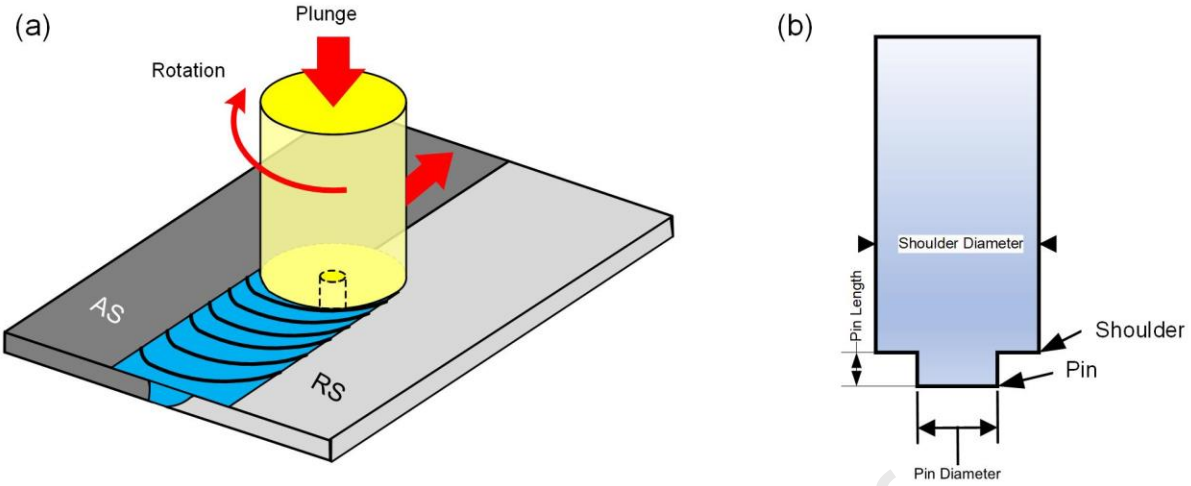

Figure 2: Schematic of (a) FSW, and (b) FSW tool.

FSW progresses through four stages. Firstly, in the plunge phase, the rotating tool is inserted into the workpiece at a predetermined rate (plunge speed) and depth (plunge depth). The second phase, dwell, involves leaving the tool submerged for a defined duration to generate heat and start mixing material. In the third phase, welding, the tool traces the joint line at a specific rotational and travel speed. Lastly, in the retraction phase, the tool is extracted from the workpiece at a predefined speed to prevent the formation of defects [58,59].

FSW's superior joint mechanical properties stem from refined microstructure and process' ability to prevent fusion welding-related defects. Microstructural and material flow-related aspects of FSW in general have been thoroughly covered in review articles by Hydrazide et al., and Ambrosio et al. respectively [60,61]. Others have investigated material flow based on either the material itself, specific FSW parameters, or a combination of both. For instance, the effects of shoulder and pin features [62], acoustic effects [63], and tool tilt angle [36,55,64,65] have been studied about material flow. Similarly, material flow has been examined for various materials such as Al/Cu [66], Mg/Mg [67], Al/Mg [68], and polymers [36]. Similarly, in the literature, one can find examples of microstructure evolution and characterization based on both material properties and specific process parameters [69–72].

1.3. FSW Parameters

Based on an extensive literature review, table 1 categorizes FSW parameters into three main groups.

Process Parameters	Tool Parameters	Workpiece Material
Rotation Speed	Tool Material	Chemical Composition
Rotation Direction	Shoulder Profile	Thickness
Welding Speed	Pin Profile	Physical Properties

Plunge Depth	Shoulder Diameter	Mechanical Properties
Tool Tilt Angle	Pin Diameter	
Tool Offset	Pin Length	

Table 1 Friction stir welding parameters and their classification.

1.3.1. Plate positioning concerning tool rotation direction

Understanding the impact of tool rotation direction involves defining the "advancing side" (AS) and "retreating side" (RS), while AS aligns with tool tangential velocity and welding direction, while RS opposes it (Figure 2-a) [15]. Material placement considers melting point and deformation response. Enhanced heat on the AS benefits higher melting point materials, as matching tool velocity and welding speed improves temperature control and outcomes [73,74]. Notably, placing magnesium on the advancing side overcomes challenges from its HCP crystal structure, resulting in defect-free joints and improved welding results due to optimized plastic deformation [75–78].

1.3.2. Tool tilt angle

The tool tilt angle (TTA), depicted in Figure 3, influences material recoalescence and flow in the stir zone, intensifying forging effects and temperature distribution [64]. This angle plays a crucial role in shaping material behavior during FSW. To enhance the material flow influenced by the tool shoulder, a tilt angle of 2° to 3° is commonly used when using a tool with a featureless shoulder [76,79]. In their study on TTA for AA6068 alloy in a T-joint configuration, Aghajani Derazkola et al. observed that increasing the TTA leads to higher temperatures at the advancing side. This is attributed to the heightened levels of frictional and axial forces resulting from the increased TTA. They also noted the presence of an optimal value of TTA, in which exceeding this will result in the formation of flash and tunnel defects [65]. Another study on AA1050 alloy also yields the same observation [55]. TTA is such a crucial parameter that its study has been extended to polymers as well [36,37]. Another crucial point to be mindful of is that during the tilting process, the trailing edge of the tool moves downward, nearing the anvil. If the degree of tool penetration into the base metal is not meticulously considered during the tilt, there's a risk of the tool colliding with the anvil and sustaining damage. This is depicted in Figure 3, where the tilting action has shifted the tool's pin plane downward from position A1 to A2, by a measure of ΔA. This shift is influenced by factors like the degree of TTA, pin diameter, and the design of the pin tip.

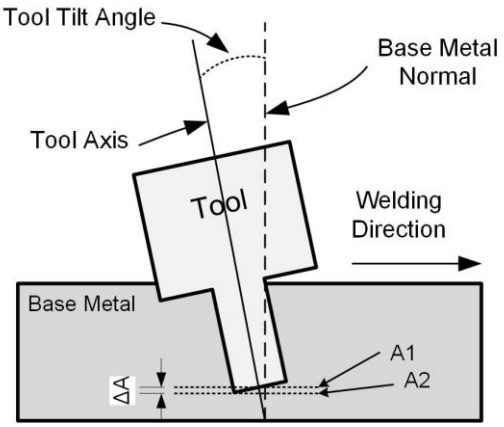

Figure 3: Visualization of tool tilt angle.

1.3.3. Tool material

Selecting an appropriate tool material for FSW involves considering properties like ambient and elevated temperature strength, stability, reactivity, machinability, and availability [80]. Tool material selection significantly influences successful FSW outcomes, with key choices summarized in Table 2.

Base Material	Aluminum Alloys	Magnesium Alloys	Aluminum-Magnesium Dissimilar
Tool Material	Tool steel	Tool steel	Tool steel
	Cobalt-Tungsten carbide (WC-Co)	Tungsten carbide (WC)	

Table 2: Tool materials for different alloys.

1.3.4. Tool Design

In FSW, the tool shoulder serves three critical functions: generating heat, facilitating material flow beneath it, and forging the plastic material to create a sound weld. Various shoulder designs, including flat, concave, and featured, have been successful, with energy input linked to shoulder radius (R) through $q \propto R^3$ [80,81]. Optimal tool shoulder design and radius are vital for effective heat generation, material flow, and weld quality [80]. The tool pin contributes to heat generation and material mixing in the bulk, with threaded pins influencing flow and microstructure, enhancing mechanical locking and texture development [45,46]. Heat generation is primarily attributed to shoulder-material interaction, exemplified by differing grain sizes and IMC layer thickness (Figure 4) along the weld's thickness [82–84]. Research highlights the interplay of shoulder diameter (D), pin diameter (d), and sheet thickness (t), revealing optimal ratios of $\frac{D}{d}$ and $\frac{D}{t}$ for defect-free FSW joints [85,86]. Pinless tools have also been documented for achieving uniform dispersion of nanomaterial additives during the processing of metal matrix composites via the

friction stir processing (FSP) route [87]. Additionally, they have been employed to eliminate the exit keyhole at the end of the FSW process [88,89]. Furthermore, these tools have been reported to find application in micro friction stir welding (μFSW) of both similar and dissimilar alloys, specifically in cases involving thin sheets [90,91]. It is noteworthy that μFSW with a pinless tool, being a low heat input method, effectively eliminates the issue of pin adhesion. Moreover, in a recent endeavor to join a 3 mm thick Mg/Fe couple in a butt configuration, four different tools with varying numbers of shoulders were employed to investigate the joint properties, as illustrated in Figure 5. Employing the tool with multiple shoulders up to three steps, the quality of the joint was improved. However, beyond that point, it was adversely affected. This phenomenon is attributed to the changes in frictional and material flow conditions [92]. The angle in the frustum cone of the pin also impacts the joint characteristics. Bokov et al. numerical analysis of the pin profile revealed that the nugget size increased with a higher pin angle. Additionally, their results demonstrated that heat generated through friction is greater when the angle is zero (cylindrical pin) [93]. Elyasi et al. have also addressed the significance of a threaded pin in material flow for dissimilar metals [66].

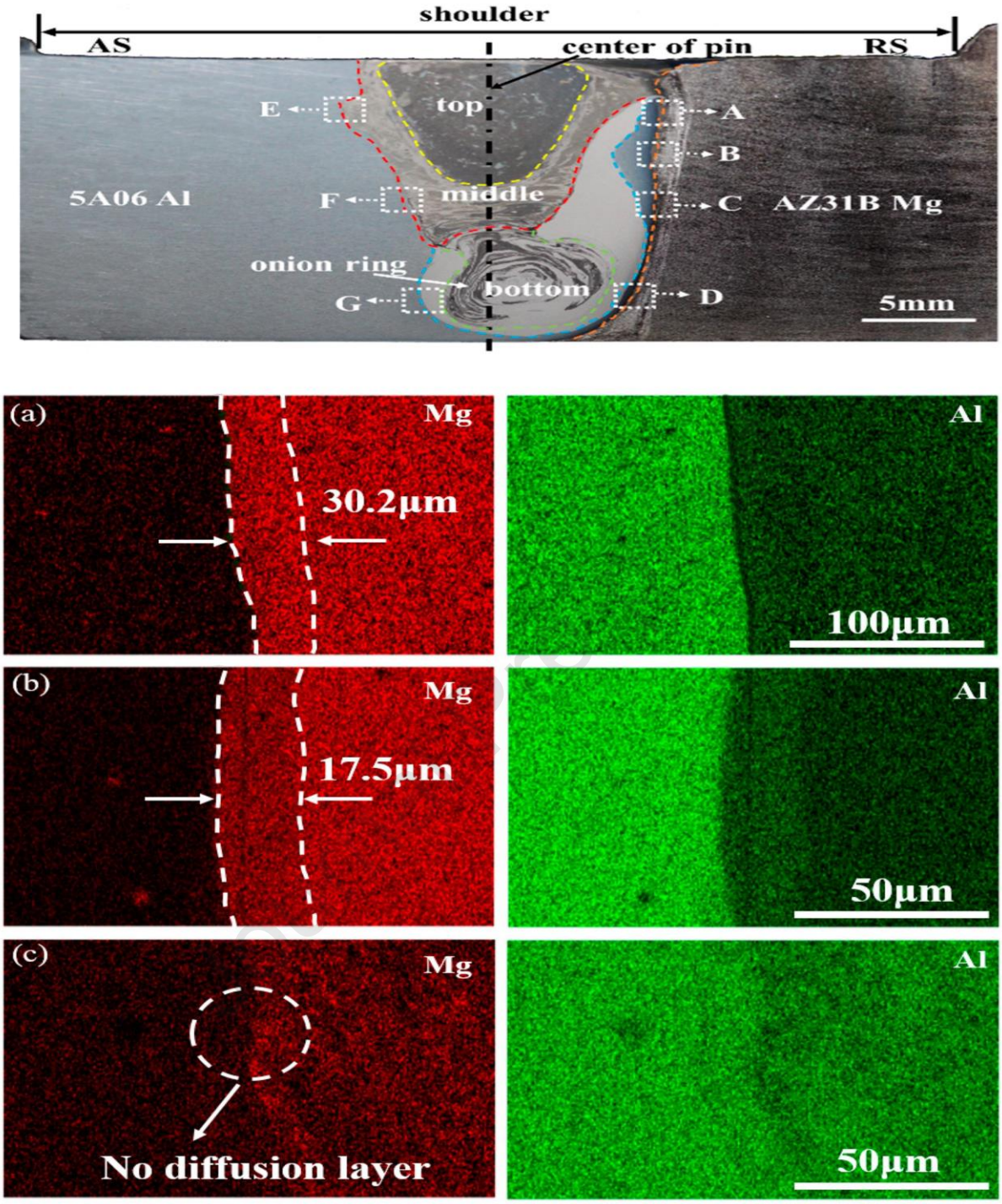

Figure 4: EDS maps (a-c) at location (E-G) depicting varying widths of the IMC layer along the thickness of the weld [84].

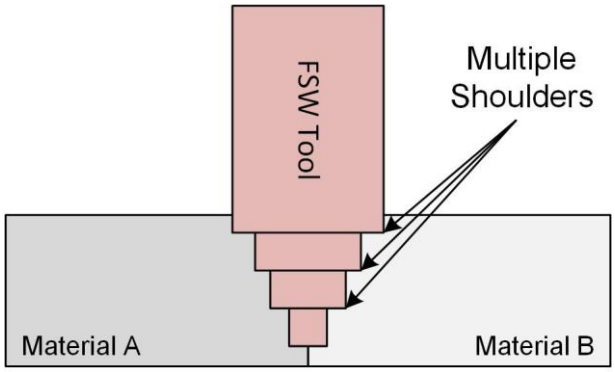

Figure 5: FSW with multiple shoulder tool.

1.3.5. Plunge Depth

The tool plunge refers to the distance the tool is inserted into the base metal. In FSW, the tool is inserted into the base metal to the point where the shoulder also penetrates the base metal to some extent, while keeping the pin of the tool away from the anvil. Plunge depth (PD) is often associated with the extent to which the shoulder penetrates the surface. This is because it is a critical factor in determining how effectively the material is worked and forged during the welding process Figure 6 (a).

The PD plays a critical role in controlling process temperature, and material flow, and providing the necessary axial force to forge the material. If the PD is insufficient, it can lead to internal cavities or incomplete filling on the surface, as the shoulder is unable to adequately plasticize the material and move it around the tool. Conversely, if the tool is too deep into the material, it can result in thinning of the weld joint and lead to excessive flash formation.

In a carefully designed experiment, Kumar and Kailas positioned a 4.4 mm thick aluminum alloy at an angle relative to the horizontal plane Figure 6 (b). As a result, while moving from point A to Point B, the tool's plunge depth increased from 3.8 to 4.6 mm, accompanied by a corresponding rise in axial force from 4 to 10.9 kN. Initially, due to inadequate shoulder contact at point A, internal volumetric defects emerged in the weld. These defects continued to shrink with increasing axial force until, at 7.4 kN, the voids completely disappeared Figure 6 (c) [94]. In a parallel study examining the influence of PD on T-joints of aluminum alloy, Memon et al. employed computational fluid dynamics (CFD) simulations. Their research elucidates that PD plays a highly critical role in regulating the temperature distribution within the joint's components, directing material flow, and effectively managing the occurrence of tunnel defects [59].

These investigations highlight the crucial role of PD in controlling internal defects in FSW. It underscores how precise adjustment of this parameter can significantly impact the quality and integrity of the weld.

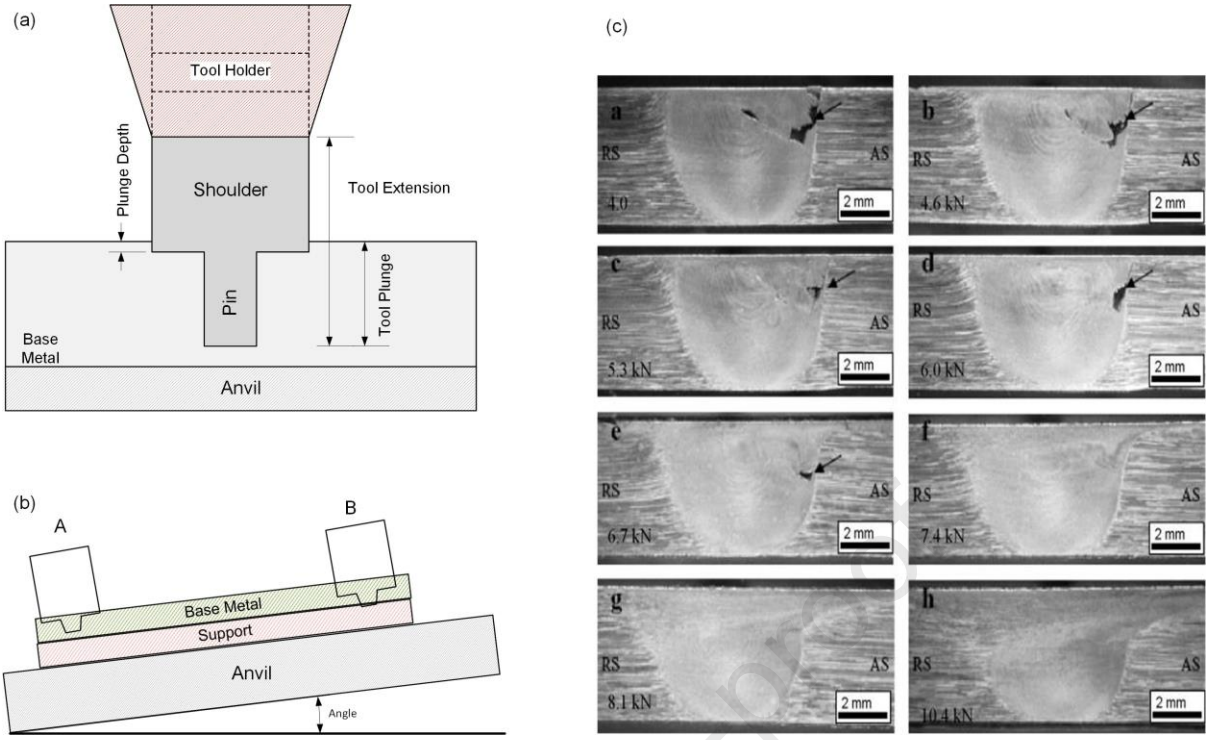

Figure 6: (a) Plunge depth, (b) experiment designed to investigate the effect of PD, and (c) size of volumetric defect as a function of PD. [(c) is cited from [94]]

1.3.6. Tool Offset

Tool offset, referring to the tool's rotation axis position relative to the joint line, gains significance in dissimilar welding due to varying material properties (Figure 7).

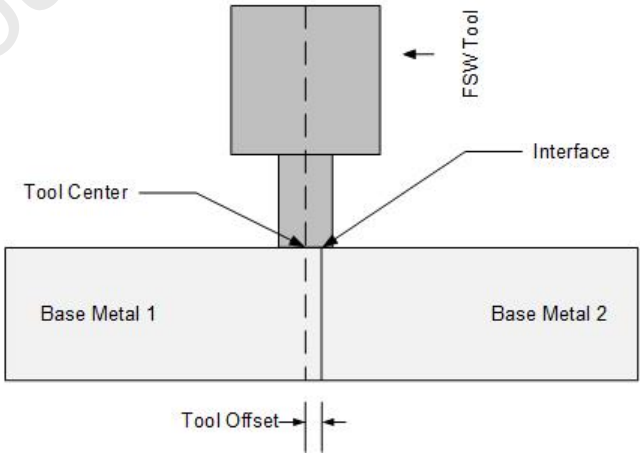

Figure 7: Graphical representation of tool offset (Front View).

It compensates for differences in hardness, and thermal conductivity, and regulates intermetallic compound (IMC) formation, affecting both heat and material flow. Tool offset direction and magnitude influence the aluminum-magnesium content in the Al/Mg interface, impacting IMC quantity [82]. Working with an Al/Cu joint, Sahu et al.

demonstrated that to achieve a defect-free joint, an effective tool offset of 1.5 mm towards the softer aluminum metal proves to be beneficial [95]. Properly selecting offset is essential for defect-free joints; for example, Fu et al. achieved this with a 0.3 mm Mg-oriented tool offset [75]. Conversely, an incorrect offset weakens the joint, leading to asymmetrical interpenetrating feature (IPF) and potential geometrical defects [96,97] as shown in Figure 8. It can be concluded that selecting the proper offset is crucial to prevent defects in dissimilar material welding, and the specific offset value depends on the combination of materials being used.

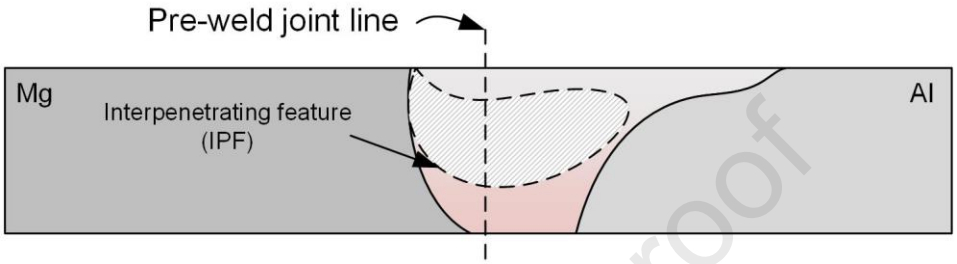

Figure 8: Asymmetrical IPF due to tool offset.

1.3.7. Tools rotational and welding speed

The tool's rotational speed (ω) and travel speed (V) are dictated by material properties, such as melting point, strength, and thickness. These parameters significantly influence heat input, and a "heat index" (HI) has been introduced to simplify heat input consideration, related to ω and V by the following equation [98,99].

$$HI = 10^{-4}\frac{\omega^2}{V}$$

ω has a more pronounced impact on heat generation due to its squared term, demonstrated by studies where peak temperature increased notably with higher ω [100,101]. ω also affects plastic deformation, material flow, and agitation during welding, leading to improved quality and reduced defects [101]. Proper ω and V adjustment eliminates heat-related defects and ensures defect-free welds, with an optimal range to prevent volumetric defects (Figure 9) [102]. Careful control and optimization of these speeds are crucial for welding quality.

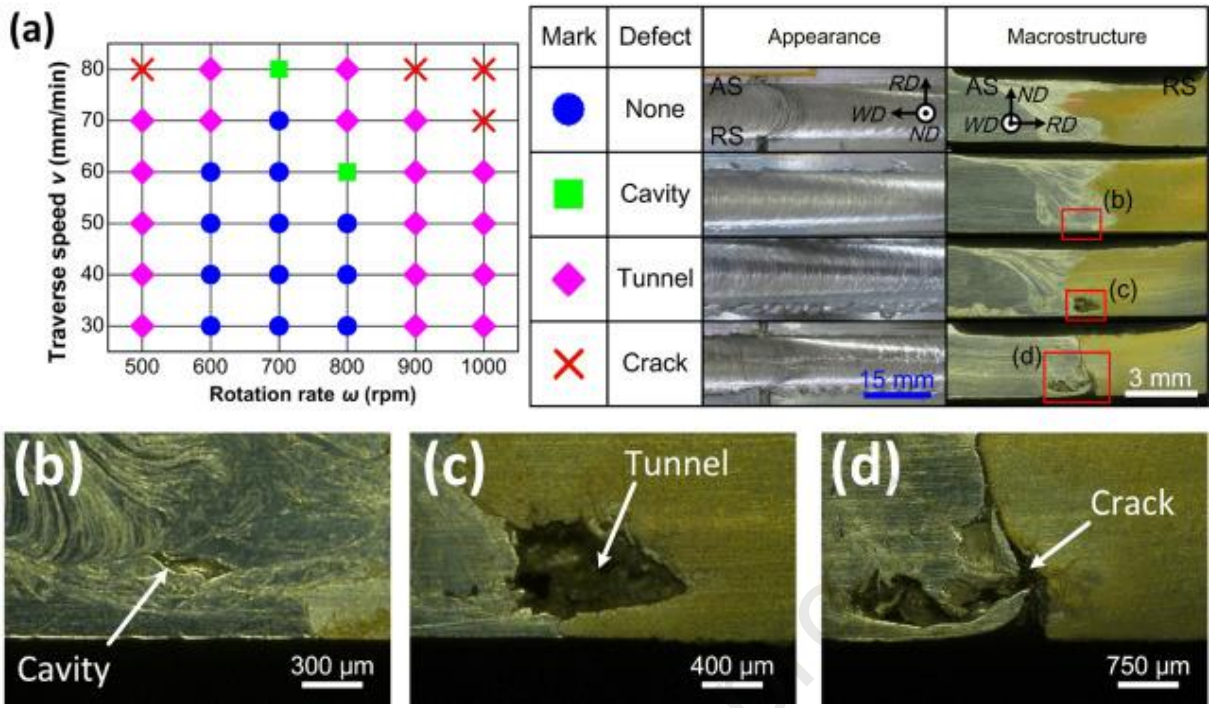

Figure 9: Travel speed and rotation rate range and their relation with defects [75]

1.4. Microstructural aspects of FSW

The mechanical properties of a friction stir weldment are dependent on the resulting microstructure, which consists of four main sections: the base metal (BM), the heat affected zone (HAZ), the thermomechanical affected zone (TMAZ), and the stir zone (SZ) also known as the weld nugget zone (WNZ). These sections exhibit distinctive temperature (T) and strain rate (ε°) histories during the FSW process. Figure 10 illustrates the *T* values for these zones about the melting temperature (T_m) and the ε° values. Due to the higher *T* and ε° values, which facilitate dynamic recrystallization (DRX), the grain size of the TMAZ and SZ undergoes reduction during the welding process [60].

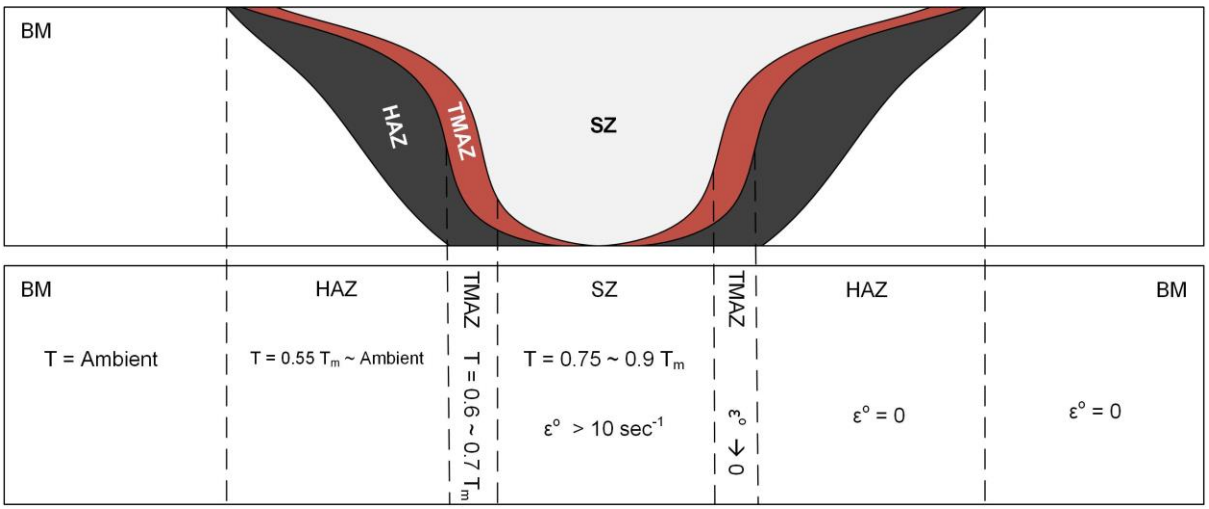

Figure 10: Different characteristic zones in a typical FSW microstructure, respective *T* concerning T_m and ε° in these zones.

In the industry, predominantly heat-treatable aluminum and magnesium alloys are employed. These alloys derive their strength from a process called precipitation hardening. Precipitation hardening is more pertinent to aluminum alloys than their magnesium counterparts [103]. However, in FSW, *T* and ε° conditions may lead to the dissolution or growth of precipitates in critical regions, which can have a detrimental effect on the strength of the material. This drop in strength is more pronounced in aluminum alloys compared to magnesium alloys [104]. This difference arises from the fact that magnesium alloys typically require coarser and more widely spaced precipitates for strengthening compared to aluminum alloys [103]. Additionally, certain alloying elements, such as yttrium (Y) and gadolinium (Gd), contribute to strengthening the solid solution in magnesium alloys [105].

Another noteworthy aspect of microstructure is the formation and morphology of IMCs. An IMC layer with a thickness in the range of 1.5 ~ 10 µm is considered indicative of a good joint [106,107]. IMCs in this amount ensure effective cementing of interpenetrating solid solution streaks across the joint line. Thicker IMC layers in the joint can serve as feasible sites for crack initiation and propagation (Figure 11) [108]. For a more detailed exploration of this topic, it's covered in the metallurgical bonding section 3.2.

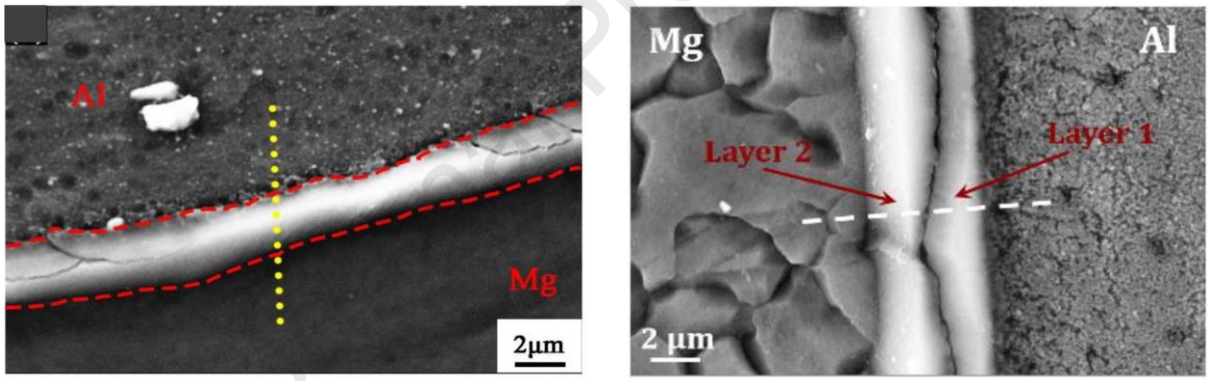

Figure 11: Crack initiation and propagation through IMC layer in Al/Mg FSW joint. (a) Crack initiation, and (b) Crack propagation [108,109].

1.5. Commonly Encountered FSW Defects

Having grasped FSW parameters' impact on heat generation and material flow, it's vital to enumerate prevalent FSW defects and their root causes, represented in Figure 12 as a fishbone diagram.

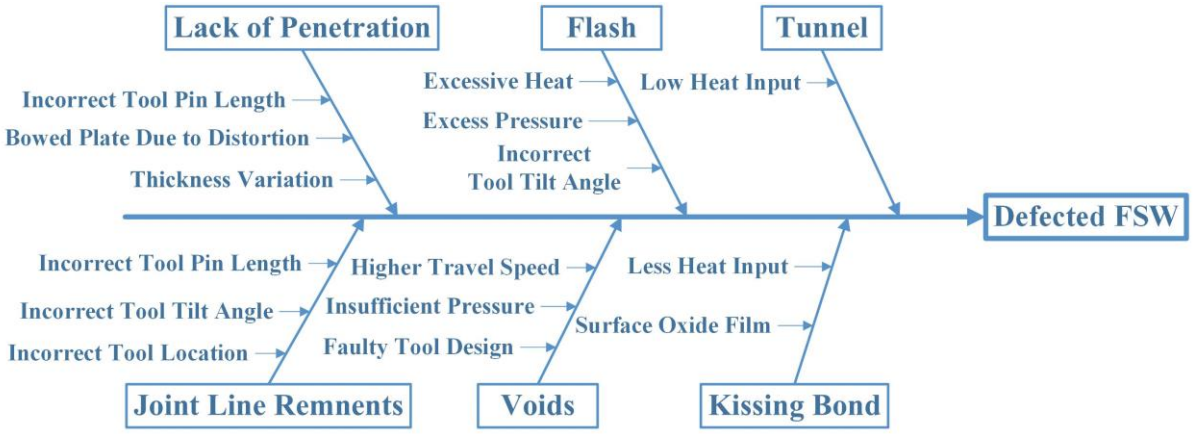

Figure 12: Ishikawa diagram for common FSW defects and their probable causes.

Note that eliminating certain defects, especially in dissimilar metal alloy welding, can be challenging due to alloy disparities and heat dissipation variations. Factors like tool and anvil materials, tool extension, and plunge depth (Figure 6-a) influence heat dissipation. Defect-free dissimilar metal alloy welds demand a holistic understanding of these variables and their interplay for successful joining and quality maintenance.

While recent reviews [110,111] have shed light on Al/Mg FSW, a critical aspect that seems missing is the discussion on strategies to enhance the interface. This review article addresses this gap by offering an analysis of Al/Mg FSW. All data analysis and textual content within this review are exclusively centered around butt joints unless otherwise specified. It provides analysis of crucial elements including FSW parameters, weld interfaces, mechanical properties, microstructure, and fractography, presenting up-to-date data. Notably, this review stands out for its dedicated focus on enhancing interfaces through the improvement in mechanical interlocking and the reduction of IMCs. Furthermore, it provides a valuable classification of methodologies aimed at enhancing Al/Mg friction stir butt weld interfaces. As such, this review article is poised to capture the attention of both seasoned researchers and engineers engaged in the realm of Al/Mg FSW. By offering a comprehensive snapshot of the current state of knowledge, it not only informs the present discourse but also pinpoints pivotal areas for future exploration.

~~Recent reviews [110,111] have provided insights into Al/Mg FSW. However, they lack strategies for enhancing the interface. This paper fills this gap by focusing on bolstering mechanical interlocks and inhibiting IMC formation. This review sequentially addresses key questions: Why Al/Mg FSW matters, crucial parameters for welding (parameter window), the significance of mechanical interlocks, IMC formation and its impact, interface classification, and finally, enhancing the interface by improving interlocking and reducing IMC growth. This comprehensive approach advances our understanding and practical methods for optimizing Al/Mg interface performance.~~

2. Retrospective data analysis on Al/Mg FSW

Past data for FSW of Al/Mg butt joint configurations has been collected and referenced sequentially for different magnesium alloys in Table 3. The following paragraphs present an analysis of 43 studies, focusing on research trends, the most researched materials, and thicknesses, ω and V, the tool's rotation direction, the tool's material, and the tool's pin profile.

Magnesium Alloy	Aluminum Alloy	Reference	Frequency	Accumulative studies for each magnesium alloy
AZ31	AA1050	[112]	1	9
	AA1060	[113]	1	
	AA6040	[114]	1	
	AA2024	[115]	1	
	AA6013	[116]	1	
	AA6061	[101,117–119]	4	
AZ31B	AA5083	[77,120]	2	24
	A5052	[25,121]	2	
	AA6061	[75,78,109,122–132]	14	
	Al6063	[96,98]	2	
	AA5A06	[82,133]	2	
	AA2024	[134]	1	
	AA7075	[135]	1	
AZ31C	AA5083	[136–138]	3	3
AZ61	AA6061	[139]	1	1
AZ91	AA6063	[140]	1	4
	A383	[141]	1	
	AA6082	[142]	1	
	EN AC-48000	[143]	1	
Mg	AA6013	[144]	1	2
	AA6061	[145]	1	

Table 3: Classification of studies on Al/Mg FSW based on Mg alloys and respective referencing.

Early FSW research primarily concentrated on identifying the appropriate FSW parameters and comprehending the kinetics and mechanisms of IMC formation. Researchers observed that uncontrolled formation and growth of IMC resulted in poor mechanical joint efficiencies. As a result, the focus of subsequent research shifted toward finding ways to mitigate the formation of IMC. Various strategies were explored, including submerged FSW, stationary shoulder FSW, the application of ultrasonics, and pulse current. Most of these methods were found to be effective in controlling the formation and growth of IMC. For a more detailed discussion, please refer to section 4.3.

In terms of base metal thickness, a significant majority, 79% to be precise, of the research has been conducted on materials with a thickness ranging from 1 to 4 mm. This is pictorially represented in the form of a histogram in Figure 13. The most researched alloys are the 6xxx series of aluminum alloys, with a particular focus on AA6061 within this series. This information is visually represented in Figure 14 (a) through a pie of pie chart. For magnesium alloys, the AZ series is the most studied composition, with AZ31 being the most frequently chosen alloy for research purposes. This data is presented graphically in Figure 14 (b). Collectively, the 6xxx series of aluminum alloys and the AZ series of magnesium alloys account for 62% and 95% of the selected research, respectively. The selection of these alloys and thicknesses is primarily influenced by factors such as their good mutual weldability, easy availability, industrial importance, and the kind of FSW setup available.

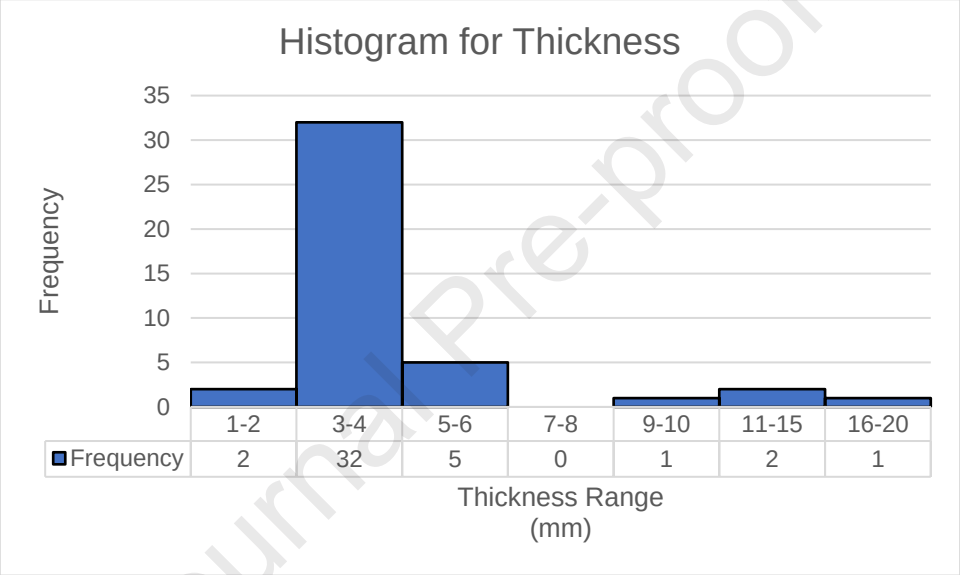

Figure 13: Histogram for thickness ranges.

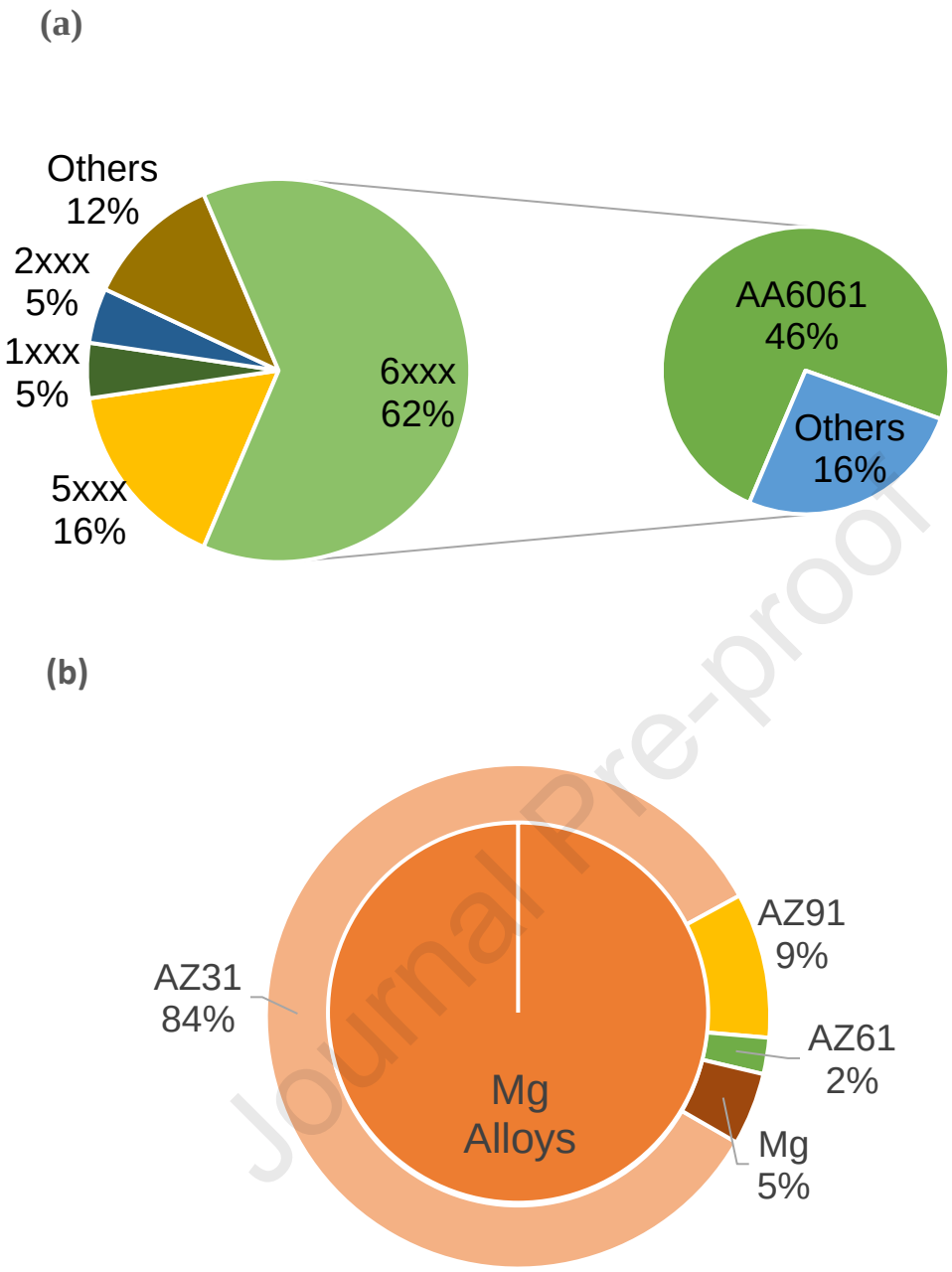

Figure 14: Aluminum and magnesium alloys used for Al/Mg dissimilar FSW based on data in Table 3. (a) Aluminum and (b) Magnesium.

When considering the FSW of Al/Mg alloys, the first parameters that receive significant attention are ω and V. To gain insights into the parameter window, individual studies provide ranges for these two parameters. By averaging and plotting these averaged values against each other, an initial estimate can be made. This estimate suggests that the ω and V can be chosen within the parameter window indicated by the dashed rectangle in Figure 15. This range covers approximately

84% of the data points and includes values between 250 to 1500 rpm for ω and 6 to 100 mm/min for V.

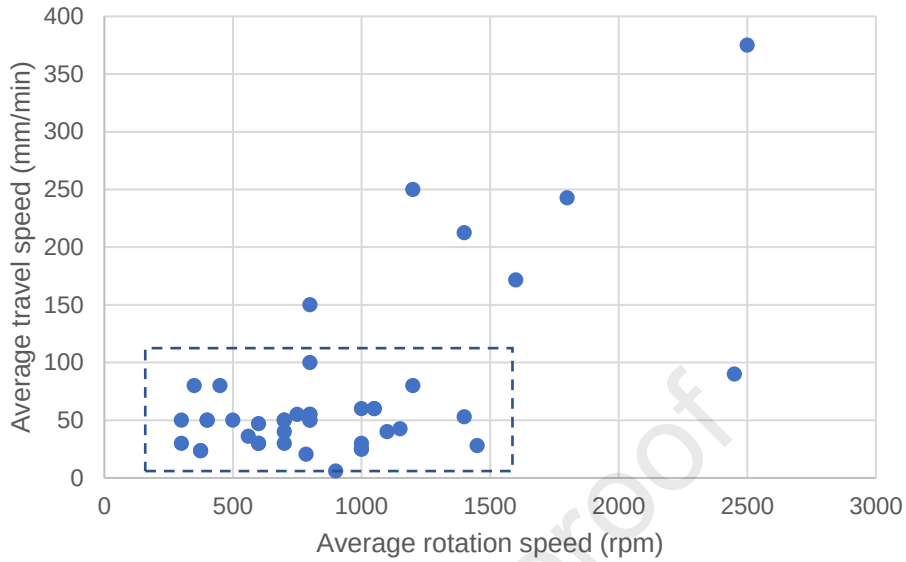

Figure 15: Most researched parameter window (84% data - dashed rectangle) for rotation and travel speed (Table 3).

Out of the 43 studies, only 35 reported the material positioning in the FSW of Al/Mg alloys. Among these 35, 17 studies chose to place magnesium on the advancing side, while 13 studies placed it on the retreating side. Additionally, 5 studies investigated the effect of positioning by alternating between placing Mg on both sides. This information is presented in Figure 16. The decision to select an alloy for the advancing or retreating side depends on the specific alloys under consideration. For AA6061, 83% of the research has been conducted with the placement of Mg alloy on the advancing side.

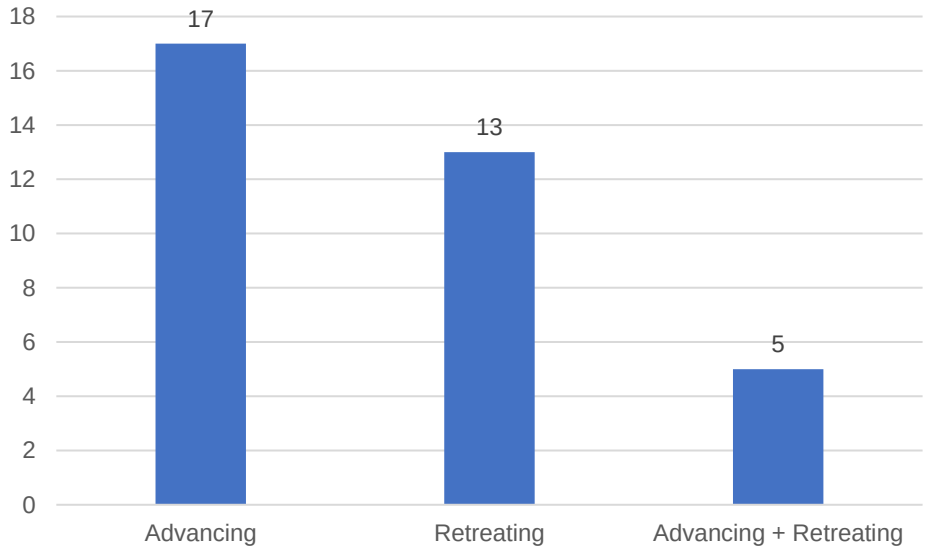

Figure 16: Number of studies with the selection of advancing side for magnesium (data from Table 3).

In the literature, only 13 reported values for shoulder PD. Among these, the most frequently used PD values are 0.1, 0.15, and 0.2 mm, occurring 6, 5, and 2 times in the literature respectively. All these reported values are within the thickness range of 3 to 5 mm, with 3 mm thickness being the most used, appearing 11 times in the literature. Moreover, for 3 mm thickness, the PD values most employed are 0.1 mm, which appeared in 6 instances, and 0.15 mm, which occurs 4 times in the literature.

In the analysis of tool selection, two aspects were considered: the tool material and the pin profile. Among the studies included in this analysis, tool steel was the only material used for the tools. As for the pin profiles, five different types were adopted: plain cylinder, cylindrical threads, frustum cone, threaded frustum cone, and tapered with 5 flats and threads. It is worth noting that the "tapered with 5 flats and threads" pin profile was used only once in the studies. On the other hand, the other four profiles have been commonly employed. In particular, the threaded frustum cone pin profile stands out as the most frequently utilized. This data on tools has been summarized in Figure 17. Approximately 75% of the reported pin profiles utilized threads. This choice of pin profile is made to ensure proper mixing of the alloys both in the horizontal and vertical directions during the FSW process.

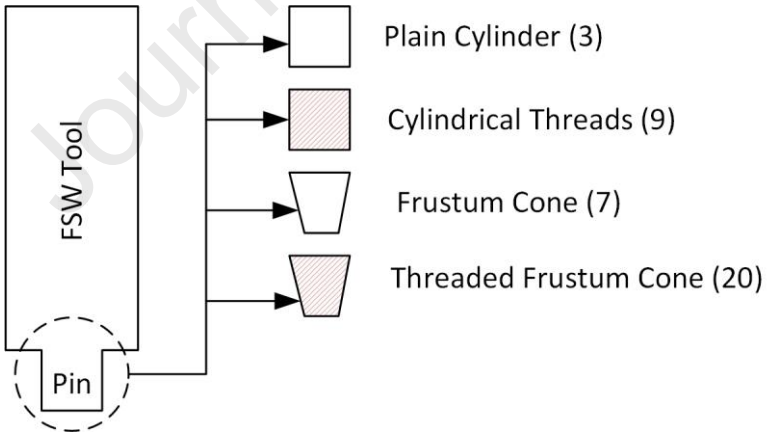

Figure 17: Most used tool pin features in literature. The numbers in parenthesis describe the number of studies that used the specific pin characteristic.

2.1. Mechanical properties of weldment

The acceptability of an Al/Mg joint hinges on the mechanical properties exhibited by the weldment. In the literature, these weldments are typically characterized through assessments involving hardness, tensile strength, and mode of fracture.

2.1.1. Vickers Hardness

The Vickers Hardness (HV) measurement method is preferred for assessing the hardness of dissimilar FSW joints due to its reliability. For dissimilar weldments, the reported hardness values in the literature vary due to several factors: alloy type, grain refinement, dissolution of precipitates, presence of brittle phases, and distribution of phases.

In Al/Mg joints, the hardness values within the WNZ range from 54 to 220 HV [112,114]. Khodir and Shibayanagi noted a minimum hardness of 65 HV in the WNZ adjacent to the Mg alloy, which had a reported hardness of 60 HV. This increase in hardness is ascribed to grain refinement in the WNZ due to DRX [115]. For heat-treatable alloys, the hardness of the aluminum side is adversely affected due to the dissolution of strengthening precipitates. Venkateswaran and Reynolds reported a base metal hardness of 63 HV for AA6063, whereas, in the WNZ adjacent to the aluminum, the hardness measured was 50 HV, attributed to the dissolution of Mg_2Si precipitates [96]. Sharp peaks observed during the transition from the TMAZ to the WNZ are attributed to the presence of IMCs. Fluctuations in hardness values indicate the clustering of brittle IMCs. Figure 18 (a) illustrates a standard hardness profile of the Al/Mg interface at three distinct positions: top, middle, and bottom. The variations in HV values during the transition from TMAZ-WNZ-TMAZ are attributed to the presence and distribution of IMCs.

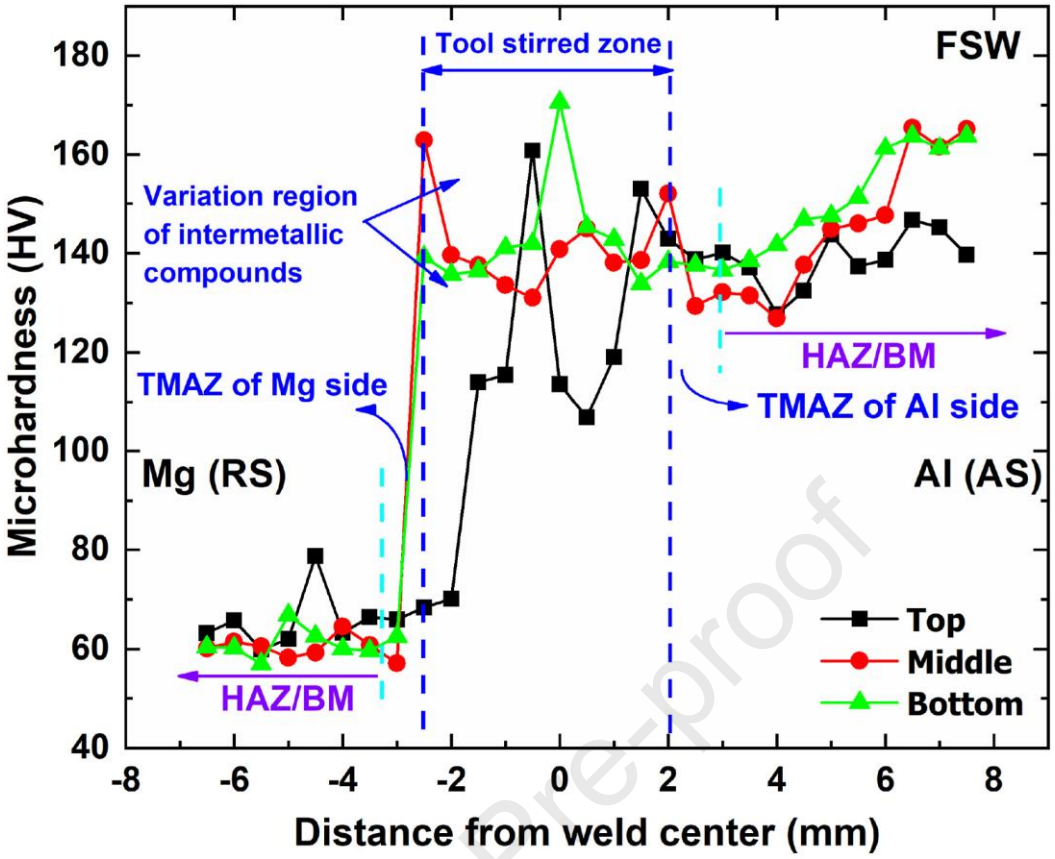

(a)

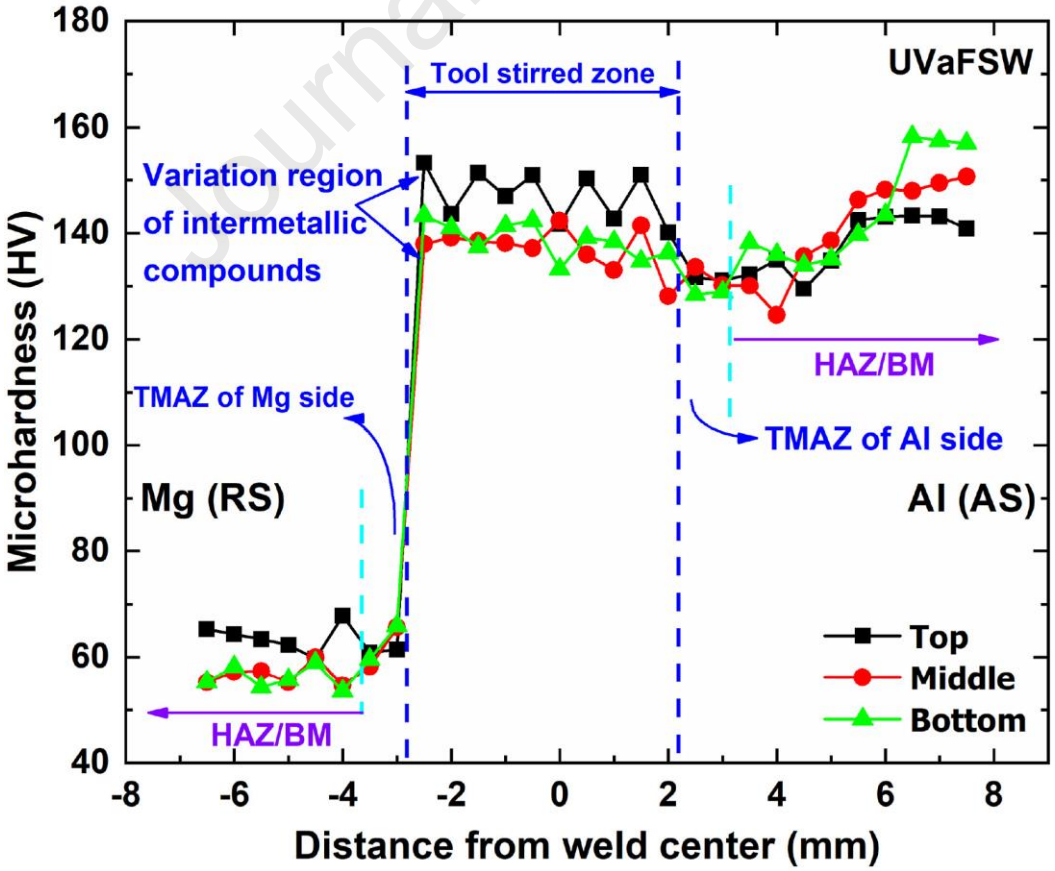

(b)

Figure 18: Microhardness (HV) profiles. (a) A typical curve showing HV values at different spatial points at the Al/Mg interface, and (b) Smoothening of HV within TMAZ of both materials [135].

2.1.2. Ultimate tensile strength

The ultimate tensile strength (UTS) is a key metric reflecting the integrity of the weldment. To illustrate this, UTS data for Al/Mg weldments has been compiled from the literature and represented in the form of a box and whisker plot in Figure 19.

From the plot, it is evident that the significant UTS spans from 82.4 to 215.7 MPa, with an average of 143.16 MPa for all data points. There are two data points with values of 32.8 and 36.14 MPa, which can be considered statistically insignificant (outliers). The former value pertains to a study involving an innovative butt joint with serrations [133], while the latter was obtained after 1 hour of heat treatment of the weldment [144], representing the maximum in the study. Furthermore, 50% of the UTS values fall within the range of 119-172 MPa. The highest recorded value of 215.7 MPa was achieved through the application of a pulse current of 500A [131].

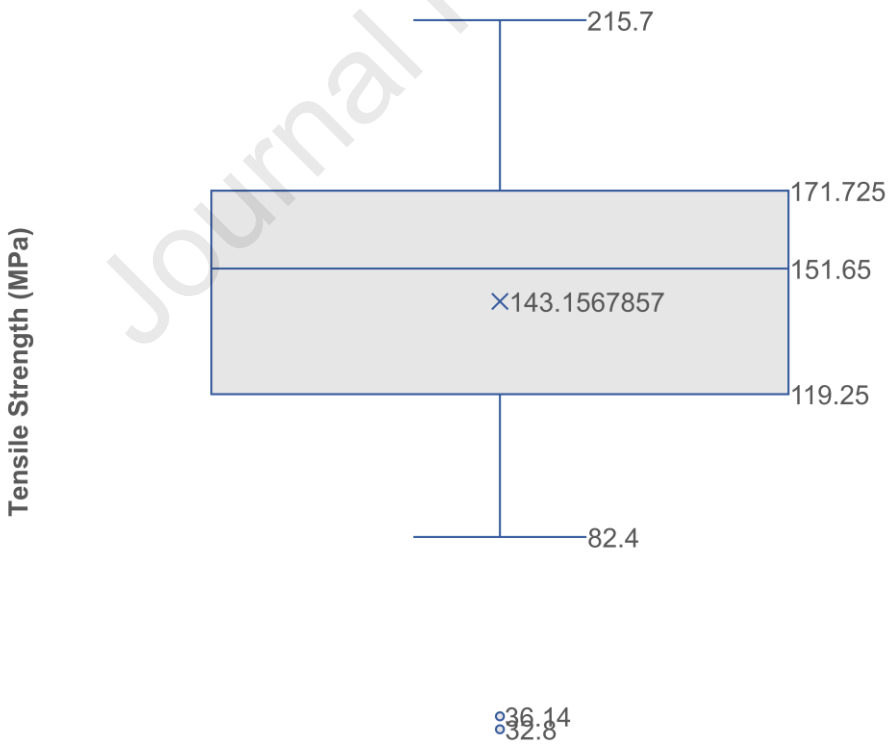

Figure 19: Box & Whisker plot for the UTS (MPa) values.

2.1.3. Fracture behavior of weldment

Fractography examines fracture surfaces, revealing fracture type, fracture initiation, fracture propagation, and contributing factors like defects or overloading. This data informs preventive measures, improving material and design reliability.

In this study, Al/Mg joints were examined in terms of fracture location and type. The fractures were categorized into five classes based on location: Mg side [122,123,125,127,131,144], Al side [78,123], banded zone (BZ) [78,119,128], and WNZ [112,113], dual location at the interface and BZ [78], and HAZ [139]. The fracture locations are primarily influenced by the presence and distribution of IMCs, followed by overloading, and the presence of volumetric defects within TMAZ and WNZ. Figure 20 illustrates all five scenarios.

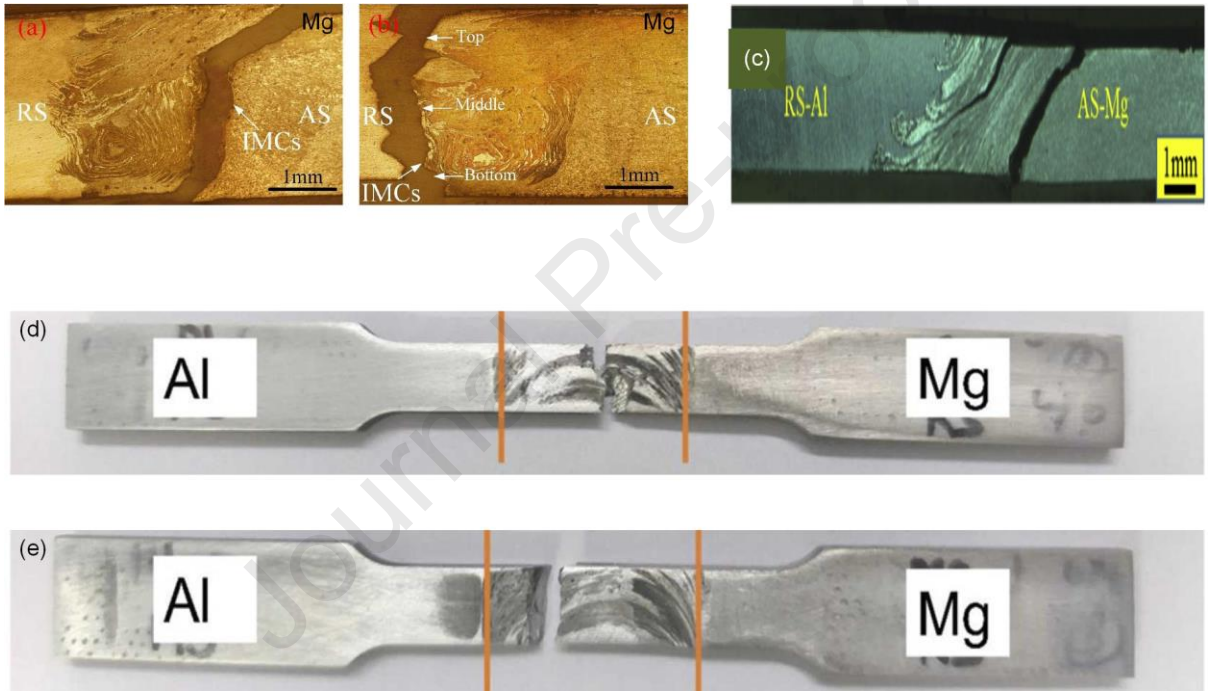

Figure 20: Typical fracture locations in Al/Mg FSW. (a) Mg side, (b) Al side, (c) both at the interface and banded zone, (d) WNZ, and (e) HAZ [78,123,139].

In scanning electron microscope (SEM) images, the mode of fracture is identified by the presence of plateaus and ridges, indicative of brittle fracture, as well as voids, associated with ductile fracture. In the case of Al/Mg welds, most fractures have been documented as brittle [77,112–114,118,121,122,122,124,142], or mixed fracture type [25,78,96,117,123,127,128,131,133,135,137,139,141,145], combining elements of both ductile and brittle characteristics. These features are represented in Figure 21.

Adaptations like the incorporation of ultrasonic vibrations, the application of water or liquid nitrogen, the use of pulse current, alterations in joint design, and the introduction of interlayers affect the distributions of IMCs. These process variations are responsible for smooth HV transitions across the microstructure, improved

tensile strength, and introduction of the ductile component in fracture. Smoothening in HV peaks due to ultrasonic vibrations is depicted in Figure 18 (b).

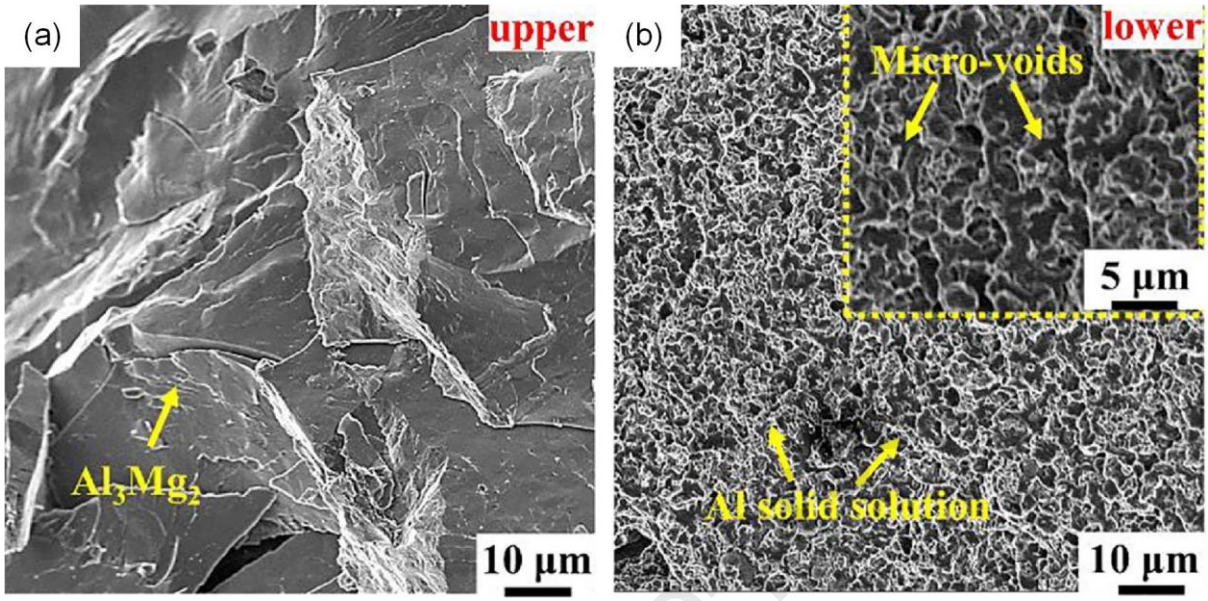

Figure 21: characteristic features of fracture mode. (a) brittle fracture, and (b) ductile fracture [133].

3. Joining mechanisms

The objective of joining Al/Mg alloys through FSW is to achieve a weld with satisfactory efficiency that meets its intended purpose. To achieve such a structure, a comprehensive understanding of the underlying principles of joining is crucial. The strength of the joint in dissimilar metal welding relies on several factors, including mechanical interlocking, the formation of IMC, and their distribution at the interface.

A closer examination of these joining mechanisms is presented in Figure 22, with Figure 22(a) illustrating the macrostructure of the Al/Mg joint. Figure 22 (b) and (c) depict the optical microstructures of the upper and lower sections of the WNZ, respectively. These micrographs vividly display interpenetrating streaks of dissimilar materials extending across the interface, representing mechanical interlocks. These interlocks are further reinforced by the presence of IMCs, establishing a robust metallurgical bond. In Figure 22 (d), the FESEM image of the Al/Mg interface provides a visual confirmation of material mixing and bonding at the interface. Figure 22 (e) showcases an SEM image of the WNZ boundary, revealing lamellae of different phases that actively contribute to the joining process through a combination of mechanical interlocking and metallurgical bonding.

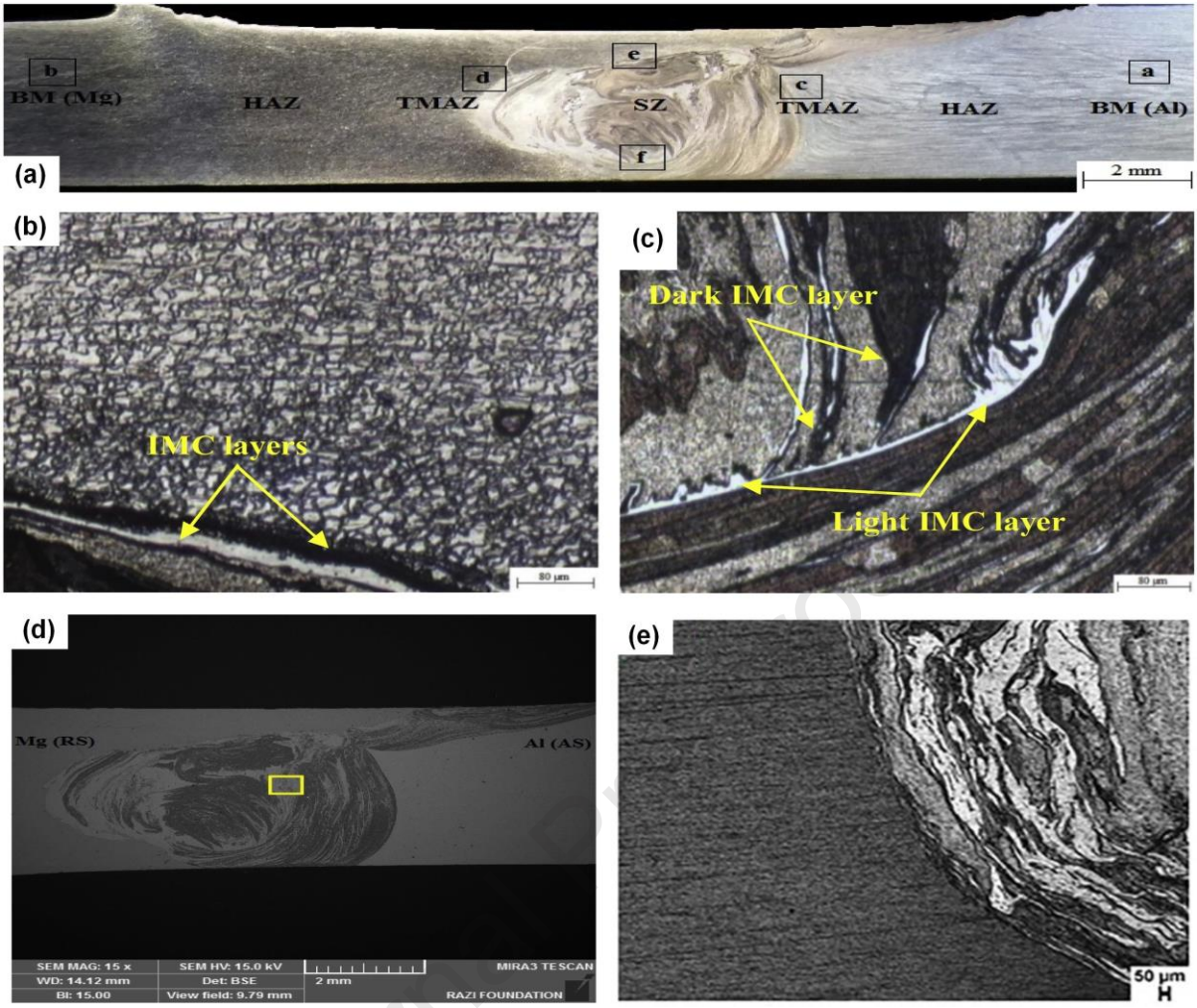

Figure 22: A cross-section of the joint showing a glimpse of joining mechanisms at the Al/Mg interface. (a) Macrostructural features of the joint, (b) Optical micrograph of the top side of the WNZ, (c) Optical micrograph of the bottom side of the WNZ, (d) FESEM image of the Al/Mg interface, and (e) SEM image of WNZ [98,146].

In this section, the focus is on understanding the processes of mechanical mixing and the mechanisms involved in the formation of IMC. This includes studying the kinetics of these reactions and the role they play in "cementing" different phases at the joint interface. A thorough comprehension of these aspects is essential to ensure the quality and reliability of the Al/Mg joint obtained through FSW.

3.1. Mechanical interlocks

The strength of dissimilar metal friction stir welds is primarily influenced by mechanical interlocking, which is a result of the complex geometry at the joint interface. Mechanical interlocking plays a significant role in enhancing joint strength, especially in cases where the metals being joined are not compatible [78,96]. The effectiveness of mechanical interlocks is closely tied to the relative displacement of materials across the initial joint line. This displacement is influenced by various FSW parameters that impact heat generation and material flow during the welding process. Among these parameters, the most crucial ones are the tool rotation

direction, tool pin profile, ω, and V [77]. These factors collectively determine the quality and strength of the joint, making them essential considerations in optimizing the FSW process for dissimilar metals.

3.1.1. Macro & micro-mechanical interlocks

To gain a fundamental understanding of mechanical interlocking and its significance, it is valuable to visualize specific variations of the FSW process that are specially designed to enhance mechanical interlocks between immiscible metals. These visual representations will aid in comprehending the concept of mechanical interlocking at the micro-scale. Various FSW process variants, such as friction stir scribe welding (FSSW), friction stir groove filling (FSGF), and friction stir dovetailing (FSD), have been developed and focused on enhancing mechanical interlocks between different base metals in lap joint configurations. These FSW variants are primarily applied to thicker combinations of dissimilar metals with considerable differences in melting points. In these techniques, the material with the higher melting point is placed at the bottom of the lap joint configuration [147].

In FSSW, a small offset cutting tool referred to as the "scribe insert", machines the top surface of the bottom plate while simultaneously softening the upper (lower melting) metal. The plastic material is then forged around the scribe produced by the tool, creating a mechanical bond between the metals (Figure 23a) [148]. In FSGF, the upper component in the lap joint fills an existing groove in the bottom component just by a 'weld throw', enhancing mechanical bonding, as depicted in Figure 23(b) [147]. Lastly, FSD utilizes a tool with a tungsten carbide FSD insert to make a dovetail groove in the lower component. This groove is then filled with the upper material, generating controlled heat to further "cement" the material in the groove with a fine layer of intermetallic compounds (Figure 23c) [149]. The concept of "cementing" is further discussed in section 3.2.2.

These variants of the FSW process demonstrate the innovative ways researchers have explored to enhance mechanical interlocks between different base metals in dissimilar metals lap joint configurations, contributing to improved joint strength and overall performance.

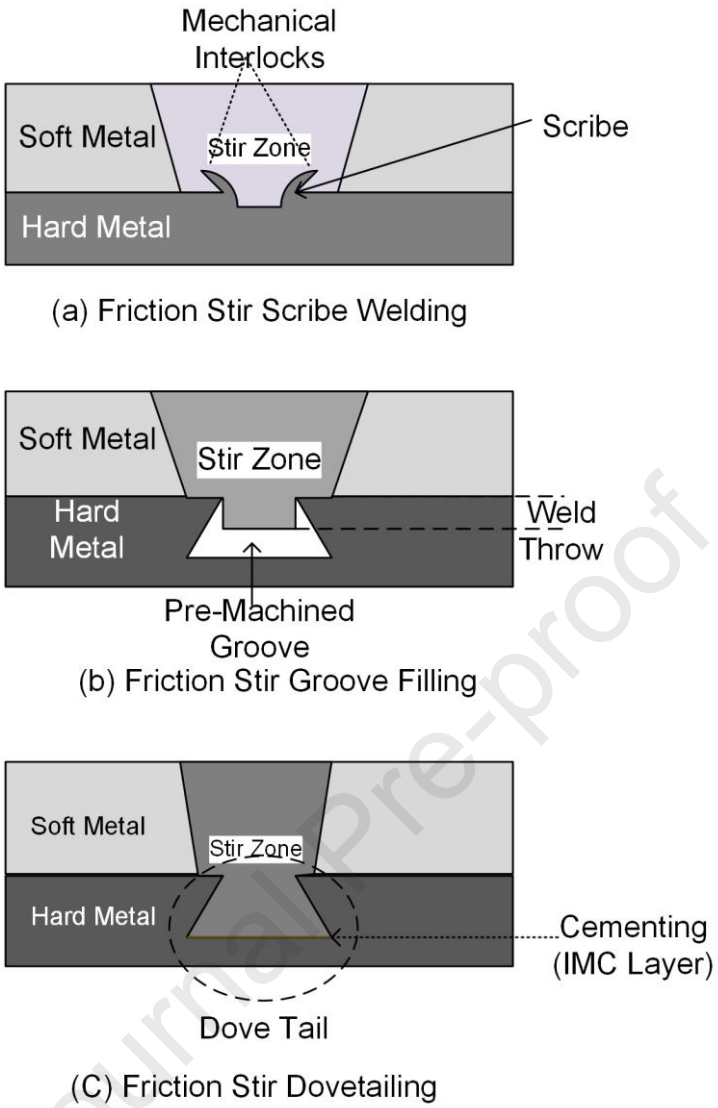

Figure 23: Macroscopic understanding of mechanical interlocking. a) Friction stir scribe welding, b) Friction stir groove filling, and c) Friction stir dovetailing.

Similarly, in Al/Mg FSW with a butt configuration, material flow streaks are generated and traverse across the joint line, leading to the formation of mechanical interlocks at the micro level (depicted in Figure 24). These micro-mechanical interlocks play a crucial role in enhancing joint strength and integrity for dissimilar metal combinations.

The shape and extent of these interlocks are influenced by the specific FSW parameters chosen for the welding process. The joint efficiency of friction stir welds is primarily determined by the degree of tortuosity of these micro-mechanical interlocks. In other words, the more intricate and convoluted the interlocks are, the stronger and more reliable the joint will be. Proper control and optimization of FSW parameters are, therefore, essential to ensure the desired extent and quality of these micro-mechanical interlocks, ultimately leading to improved joint performance and mechanical properties.

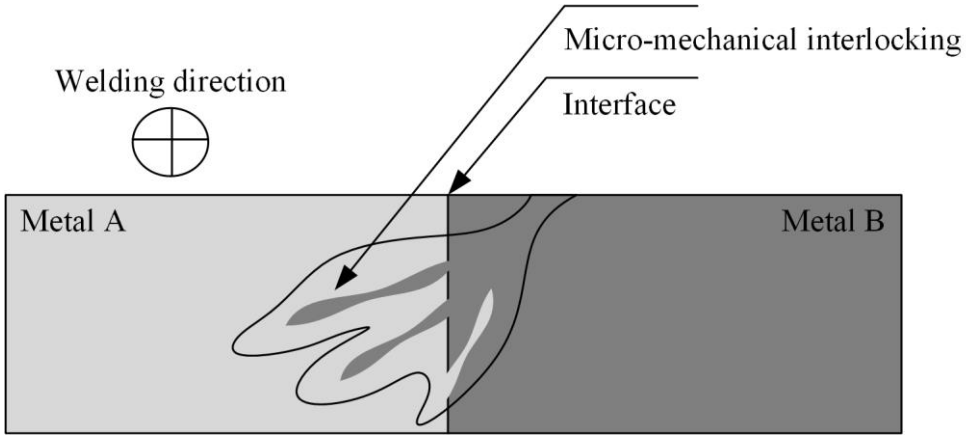

Figure 24: Micro-mechanical interlocking in friction stir welding.

3.2. Metallurgical bonding

To comprehend metallurgical bonding in the context of Al/Mg welding, it is beneficial to discuss the Al/Mg binary phase equilibrium diagram (depicted in Figure 25). This diagram provides valuable insights into the potential phases that may form during the welding of these dissimilar materials.

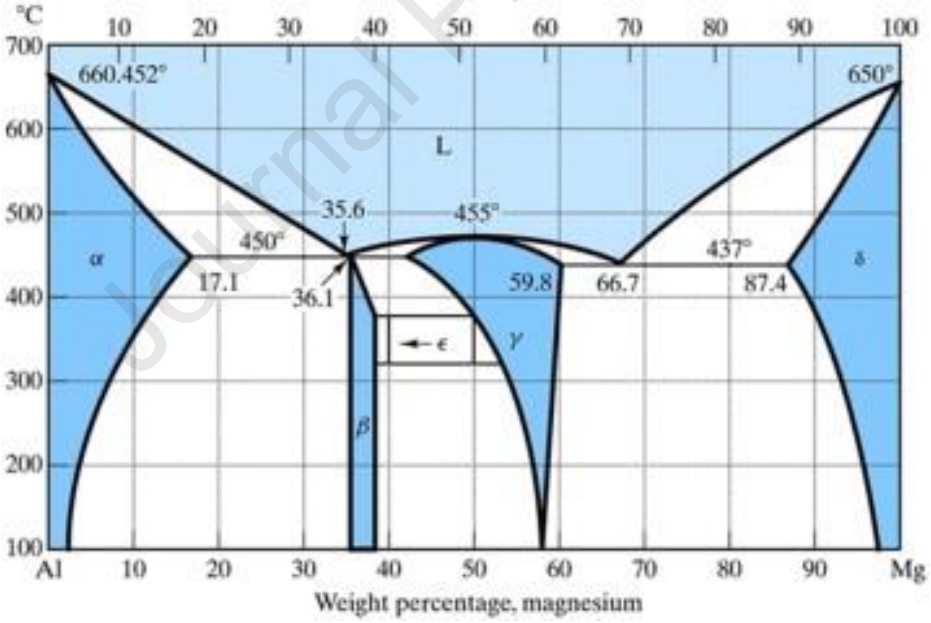

Figure 25 Al-Mg binary phase diagram [150].

As indicated in the binary phase diagram, Al and Mg have limited mutual solubility. Consequently, IMC are likely to form, in addition to aluminum-magnesium single-phase solid solutions. Specifically, three intermetallic compounds are known to be formed in this combination: β phase (Al_3Mg_2), also referred to as the Samson phase [151], ɣ phase ($Al_{12}Mg_{17}$), and R phase (AlMg) [152,153].

While consulting equilibrium phase diagrams during FSW, it is essential to recognize that FSW is a non-equilibrium process [82]. Nevertheless, the phase diagram can still offer some guidance on the potential reactions that might occur and the expected

phases that may form because of these reactions during the welding process. It provides valuable information to understand the complex metallurgical transformations that take place during the Al/Mg welding and the formation of various IMC and solid solutions, which significantly influence the joint's microstructure and mechanical properties.

An essential aspect to highlight is the occurrence of the eutectic reaction during the welding of dissimilar materials. Due to the difference in melting points, with aluminum having a higher melting point (660°C) than magnesium (650°C), the eutectic reaction on the aluminum side occurs at a slightly higher temperature of approximately 450°C. On the other hand, the eutectic reaction on the magnesium side takes place at around 437°C.

$$\text{Liquid} \rightleftharpoons Al_{12}Mg_{17} + Mg \ (437°C)$$

$$\text{Liquid} \rightleftharpoons Al_3Mg_2 + Al \ (450°C)$$

The formation of IMC during the FSW process is strongly influenced by its thermomechanical nature. The intense mixing and heat generation in FSW create an environment where the formation of IMC depends on several factors. One crucial factor is the relative concentration of aluminum and magnesium in the welded region. The composition of the base metals plays a significant role in determining the type and amount of IMC that may form at the joint interface. Additionally, the temperature distribution during the welding process is a critical determinant. Different regions experience varying temperatures, and these temperature gradients influence the kinetics of IMC formation. The applied pressure, which can be in the form of axial force or plunge depth, also affects the IMC formation. The pressure applied during the welding process can affect the material flow and distribution, influencing the reaction rates that lead to IMC formation. All these factors, including composition, temperature distribution, and applied pressure, work together to influence the formation of IMC during FSW.

The formed IMCs have been identified as a contributing factor to weak joint strength in dissimilar alloy welding [10,128,154]. In the case of Al/Mg FSW, it is challenging to completely avoid the formation of IMC, as referenced in [72,155,156]. Given the inevitable presence of IMC in Al/Mg FSW, recent research efforts have shifted towards exploring various strategies to impede the growth of these IMCs [137,154,157–159]. These strategies aim to control the process parameters and conditions to reduce the extent of IMC formation, thereby improving the overall mechanical properties and joint strength of the welded materials. By mitigating the negative effects of IMC, researchers aim to enhance the performance and reliability of Al/Mg FSW joints for practical applications.

It is worth noting that IMCs are a common feature in most dissimilar systems. They have been documented in systems such as Fe/Al [160], Al/Cu [161], and Al/Ti [162]. The joint interface is the most favorable location for the formation of IMC during Al/Mg FSW. At this interface, IMCs are commonly observed in the form of overlapping layers, with the ɣ phase on the magnesium side and β phase on the aluminum side.

3.2.1. Mechanical properties of β and ɣ IMC

Given that β and ɣ IMCs are implicated in creating weaker joints during Al/Mg FSW, it is crucial to substantiate this assertion with mechanical property data for these compounds. Wang and Prangnell have addressed this in their research on Al/Mg IMCs, providing relevant properties, summarized in Table 4.

IMC	Fracture Toughness	Micro Hardness	Nano Hardness
	MPa√m	H_v	GPa
$Al_{12}Mg_{17}$	0.105	268.3 ± 3.6	3.82 ± 0.18
Al_3Mg_2	0.062	289.4 ± 3.6	4.09 ± 0.10

Table 4: Mechanical properties of β and ɣ IMCs [163].

It's important to highlight that while there may be variations in nano hardness values reported by Wang and Prangnell compared to others [164,165], the overarching conclusion remains consistent: both β and ɣ phases exhibit elevated hardness and diminished fracture toughness, rendering these IMCs prone to brittleness. Notably, the β phase demonstrates greater brittleness than the ɣ phase.

3.2.2. The cementing effect

Thicker IMC layers might be perceived as a source of stronger joints due to the potential for chemical bonding. However, the presence of thick IMC layers hampers mechanical interlocking, negatively affecting joint strength [77]. This was confirmed by Sameer and Birru et al. during experiments on AZ91 and AA6062, where they observed poor adhesion between aluminum and magnesium due to thick IMC layers [142]. Due to their brittleness, microcracks form and propagate within these IMC layers under stress.

Conversely, thin layers of IMC are known to enhance the strength of weldment by acting as a ‘cementing agent’ at the complex material interface. These thin IMC layers also effectively mask defects at the interface [96]. The cementing effect of IMC is explained in Figure 26, where controlled growth of IMC at the A/B metallic interface significantly improves interface strength, uniformly distributes the stress, and shifts the location of failure outside the interface.

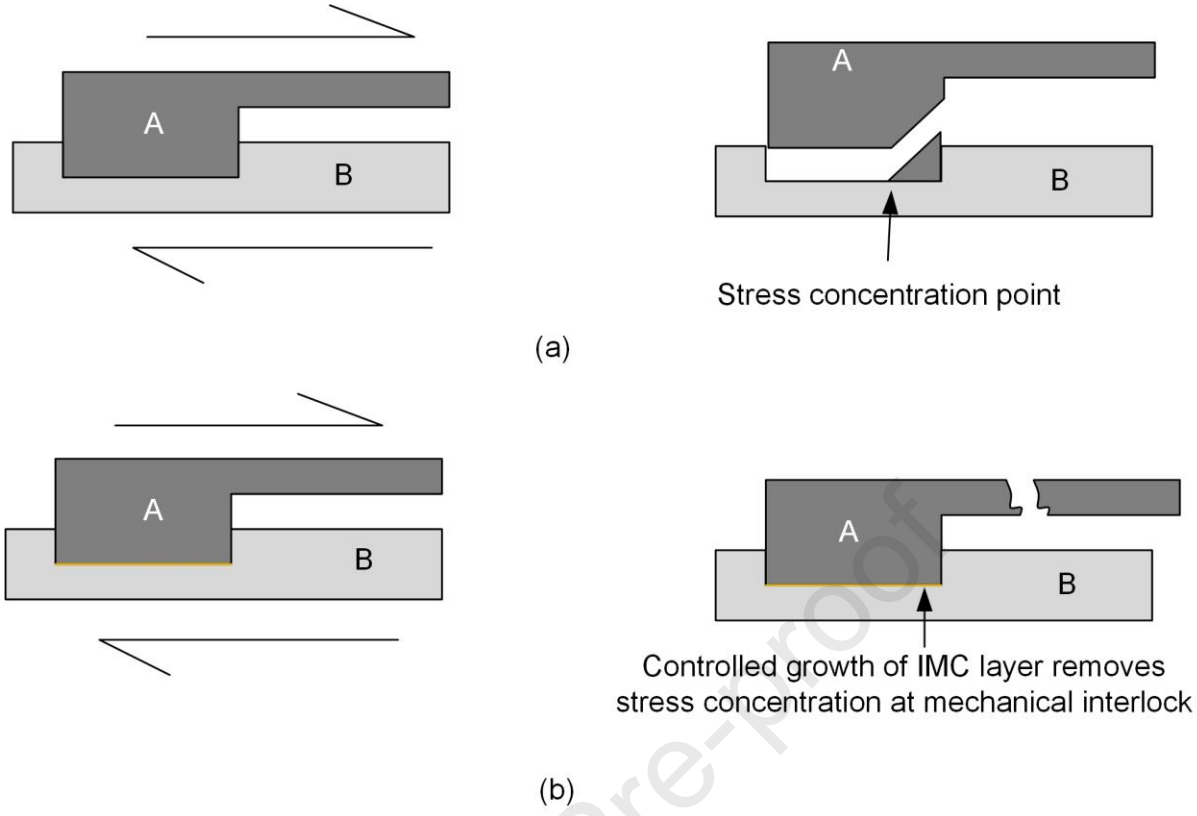

Figure 26: The cementing effect a) Mechanical interlocking alone causes the force to concentrate on a single point b) Metallurgical bonding (IMC) along with mechanical interlocking distributes the forces over a large area and shift fracture location.

Reza-E-Rabby et al. focused on a joint design in an Al/Fe couple, aiming to control the growth of IMC at the interface to enhance strength through metallurgical bonding [149]. Their study concluded that an IMC layer with controlled thickness at the interface of Al/Fe efficiently distributes the acting force over a larger area, thereby reducing stress concentration at localized points and increasing joint strength.

These findings underscore the critical importance of controlled IMC thickness in dissimilar alloy joints to achieve optimal joint strength and overall performance.

3.2.3. Mechanism of IMC formation

IMCs are an unavoidable outcome of Al/Mg welding [96]. However, their excessive presence is undesirable as it can lead to a deterioration in joint strength. To address this, a deeper understanding of the formation mechanism of IMC is crucial. The formation of IMC in Al/Mg FSW is influenced by factors such as process peak temperature, the relative concentration of Al and Mg, and strain rate [166].

One theory proposes that IMC are formed through constitutional liquation, where the concentration of Al and Mg atoms at a localized point on the Mg side reaches a suitable level, and the temperature exceeds the eutectic temperature, resulting in the formation of β phase [112,138,167]. Figure 27 (a) illustrates this proposed mechanism of IMC formation.

However, in cases like AZ31B and A5083 dissimilar welding, where the temperature did not reach the eutectic temperature, the formation of β and ɣ IMCs in the weld

was attributed to the react diffusion mechanism [77,101,159]. Chen et al. further demonstrated that the formation of β IMC is a strain rate-dependent phenomenon, even at temperatures below eutectic temperature [166]. They found that a strain rate of 10 s^{-1} led to increased dislocation density, promoting diffusion phenomena, and consequently, β IMC formation.

Rathod & Kutsuna provided a detailed description of the three stages involved in this diffusion-controlled mechanism [168]:

1) Formation of a supersaturated solid solution,
2) Transformation of the solid solution to IMC at a certain temperature and pressure,
3) Growth of the IMC layer due to continued diffusion of atoms.

These steps are visually presented in Figure 27 (b).

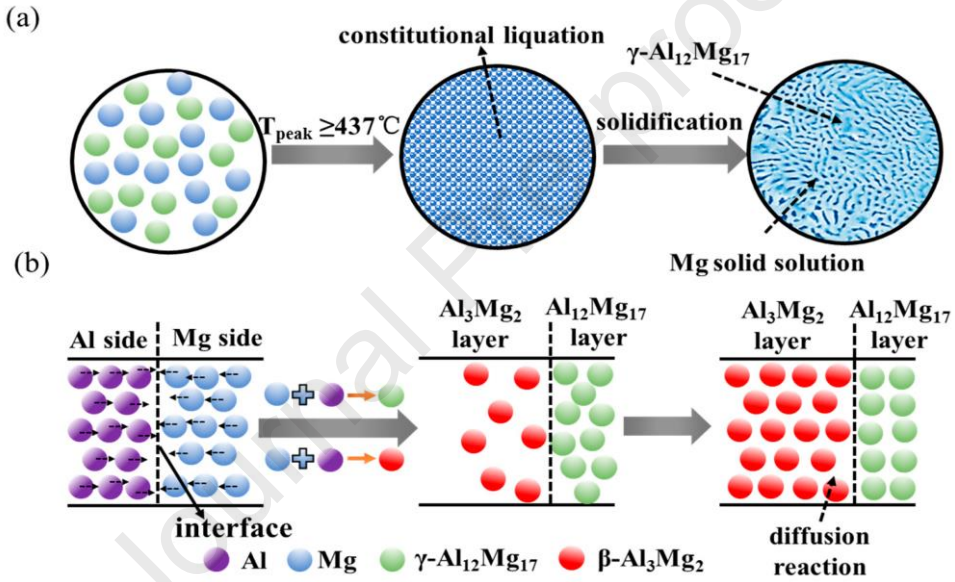

Figure 27: Schematic for IMC formation by (a) constitutional liquation or eutectic reaction (b) and react diffusion [84].

Both phenomena can coexist simultaneously in a single FSW joint, especially in thick sections, which can be attributed to the enhanced heat input at the top of the joint caused by the 'shoulder effect'. In Al/Mg FSW joints, the formation of IMC in thick sections shows a distinct pattern. ɣ phase is observed to form at the upper section of the Mg side of the weld through constitutional liquation, while both ɣ and β phases are formed at the lower section of the Mg side of the interface through the react diffusion mechanism [84].

3.2.4. Kinetics of IMC in Al-Mg Binary System

The IMC formation depends on the thermodynamics of IMC formation which in turn depends on the process peak temperature. For instance, in the Al/Cu system, the effective heat of formation (EHF) model was employed to evaluate a variety of AlCu IMCs across various temperatures [169]. Ji et al. observed only the presence of AlCu and Al_2Cu because the peak temperature in their process did not exceed 416.7 °C [161]. Eyvazian et al. also demonstrated the temperature-dependent variation of IMC layer thickness in the Fe/Al pair [160]. For the Al/Mg system, Chen et al. and Xu et al. calculated the Gibbs free energy of ɣ and β IMCs using the equations below [84,166].

$$H = U + \int Cp\, dT$$

$$G = H - TS$$

Here, *H* represents enthalpy, *U* stands for formation heat, C_p denotes heat capacity, *T* is absolute temperature, *G* symbolizes Gibbs free energy, and S represents entropy.

Their calculations showed that the *G* value of the ɣ phase is lower than that of the β phase for temperatures up to 500 °C (Figure 28). This finding was further supported by Huang et al. and Long et al., confirming the feasibility of ɣ phase formation over β phase [157,170]. Thus, it can be concluded that the formation of the ɣ phase is more favorable than the β phase.

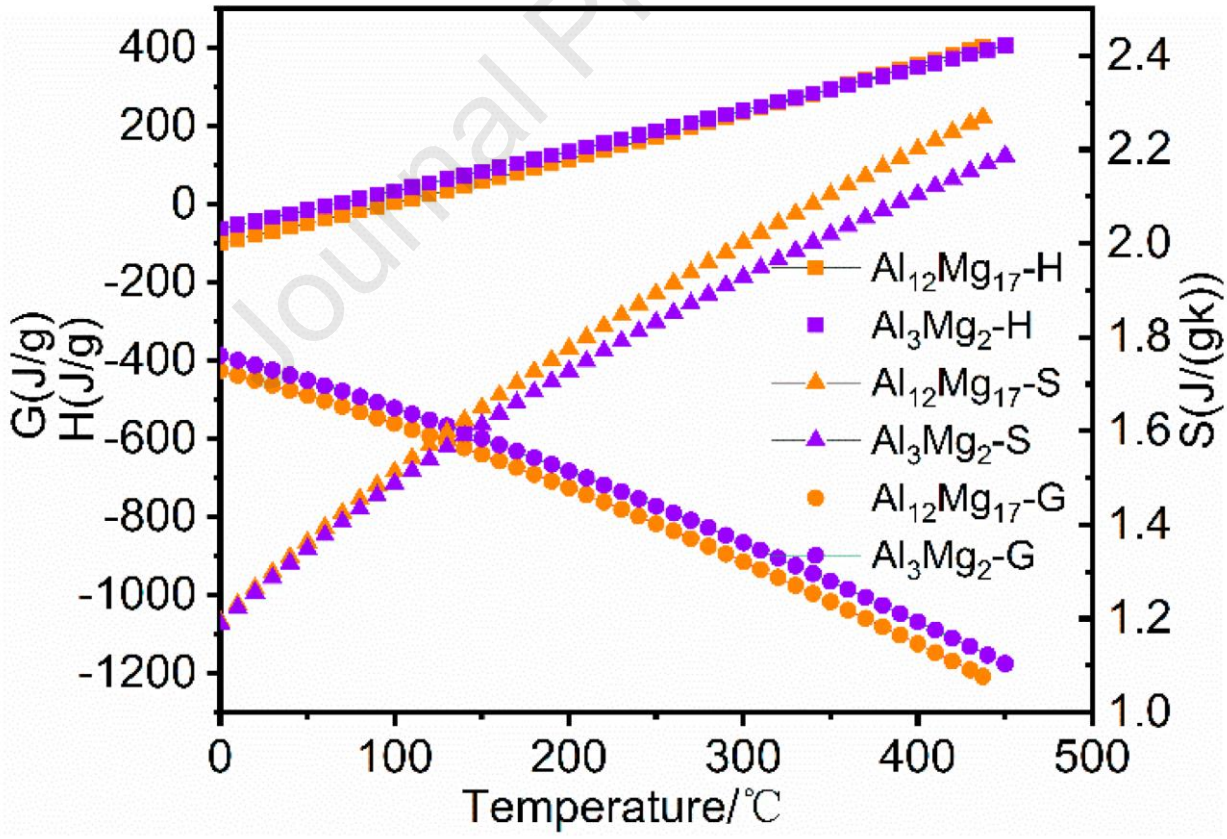

Figure 28: Gibbs free energy of $Al_{12}Mg_{17}$ & Al_3Mg_2 as a function of temperature [84].

After the IMC layer has formed, it proceeds to grow following the parabolic trend described by the equations [171].

$$d^2 = K.t$$

$$K = K_0\, e^{-\frac{Q}{RT}}$$

Where *d* = layer thickness, *K* = growth rate constant, *t* is heating time, K_0 is the pre-exponential factor, *Q* is the activation energy, *R* is Boltzmann's constant and *T* is the absolute temperature.

Studies have demonstrated that the β phase exhibits faster growth compared to the ɣ phase [77,84,159,163]. This rapid growth is believed to be temperature-independent due to the negligible temperature difference within the few micron width of the IMC layers. The dislocation density on both sides of the interface affects diffusion, consequently influencing the growth rate of intermetallic (IMC) layers. [159]. This dislocation density results from plastic deformation and impacts the diffusion coefficients of Al and Mg [84]. In contrast, the overall thickness of the IMC layer is influenced by temperature variations. For instance, during FSW, increasing the peak temperature from 259°C to 402°C led to an increase in the IMC layer thickness from 0.41 μm to 1.31 μm [101].

4. Enhancement of mechanical properties by improving the interface

4.1. Classification of Al/Mg joining interface

Having examined mechanical interlocking and IMC formation independently, it becomes essential to discuss the Al/Mg interface, which serves as the cornerstone of joint strength. By studying the joining mechanisms in FSW of dissimilar metals and alloys, it is evident that the strongest welds are achieved when the joint exhibits a complex interpenetrating morphology while simultaneously having thin IMC layers.

A thorough analysis of the literature on dissimilar alloys FSW, particularly Al/Mg, reveals that although Shah et al. [111] earlier categorized the bonding interface in three groups namely (i) distinct boundary, (ii) lamellar structure with distinct boundary, and (iii) complex lamellar structure with distinct boundary, the FSW interface can be classified into four distinct types [96,172]. These are:

Class I: The first class exhibits a distinct boundary in the weld joint (Figure 29 a). These joints feature a continuous layer of IMC at the interface, and weld failure occurs along this IMC layer.

Class II: The second type includes an additional 'interpenetrating feature' (IPF) alongside the delineation at the interface (Figure 29 b). The symmetrical IPF is believed to pin bimetals, enhancing the joint's strength by holding them firmly across the interface.

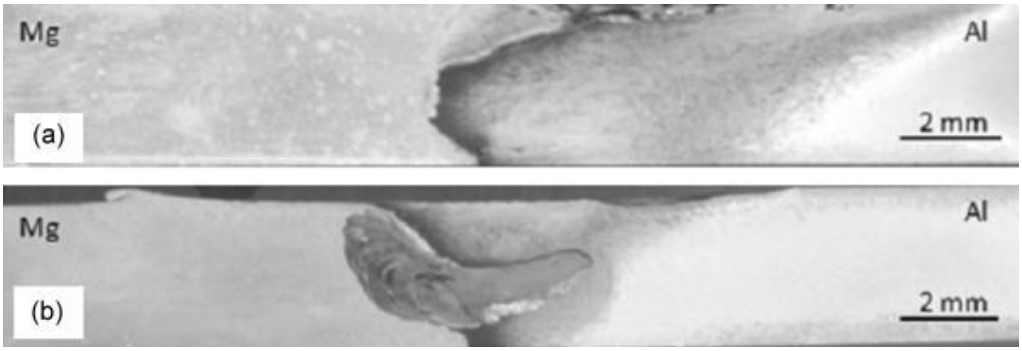

Figure 29: Class I (a) and Class II (b) interfaces [96].

Class III: The third type displays a distinctive lamellar structure, commonly referred to as a banded structure, at the interface (Figure 30). This interface demonstrates superior material mixing across the joint compared to Class I. The bands in this structure comprise alternating layers of Al and Mg, interspersed with IMC within these layers.

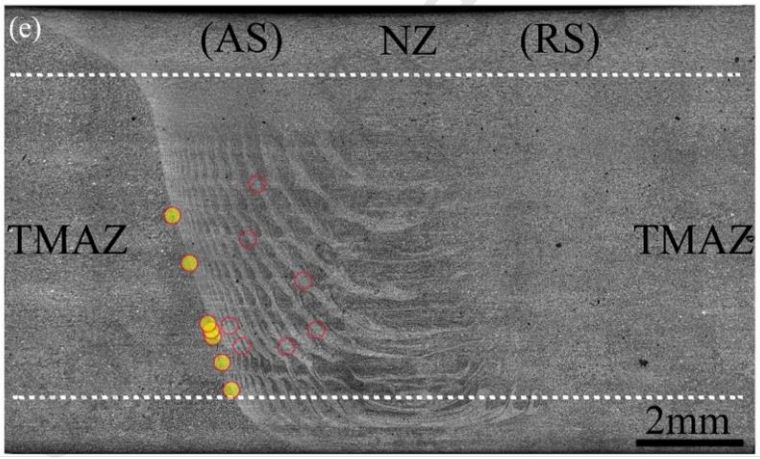

Figure 30: Depiction of class III interface with prominent banded structure [173]

Class IV: The fourth type has an interface that combines the characteristics of both Class II and Class III. This interface is highly desirable due to its extended and convoluted path, which effectively hinders the propagation of cracks, thus consequently retards the failure. The work of Fu et al. demonstrates this interface and is presented as an SEM image in Figure 31 (a). In this study, three distinct zones within the weld nugget have been identified. Firstly, the shoulder-affected zone (located just below the shoulder) involves material from the advancing side being carried away into the retreating side by the action of the rotating tool. Secondly, the banded zone, located in the upper and middle regions of the joint on the advancing side, exhibits alternating lamellae of Al and Mg, as indicated by the red and blue lines. Thirdly, the severe intercalated zone at the bottom is characterized by complex flow patterns, caused by vortex and swirls of Al and Mg, resulting from the use of a threaded pin (area bounded by the green line).

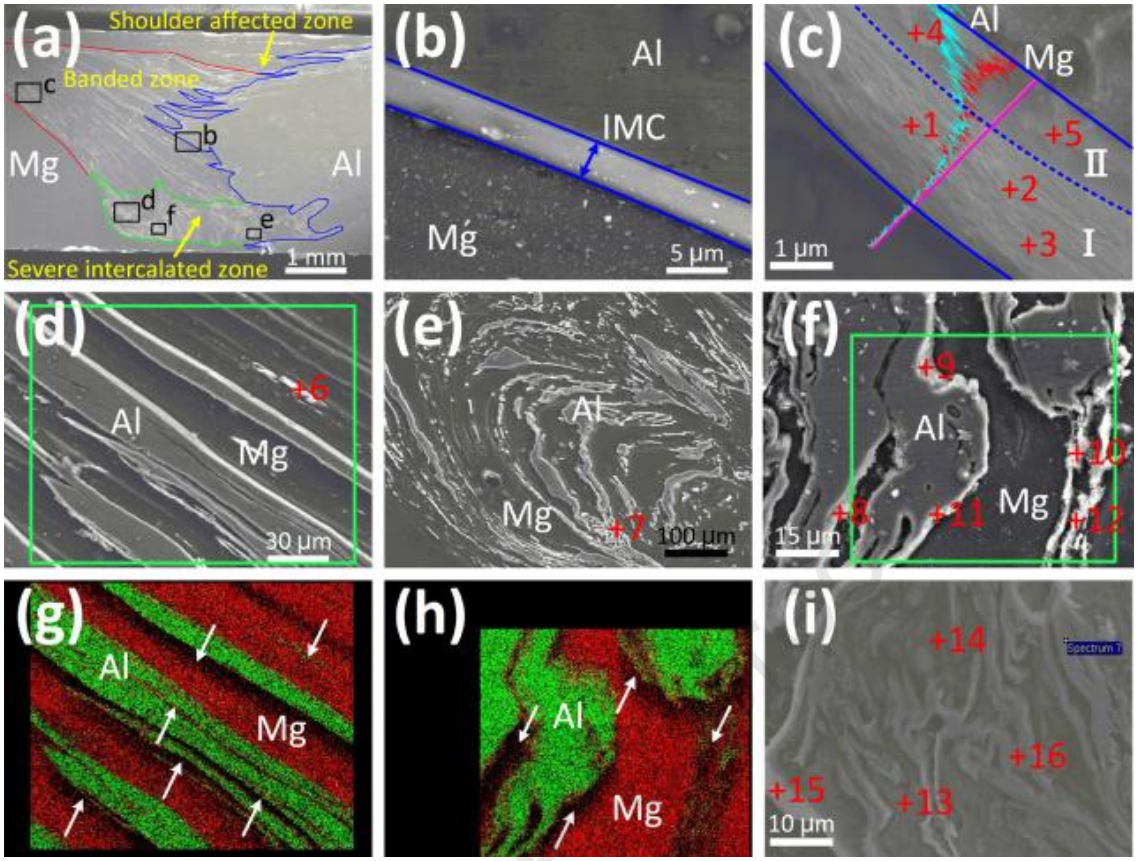

Figure 31: a) Features of Class IV joint in SEM image. Banded zone (Blue Boundary). Severe intercalated zone (Green Boundary). b-f) Magnified images of the regions marked in (a). g) EDS mapping of the region marked in (d). h) EDS mapping of the region marked in (f). i) magnified image of the severe intercalated region in (a) [75].

The importance of the Class IV joint can be better understood by taking a closer look at the work of Venkateswaran and Reynolds [96]. In their study, three primary parameters for the Class IV joint were defined: interface length (*l*), the thickness of the base metal (*t*), and the height of the interpenetrating feature (*h*) (Figure 32). It was found that a stronger joint can be achieved with larger values of $a = \frac{l}{t}$ and $b = \frac{h}{t}$. This is because larger values of '*a*' and '*b*' result in a longer interface length and a more challenging path for cracks to propagate, thus contributing to a stronger joint.

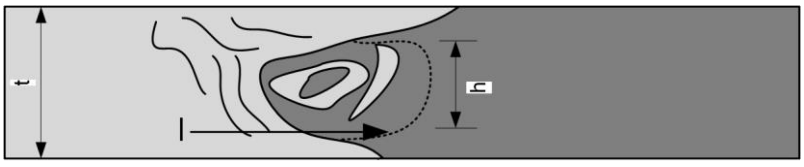

Figure 32: Class IV joint characteristic features.

4.2. Improving micro-mechanical interlocking

Better joint efficiencies in dissimilar alloy friction stir welds can be achieved by increasing mechanical interlocking. To improve mechanical mixing at the interface of butt joints, researchers have employed various strategies. This section primarily focuses on the aluminum-magnesium combination but also includes examples from other bimetals within the scope of either aluminum or magnesium to cover a wide range of domains. Moreover, the methods of enhancing mechanical interlocks at the interface have been thoroughly discussed. These methods enhance the values of the '*a*' and '*b*' parameters for Class IV joints (Section 4), leading to improved interlocking.

The application of ultrasonic waves has proven to be effective in enhancing mechanical bonding in dissimilar metals friction stir welds [78,109,174,175]. As depicted in Figure 33 b, the use of ultrasound energy results in improved interlocking, leading to increased interface length '*l*' and parameter '*a*' in Class IV interfaces.

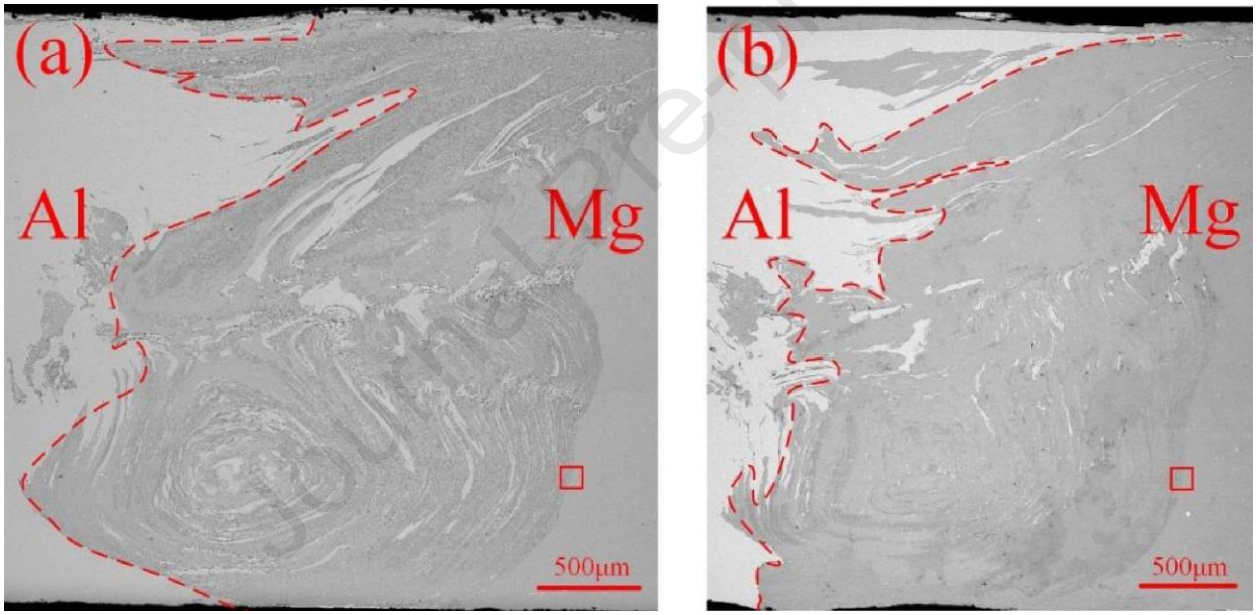

Figure 33: Effect of ultrasound energy on the mechanical interlocking at the Al/Mg interface [123].

To achieve better results, a combination of stationary shoulder and ultrasonic waves has been employed. This approach aims to lower the peak temperature by reducing the 'shoulder effect' while simultaneously enhancing mechanical interlocking through ultrasonic vibrations. Experimental studies have successfully demonstrated that this combined approach results in complex mechanical bonding in Al/Mg joints [123,176].

Increasing the *V* has also been found to be beneficial for enhancing mechanical interlocks. It has been proven that raising the *V* to an optimal level reduces the peak temperature and results in less pin adhesion, leading to increased complexity of intercalation at the interface [177]. An appropriate value of *V* can promote the optimum width of the nugget zone, resulting in improved mechanical properties. Figure 34c illustrates the optimum width of the banded zone (BZ) (2mm) at a constant ω of 800min^{-1} and *V* of 50 mm/min. These welding parameters provided the

maximum tensile strength, reaching 175 MPa, among all three travel speeds, owing to the optimized width of the banded zone [78]. This phenomenon arises due to increased material flow at lower travel speeds, while higher travel speeds constrain material movement. In this context, the optimal width of the BZ is attained at an intermediate travel speed.

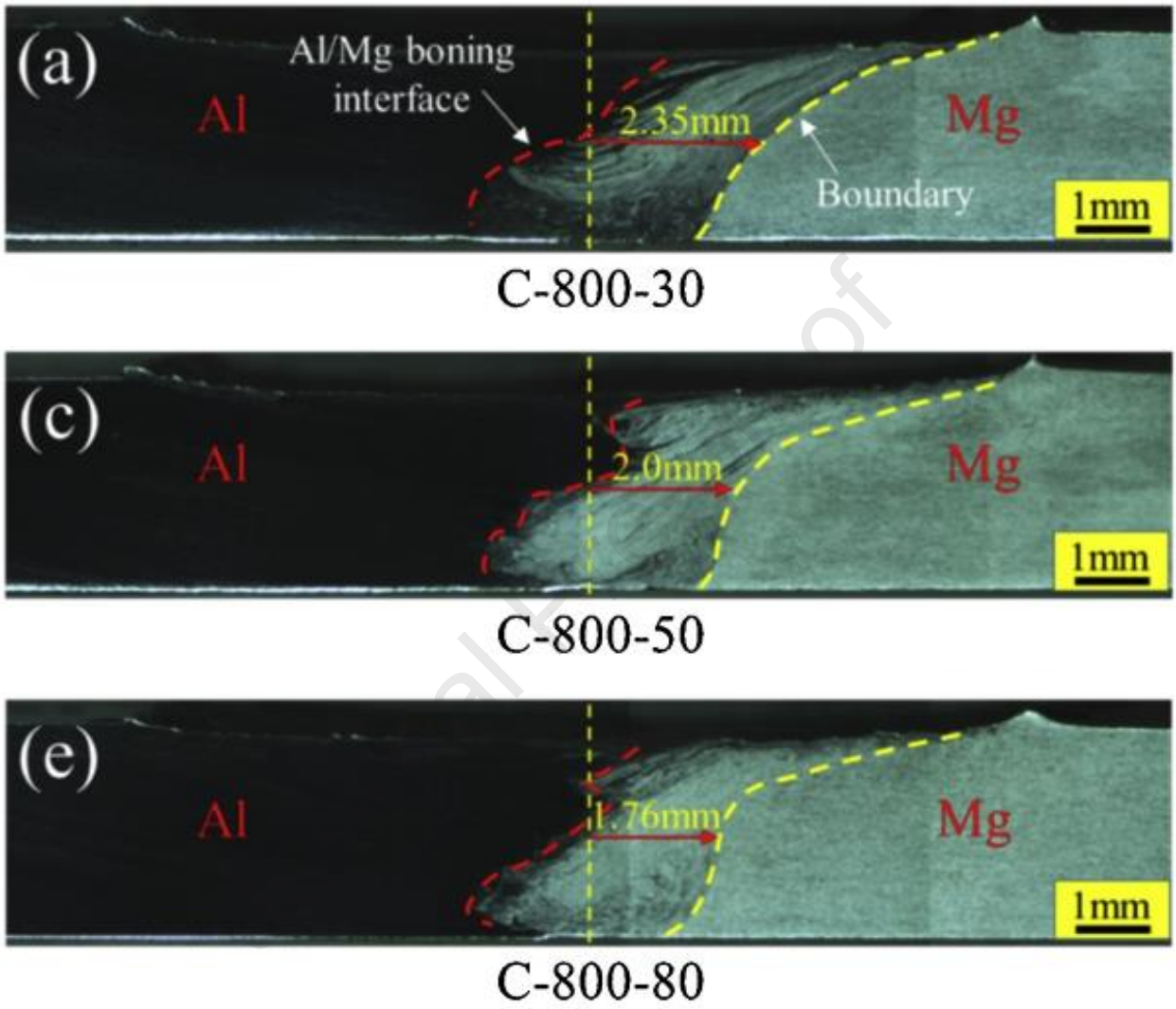

Figure 34: Effect of travel speed on AA6061/AZ31B dissimilar joint made at a constant tool rotation speed of 800 RPM. a) 30 mm/min c) 50 mm/min e) 80 mm/min [78].

Pulse current has been demonstrated to effectively enhance the interfacial mechanical bonding in Al/Mg FSW. In a study conducted by Xiaoqing et al., it was shown through experimentation that applying pulse current during FSW resulted in the formation of micro-interlocking at the interface (Figure 35). This micro interlocking significantly improved the mechanical properties of the joint [131]. This is credited to the increased material flow induced by pulse current.

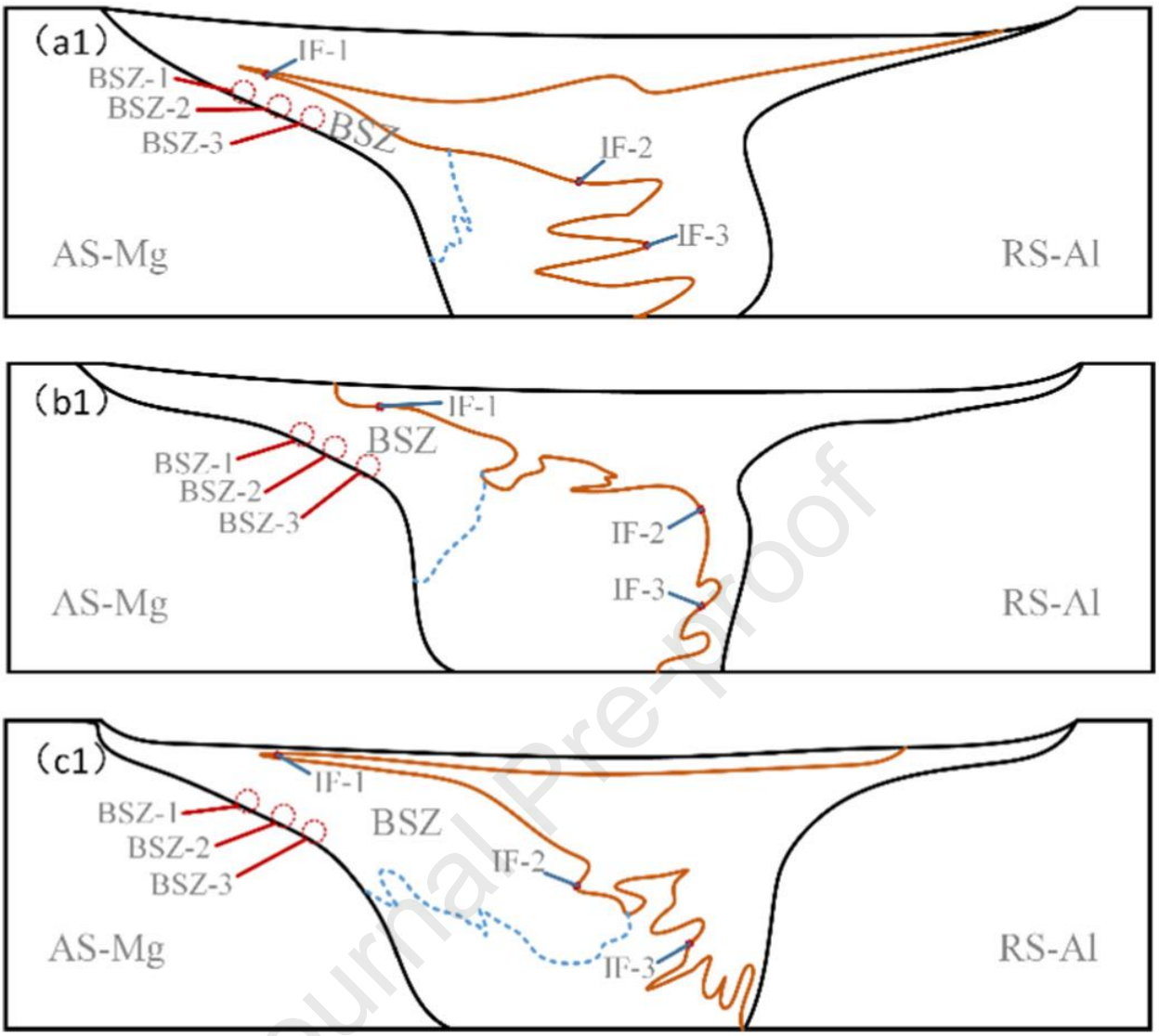

Figure 35: Effect of pulse current on the location and intricacy of Al/Mg interface. a1) 0A b1) 300A c1) 500A [131].

Tool offset is a significant factor affecting mechanical mixing in the FSW joint. In an experimental study involving Al/Cu FSW, researchers observed that the highest tensile strength was achieved with a tool offset of 1.2 mm towards aluminum. This offset facilitated excellent intermixing at the interface, as depicted in Figure 36 (c). However, when the offset was further increased to 1.6 mm, the extent of uniform material mixing at the interface decreased, leading to a reduction in tensile strength [178].

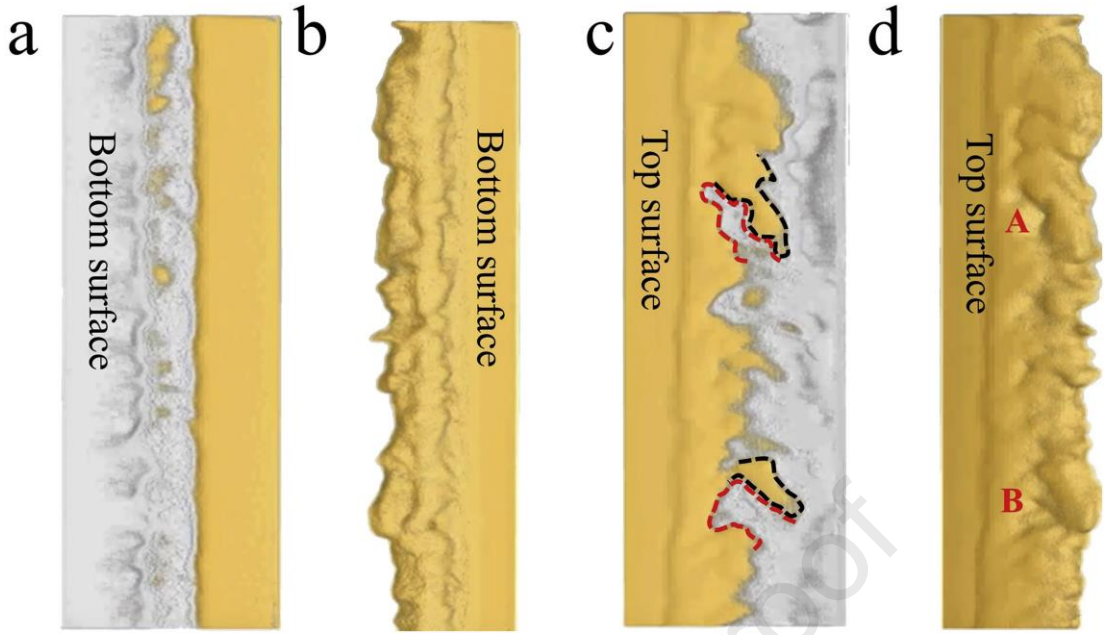

Figure 36: Radiography images of Al/Cu joint from different locations with tool offset of 1.2 mm [178].

A second pass in double pass FSW has proven to be effective in enhancing the mechanical bond between dissimilar alloys. Chen et al. demonstrated that applying a second pass in the opposite direction improved mechanical interlocking, as shown in Figure 37. This improvement is attributed to better vertical flow achieved by reversing the direction [179].

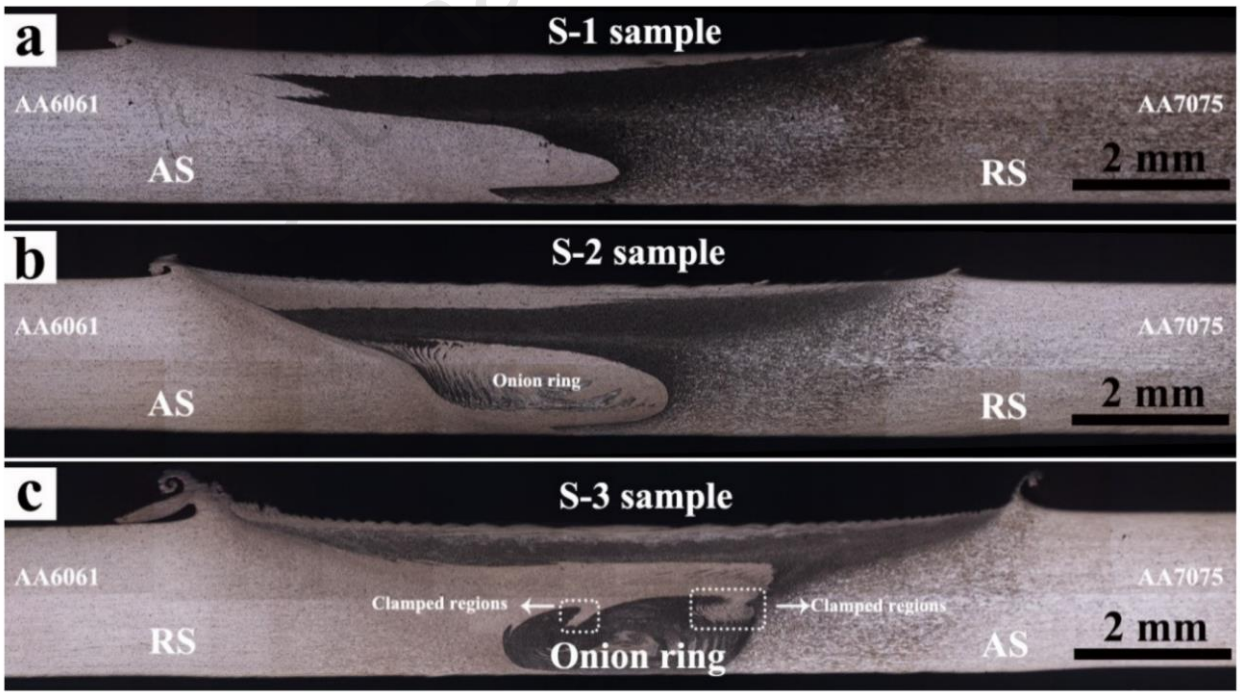

Figure 37: Improved mechanical interlocking. a) Single Pass FSW b) Double pass with 2nd pass in the same direction c) Double pass with 2nd pass in opposite direction [179].

Some researchers have investigated the use of interlayers and their potential positive effects in creating mechanical interlocks. Notably, FSW experiments involving dissimilar Al 7075 and Mg AZ31 alloys in butt configuration with a cadmium (Cd) interlayer demonstrated that the presence of Cd significantly improved interlocking [180]. In friction stir lap welding (FSLW), hooks are formed at the Al/Mg interface on both the AS and RS [181]. Al/Mg FSLW can be characterized by two parameters: effective sheet thickness (EST) and effective lap width (ELW), in the presence of a hook defect [182]. The former is defined as the smallest distance between the hook's crack tip and the joint's upper surface, while the latter is the horizontal separation between the AS and RS hooks' crack tips. Higher EST and ELW values promote stronger joints by providing increased contact at the Al/Mg interface. Niu et al. have reported enhanced EST and ELW, which they attribute to the presence of a Zn interlayer (Figure 38) [183]. In specific cases, molten Zn (419 °C melting point) can infiltrate the cold laps at the Al/Mg interface, aiding in their elimination. Ji et al. found that incorporating a zinc interlayer and using ultrasound energy in dissimilar Al/Mg joints enlarged the ELW, improving tensile shear load significantly. Conventional joints had the smallest ELW due to a large cold lap. This combined approach enhances joint performance in FSLW [184].

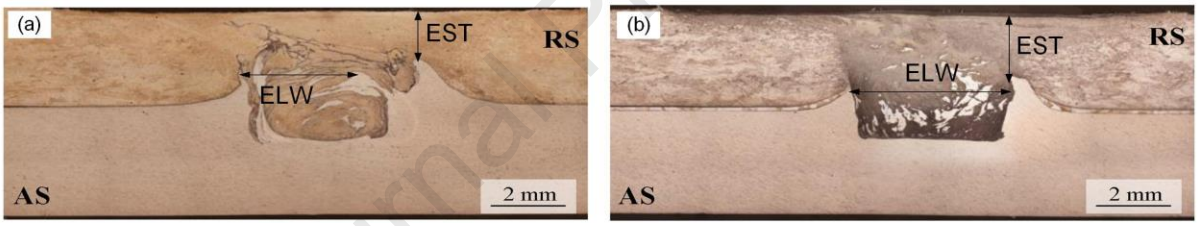

Figure 38: Effect of Zn interlayer in enhancing mechanical interlocking through increased EST and ELW [183].

Another approach to enhance mechanical interlocking in FSW is through innovative butt joint design. Xu et al. devised a serrated interlocked joint and conducted FSW, as shown in Figure 39. The study concluded that this design led to superior mechanical locking at the interface (Figure 39 d), resulting in a threefold increase in tensile strength compared to a conventional butt joint [133].

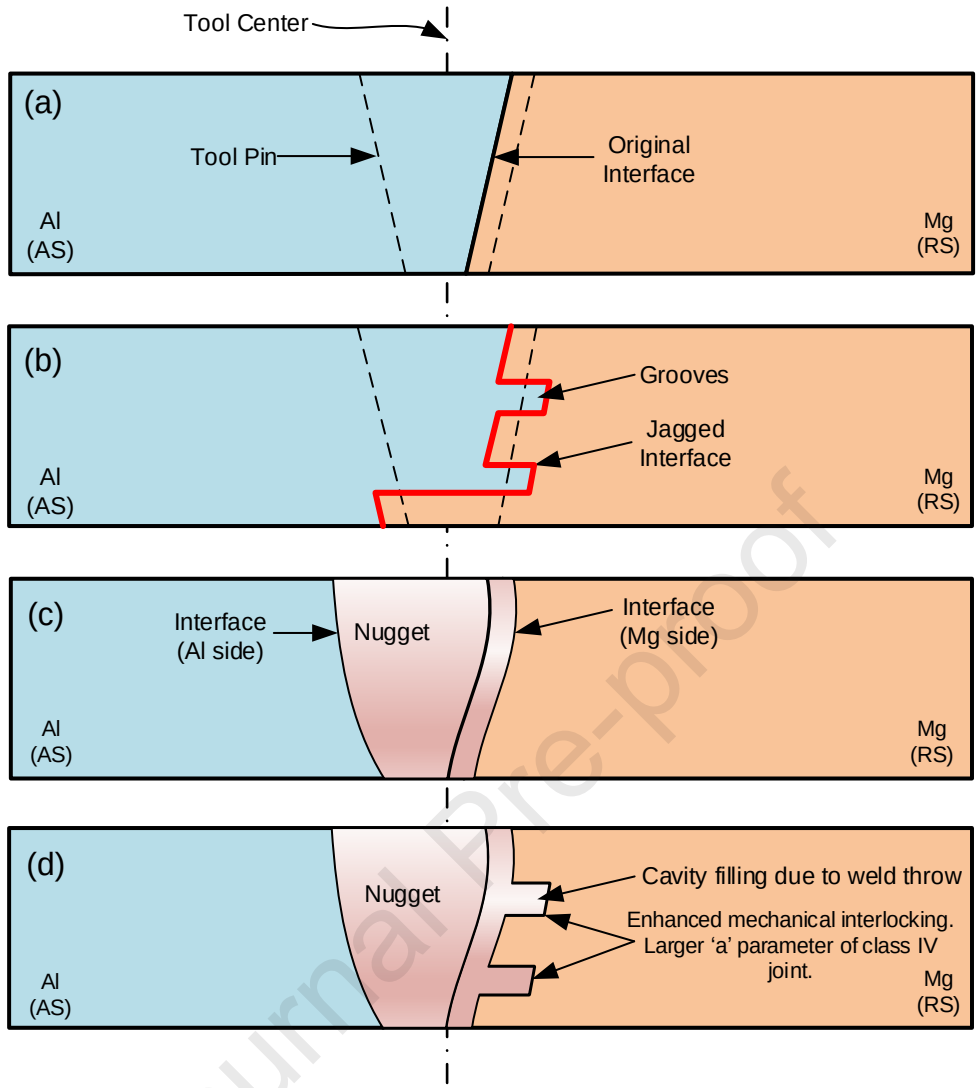

Figure 39: (a) Conventional butt joint, (b) Innovative butt joint with serrations to improve mechanical interlocking, (c) Weldment structure in conventional joint, (d) Weldment structure in innovative joint.

The utilization of external cooling media to reduce the peak process temperature has been found to improve interlocking. In a specific experimental study, submerged friction stir welding (SFSW) was employed for the Al6061/AZ31B pair, resulting in an enhanced tensile strength of 171 MPa compared to conventional FSW. This improvement was attributed to the superior mechanical interlocking achieved using SFSW [157].

In summary, the factors that contribute to enhancing mechanical interlocking in FSW include lowering peak temperature, the use of ultrasonic waves, application of pulse current, optimum travel speed, and improved joint design. Additionally, for specific combinations like Al/Cu and AA6061/AA7075, tool offset, and double pass have shown positive effects on mechanical interlocks. However, their impact on the Al/Mg interface interlocks presents an area with significant research potential. Further investigations in this direction could yield valuable insights and advancements in Al/Mg FSW.

4.3. Mitigating intermetallic compounds

Based on the current findings, the preference for a stronger FSW dissimilar joint is given to the class IV interface. In Al/Mg FSW, joint properties are significantly influenced by the volume fraction and morphology of IMC [185]. The methods to enhance mechanical interlocking at the interface have been discussed in section 4.2. Now, the retardation of IMC will be explored. IMC formation is believed to be a eutectic or react diffusion-based phenomenon, both of which can be impeded by reducing the process temperature. In essence, the reduction of process temperature can effectively decrease IMC formation and growth. Additionally, techniques such as pulse current or the use of ultrasound vibration have been found to thin, disintegrate, or even completely diminish the presence of IMC. A more detailed examination of these control phenomena will be undertaken in the following paragraphs of this section.

4.3.1. Lowering peak temperature

The mechanism of IMC formation, whether eutectic or react diffusion, can be hampered by reducing the process temperature, as discussed in section 3.2.4. Various strategies have been employed to achieve lower FSW process temperatures, including the selection of appropriate parameters, changes in tool technology, and the utilization of external cooling media such as air, water, and liquid nitrogen.

4.3.1.1. Parameters

The peak temperature and IMC layer thickness at the Al/Mg interface are influenced by the ω. Fu et al. demonstrated that varying ω from 400 to 1000 rpm resulted in a 3.25-fold increase in IMC layer thickness [101]. The placement of materials on the AS or RS also impacts heat input. Firouzdor and Kou's experiments with Al/Mg showed that placing Mg on the advancing side reduces the heat input, leading to a considerable reduction in IMC content within the joint [122]. This is due to the lower coefficient of friction between the tool and magnesium.

In FSW, the rotating shoulder and metal interface generate the maximum heat, creating a thermal gradient across the workpiece thickness [48]. To mitigate this, stationary shoulder friction stir welding (SSFSW) has been introduced, which reduces heat input from the tool's shoulder. Stationary shoulder FSW has been reported to improve surface finish, and fatigue properties, reduce pin adhesion, and decrease IMC layer thickness [186].

4.3.1.2. External cooling media

To reduce the peak temperature and decelerate the growth of IMC during Al/Mg FSW, several FSW variants employing various cooling media have been developed.

Two notable approaches are submerged friction stir welding (SFSW) and cooling-assisted friction stir welding (CFSW). In submerged friction stir welding (SFSW), the joint is submerged in different cooling media like water or liquid nitrogen. This helps in lowering the peak temperature during the welding process and thus retards the growth of IMC. On the other hand, cooling-assisted friction stir welding (CFSW) involves the use of cooling media to cool the joint behind the tool. This method also helps in reducing the peak temperature of weldment and slows down the growth of IMC. Both SFSW and CFSW have shown promising results in improving joint quality and reducing the formation of IMC in Al/Mg FSW.

In an experimental study using SFSW on the AA5083/AZ31, FSW was conducted at 400 rpm and 50 mm/min, while three different cooling media were employed: air, water, and liquid nitrogen. Among these, the sample cooled with liquid nitrogen exhibited the lowest peak temperature compared to the other environments. The recorded peak temperatures were 435°C in air, 389°C in water, and 382°C in liquid nitrogen. Samples welded in air showed the presence of three types of IMC: β, ɣ, and Al_2Mg_3, with micro-cracks observed in the IMC layers on the Al side of the joint. However, when either water or liquid nitrogen was used as the cooling media during welding, the volume fraction of the IMC was significantly reduced, and no cracks were observed. This improvement was attributed to the higher cooling rate and lower process temperature achieved with the cooling media [167]. Similarly, in another study involving AA6061/AZ31B, water was used as the cooling media, resulting in a reduction of IMC and an improvement in ultimate tensile strength [157]. In a different CFSW study involving the AA6061/AZ31B pair, a water-cooling nozzle was positioned 15 mm behind and at a specific angle from the FSW tool, with a water flow rate of 15 ml/min. The results demonstrated a significant reduction in the IMC content in the joint. As a result, the tensile strength of the CFSW joint improved by 42% compared to the conventional FSW joint [187].

These findings highlight the effectiveness of using cooling media during SFSW and CFSW to control the formation of IMC and enhance the overall strength of the welded joints.

4.4. Thinning or breaking continuous IMC layer

To achieve an effective cementing effect, it is crucial to carefully control the generation, growth, and form of IMCs. Recently, research to manipulate IMCs using ultrasonic vibration and pulse current is in trend.

Ultrasonic energy lowers the flow stress and viscosity of the material [188]. Ultrasonic waves have been applied in different configurations i.e., horn attached to one of the base metals [176], transducer assembled axially with tool [189], ahead of the tool directly on base metal via sonotrode [129] and exerted horizontally on the tool through horn [135]. This is graphically presented in Figure 40.

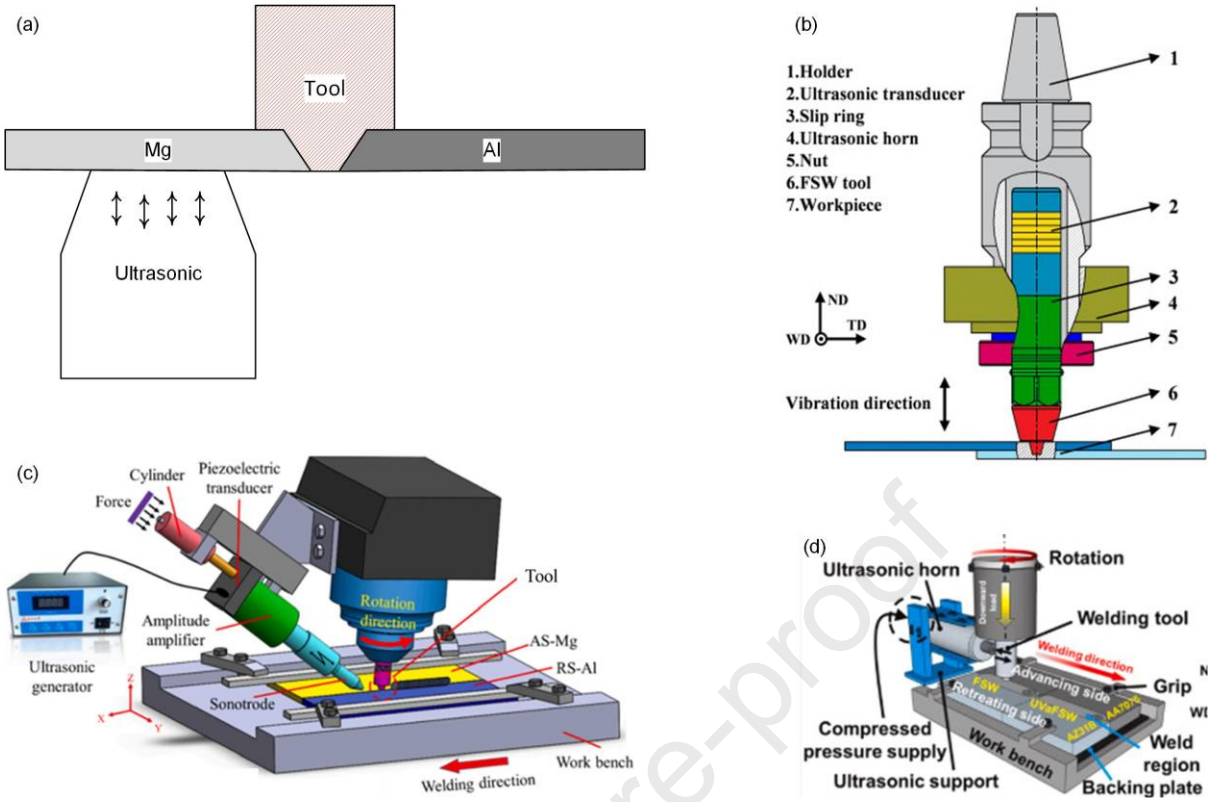

Figure 40: Different configurations to apply ultrasound vibrations in FSW. (a) Horn attached to a base metal, (b) Transducer axially attached to the tool [189], (c) Sonotrode ahead of the tool [129], and (d) Horn attached horizontally to the tool [135].

Ultrasonic vibrations have been reported to affect the IMC in the Al/Mg FSW combination in three ways.

1) Thinning of IMC layer
2) Disintegration of IMC layer
3) Annihilation of IMC

But one thing should be considered, only an optimum value of energy is beneficial to cope with IMC. Too low or too high energy is not beneficial to impede IMC. All these effects are discussed to give a bit deeper reference to the reader.

4.4.1. Ultrasonic assisted thinning

Ultrasonic vibration has been found to effectively thin the IMC layer at the Al/Mg interface. Through ultrasonic vibration-enhanced friction stir welding (UVeFSW), the application of ultrasonic energy has shown a significant reduction in the thickness of the IMC layer [78,109,126,159,175,190], as illustrated in SEM images in Figure 41. In this context, *S* and *T* represent the same locations, with *S* depicting the condition without ultrasonic application, and *T* representing the condition with ultrasonic energy applied. The comparison reveals that at locations 1, 2, 3, and 4, the thickness of the IMC layer decreases by 27%, 60%, 22%, and 58%, respectively. This confirms

the efficacy of ultrasonic vibration in thinning the IMC layer at the Al/Mg interface during FSW. Ultrasonic vibrations have been documented to stimulate the formation of high-angle grain boundaries (HAGB) through the motion and absorption of dislocations [191]. This, in turn, decreases diffusion rates near the interface, resulting in reduced IMC content.

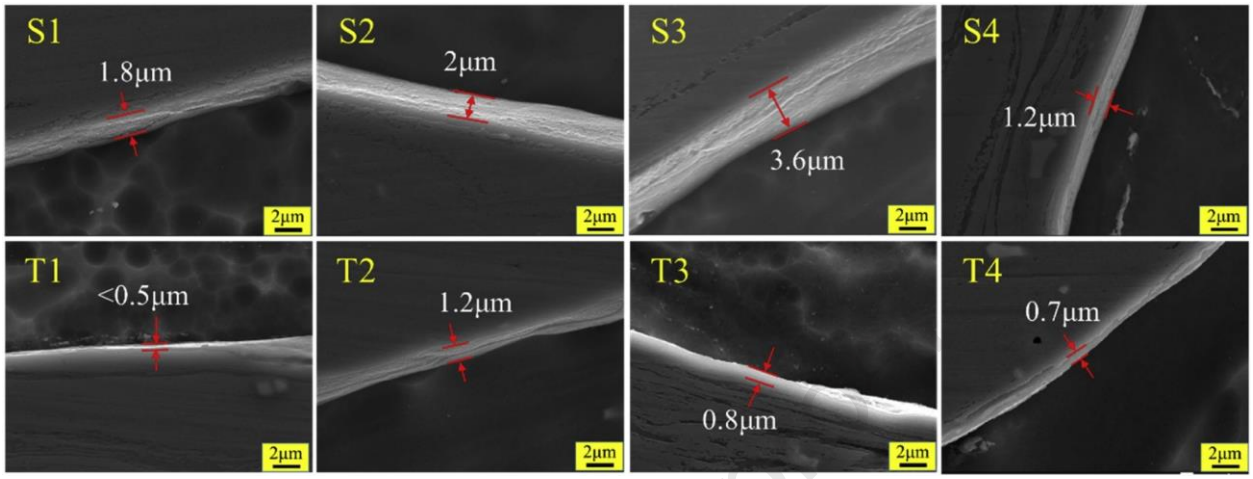

Figure 41: SEM images showing the effect of ultrasonic energy on IMC layer thickness at the Al/Mg interface. S & T correspond to the same location; S is without ultrasonic assistance while T is with ultrasound assistance [78].

4.4.2. Ultrasonic disintegration

The use of ultrasound energy in FSW has the potential to break the continuous layer of IMC into smaller fragments, thereby reducing their negative impact on mechanical properties. The disintegration of the IMC layer leads to a diminished continuous path for crack propagation [174]. Liu et al., in their research, demonstrated that introducing ultrasonic vibrations at 1400 watts fractured the long IMC layer into smaller pieces at the advancing side of the interface. This alteration forced the crack to take a longer path along the interface during the tensile test, resulting in an improved tensile strength of 17 MPa (Figure 42) [123]. The disintegration phenomenon has been further supported by the work of Bai et al., who demonstrated that the disintegration of IMC occurs not only at the interface between aluminum and magnesium (Al/Mg) but also within the magnesium matrix (Figure 43 c, d) [192]. This disintegration is ascribed to the synergistic impact of severe plastic deformation inherent in FSW, along with ultrasonic energy. Although IMC nucleation occurs at multiple sites, the absence of diffusion pathways hinders its growth in the continuous films, resulting in a disintegrated appearance.

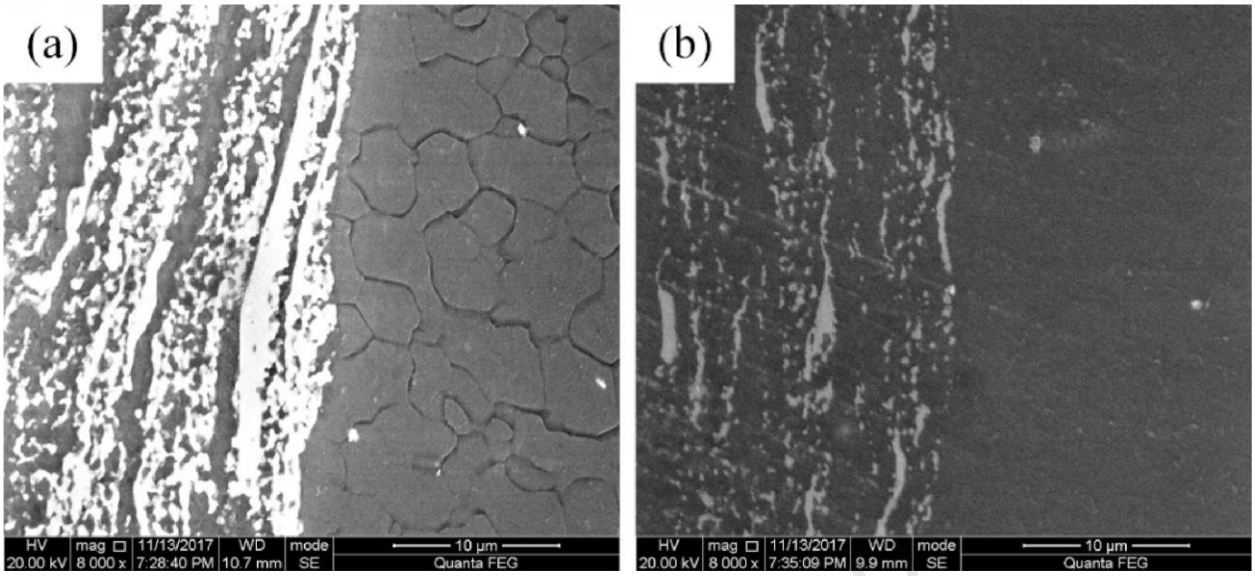

Figure 42: SEM image of disintegrated IMC layer due to acoustic effects at Al/Mg interface [123].

4.4.3. Ultrasonic annihilation

Ultrasonic vibrations (UV) are also effective in eliminating certain IMCs at the Al/Mg interface. Research has demonstrated that by applying UV during Al/Mg FSW, the β phase was entirely eradicated [174]. This effect is evident in Figure 43 (b), where the application of ultrasound energy has diminished the β layer at the Al/Mg interface. This phenomenon is credited to the combined influence of tool rotation and ultrasonic vibrations, causing material from the Mg side to migrate towards the Al side (the retreating side in this instance). This process triggers β phase formation at the Al interface, rather than the ɣ phase on the Mg side [192].

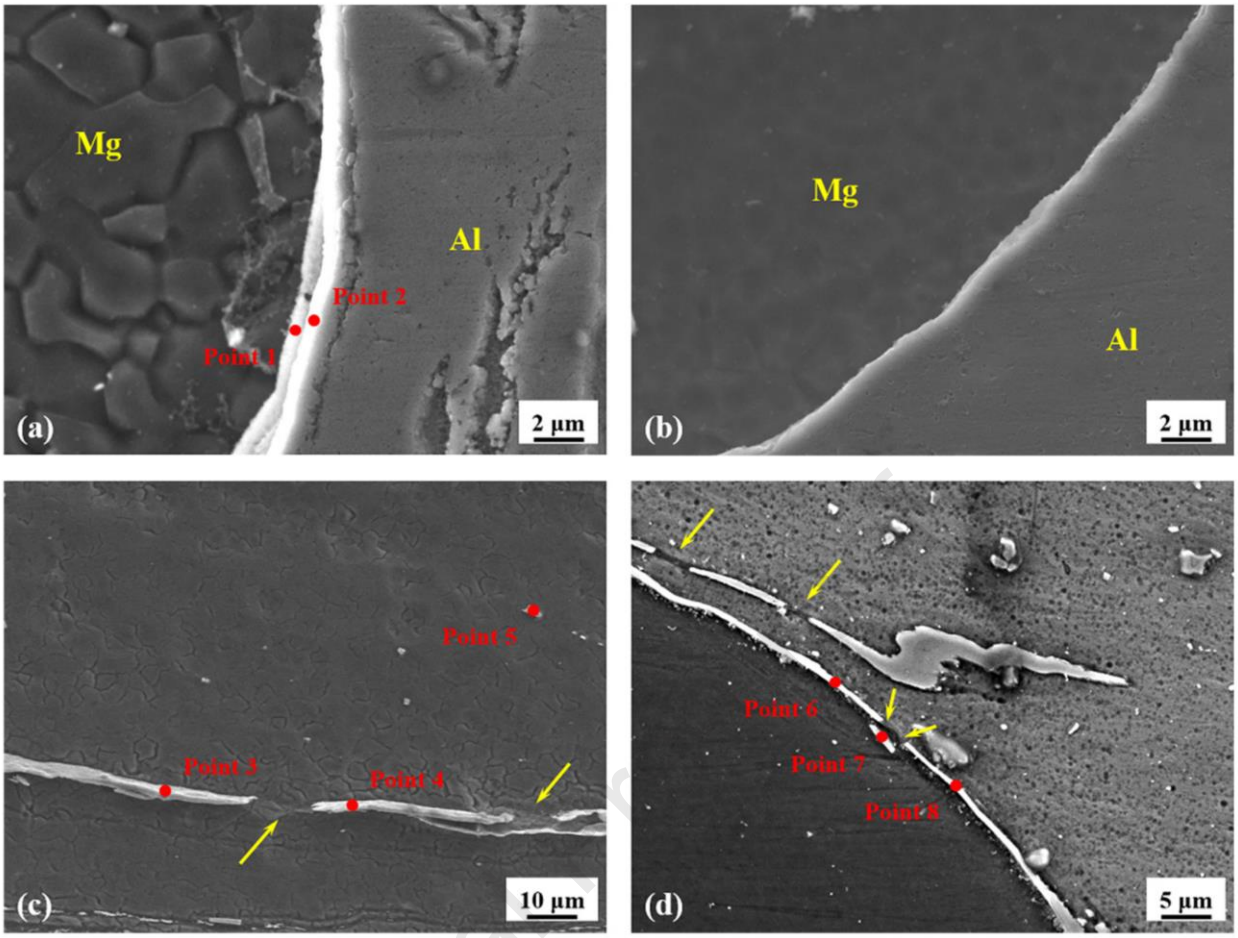

Figure 43: a) Al/Mg interface showing dual layers of IMC at 800 rpm and 50 mm/min, b) diminishing of one layer of IMC due to ultrasonic vibrations (UV), c) discontinued IMC in Mg matrix due to UV, d) discontinued IMC at Al/Mg interface due to UV [192].

The positive impact of ultrasonic energy on Al/Mg FSW suggests that higher UV energy could be advantageous for weldments. However, experiments with different UV powers (ranging from 75 W to 500 W) have revealed that only moderate power levels offer the greatest improvement in mechanical properties [193]. This indicates that there exists an optimal range of UV energy for achieving the best results in dissimilar FSW joints. This could potentially stem from the resurgence of dislocation activity at higher UV powers beyond the optimal threshold.

4.4.4. Effect of pulse current

A variation of FSW known as electrical current-aided FSW (EA-FSW) uses friction and electrical resistance to produce heat that is necessary for the process. With the extra resistance heating, less force is needed by the FSW machine, allowing for higher *V*. For metals that are hard (steel) or have a higher thermal conductivity (Al, Mg), EA-FSW is extremely effective. Both alternating current (AC) and direct current (DC) can be employed for resistance heating. However, for more precise and controlled heating, a pulsating DC power supply is often utilized [194]. This method

has also been explored for dissimilar polymer/metal FSW [51]. For Al/Mg EA-FSW, the use of pulse current has been reported to yield satisfactory properties.

Pulse current has emerged as a promising method to strengthen polycrystalline multiphase alloys [195]. Pulse current assisted FSW has gained attention for its ability to reduce the thickness and quantity of IMC while improving tensile strength. Notably, when applied in the range of 0-400 A during FSW of AZ31B Mg alloy, pulse current significantly enhanced the joint's tensile strength and shifted the crack path from the nugget zone to the heat-affected zone [196]. In their experimental study, Xiaoqing et al. used three levels of pulsed current (0 A, 300 A, and 500 A) [131]. At 300 A, the IMC transformed from a cloud-shaped morphology (Figure 44 a-c) to a micro-interlocking pattern (Figure 44 d-f). Further increasing the current to 500 A resulted in a sandwich structure of Al-IMC-Mg with an almost negligible thickness of the IMC layer, leading to the formation of the strongest joint (Figure 44 g-i).

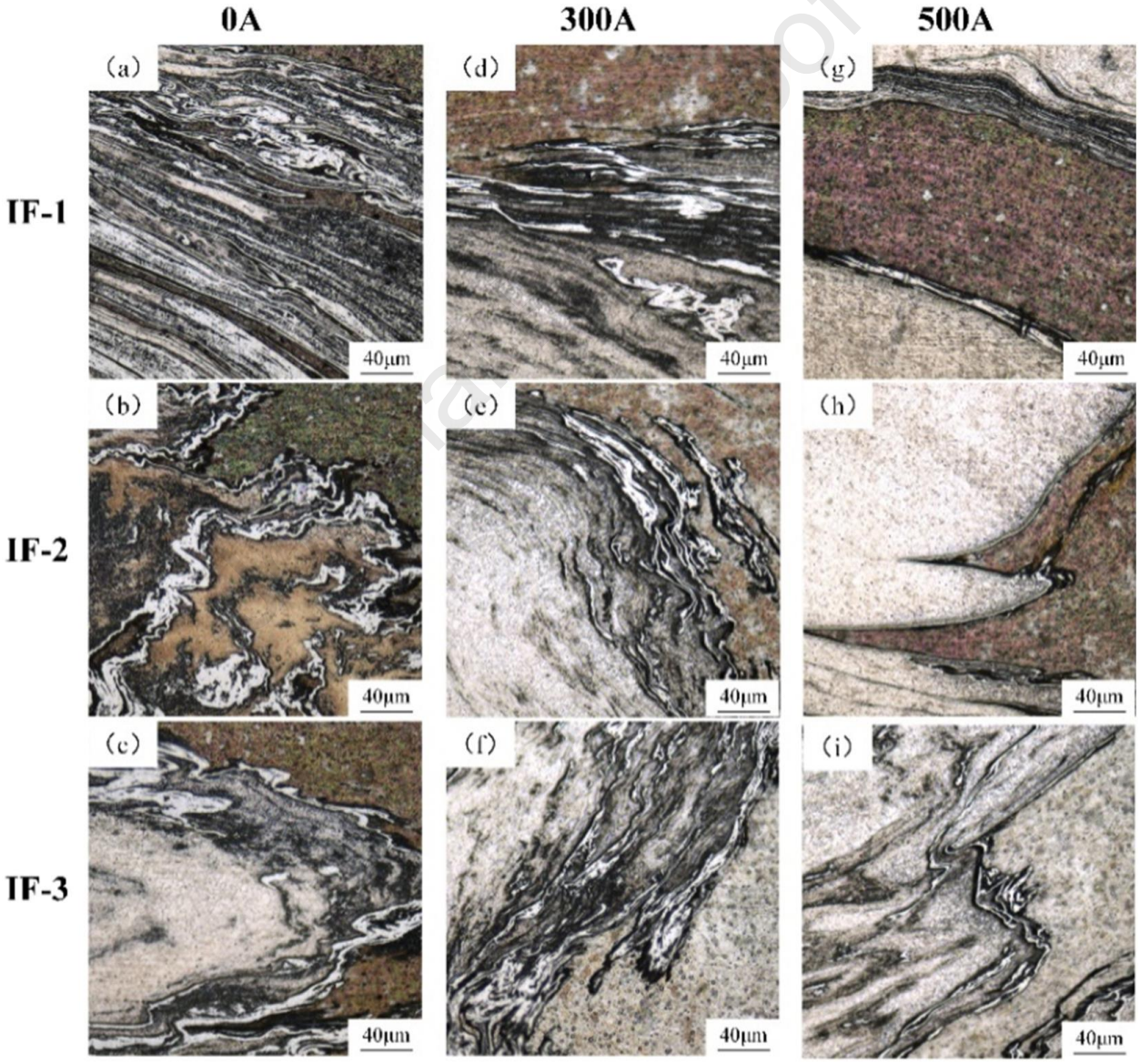

Figure 44: Effect of pulse current on IMC at different locations of Al/Mg interface (IF) [131].

As the pulse current increased, a well-defined vortex shape became apparent. This indicated that, under the influence of the pulse current's electroplastic effect, most materials in the SZ flowed in alignment with the pin's rotational direction. When the high-speed rotation of the pin is combined with a pulse current, the fluidity of the material surrounding the pin is enhanced. Consequently, this synergistic effect promotes a more rapid and thorough process of dynamic recrystallization which refines the grains in the stir zone and forces the fracture outside the stir zone [196].

4.4.5. Use of interlayer/additives

Another approach for controlling the IMC formation at the interface of dissimilar Al-Mg FSW is the use of interlayer/additives. Interlayers or additives in dissimilar FSW are used to serve one of the following purposes:

1. Acting as a diffusion barrier to slow down the growth of IMC.
2. Reducing the volume fraction of detrimental IMC by promoting the formation of thermodynamically and mechanically favorable IMC.
3. Specifically in the case of Al/Mg combinations, preventing the formation of brittle IMCs.

The following discussion will encompass all these scenarios.

To investigate the impact of the Zn additive on IMC at the Al/Mg interface, the Gibbs free energy (G) values of various possible compounds were calculated. The results revealed that $MgZn_2$ exhibited the lowest '*G*' value among all the considered compounds. This finding was further confirmed through experimental validation. Additionally, it was concluded that the addition of a Zn interlayer and the subsequent formation of $MgZn_2$ contributed to a reduction in the presence of β and ɣ compounds to some extent [166]. Al-Zn and Mg-Zn solid solutions have also been reported to replace the IMC and corresponding 1.27 times improvement in tensile strength [185]. Subsequent experiments conducted with friction stir clinch-brazing utilizing a Zn interlayer demonstrated that the introduction of Zn effectively inhibited the formation of the β layer. However, it was observed that the formation of the γ phase could not be prevented despite the presence of the Zn interlayer [197]. It's worth noting that while Mg-Zn IMCs are also reported as hard and brittle (but to a lesser extent as compared to β and ɣ IMCs), it is their dispersion that plays a crucial role in enhancing joint strength. Furthermore, Zn melting at optimized parameters favored the elimination of void and tunnel defects [117].

In another attempt to mitigate the formation and detrimental effects of IMC in welds, an Al-Si clad sheet was employed based on thermodynamic calculations. It was determined that among the expected IMC in the Al-Mg-Si ternary system, Mg_2Si had the lowest energy of formation. The utilization of Mg_2Si was expected to enhance joint strength by reducing the presence of its counterparts, the β and γ phases, owing to its higher melting point and Young's modulus. Experimental results confirmed that the incorporation of the Al-Si interlayer impeded the growth of the β phase. Furthermore, the fracture energy of the joint was significantly improved, reaching 97% of that observed in Mg-Mg welds [198].

The introduction of Cd as an additive facilitated the formation of CdMg and $CdMg_3$ compounds. The presence of a thin layer (1μm) of β IMC and fragments of γ IMC, which have been demonstrated to contribute to the improved tensile strength of 129

MPa in FSW between Al 7075 and Mg AZ31, were attributed to the Cd interlayer [180].

Moreover, the utilization of nickel (Ni) as an interlayer resulted in the complete elimination of the β and γ phases. The formation of new phases, namely Al_3Ni and Mg_2Ni, in the joint has been linked to the occurrence of dual-mode fracture, exhibiting both brittle and ductile characteristics. Similar fracture behavior has also been observed when tin (Sn) is employed as an interlayer [199]. In a separate study examining the impact of varying nickel (Ni) interlayer thicknesses, it was observed that Mg_2Ni partially replaced the β phase. The analysis revealed that the optimal outcome, featuring a 13.5% improvement in tensile strength, was achieved with a Ni interlayer thickness of 0.3 mm. This improvement was attributed to the formation of a densely packed nugget structure consisting of magnesium (Mg), aluminum (Al), IMC, and nickel particles [200].

For a deeper understanding of selecting interlayers to mitigate IMC formation in Al/Mg welding, Shah et al. have presented instructive recommendations. Their study outlines a three-step approach to ~~effectively address~~ guide interlayer selection ~~IMC formation~~ [201]. Following these guidelines is highly advisable when designing interlayer-based strategies for IMC mitigation.

4.4.6. Joint design

The growth of IMC has been reported to be hindered by modifying the joint configuration in a way that limits certain sections of the joint from experiencing high temperatures and large strain rates. In a unique and innovative approach, the joint design has been altered to minimize the formation of IMC. By utilizing a serrated joint configuration — where dissimilar Al/Mg alloys with a thickness of 15 mm are joined, with aluminum positioned on the advancing side and the tool offset towards the aluminum — the thickness of the IMC layer has been reduced from 60 μm in a conventional butt joint to 10 μm. This is attributed to the lower peak temperature at the region marked by dotted rectangles in Figure 45, which is 2.6 mm farther than the conventional joint design and observed 2.4 times less strain rate for the serrated joint [133].

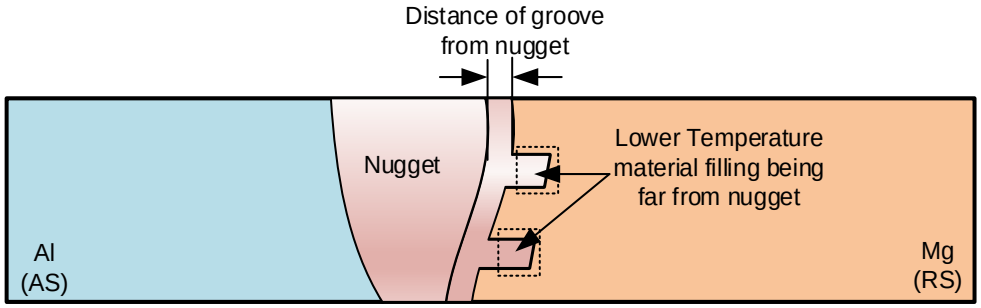

Figure 45: Lower temperature interface area being far from weld nugget bounded by a dotted rectangle.

5. Conclusion

Heat generation, heat, and material flow are critical factors that determine the quality of FSW. In the case of Al/Mg FSW, specific parameters have been identified as a good starting point for obtaining proper heat generation and material flow, thus achieving acceptable welds in butt configuration. These parameters include placing the Mg material on the advancing side, employing a tool tilt angle ranging from 1.5° to 3°, utilizing a hardened tool steel with a concave shoulder and a threaded frustum cone pin, offsetting the tool towards the Mg side, rotating the tool at speeds between 250 and 1500 rpm, and setting the travel speed between 6 and 100 mm/min. Previous research has primarily focused on the AZ31 series of magnesium alloys and the 6xxx series of aluminum alloys due to their favorable flow characteristics and extensive industrial usage. ~~However, there exists a research opportunity to explore other alloys, such as aluminum-lithium alloys and Mg-rare earth alloys, which offer unique properties and characteristics.~~

The efficiency of a joint is improved when a Class IV interface is formed, accompanied by the controlled presence of IMC (less than 10 µm thick). Achieving both complex mechanical interlocking and the controlled presence of IMC requires optimizing process parameters, utilizing ultrasonic vibration, implementing pulse current, incorporating interlayers/additives, and developing novel joint designs (FSW variants). It is important to note that enhancing mechanical interlocking and retarding IMC cannot be targeted separately; the method chosen to enhance mechanical interlocking will also impact the presence of IMC. ~~Limited research has been conducted in the domain of pulse current and customized joint design to simultaneously improve mechanical interlocking and retard IMC, presenting a potential research gap.~~

The studies mentioned in this context have documented ultimate tensile strength results for Al/Mg FSW joints, reaching about 200 MPa. The decision regarding selection parameters for FSW and the approach to enhance the interface rests with the designer, who is targeting a UTS for a specific application. Although the researchers were first drawn to the novel joint technology, it only produced a UTS of 32.8 MPa, while the application of pulse current was reported to produce a UTS of 215.7 MPa. These two FSW domains for Al/Mg have received the least research. Additionally, FSW variants offer a smooth transition of HV from HAZ-TMZ-WNZ. The introduction of ductile features into the Al/Mg fracture mode is also made possible by these modifications in the FSW process. This review article has been prepared to ~~comprehensively~~ discuss the existing potential and future direction of the Al/Mg FSW, specifically in improving the mechanical properties of the butt joint structure.

6. Future Scope

a) The utilization of pinless tools has been observed in various process variants of FSW, including µFSW and FSSW. However, the paucity of available literature highlights the need for further investigations, particularly in the context of Al/Mg joints.

b) A notable research gap exists in the exploration of tools with multiple shoulders, indicating a promising area for future study.

c) While multiple-pass FSW has shown promise in enhancing joint properties, the scarcity of data specific to Al/Mg alloys underscores a critical research gap.

d) An exciting research opportunity lies in the exploration of other alloys, such as aluminum-lithium alloys and Mg-rare earth alloys, which possess distinctive properties and characteristics.

e) The limited data available on pulse current assisted FSW, as well as the potential for modifying the joint design to enhance the interface, beckon further exploration within this domain.

f) Another promising avenue for future research lies in the simulation of Al/Mg joints. This involves predicting material flow, temperature distributions, and residual stresses. Delving into this area holds great potential for advancing our understanding and optimization of the welding process.

Acknowledgements

This work is funded by the Distinguished International Associates program, Royal Academy of Engineering (No. IF013-2023) received by Mohd Ridha bin Muhamad.

References

[1] Nations U. Population. United Nations n.d. https://www.un.org/en/global-issues/population (accessed December 22, 2022).

[2] Martins T, Barreto AC, Souza FM, Souza AM. Fossil fuels consumption and carbon dioxide emissions in G7 countries: Empirical evidence from ARDL bounds testing approach. Environmental Pollution 2021;291:118093. https://doi.org/10.1016/j.envpol.2021.118093.

[3] Zhang W, Xu J. Advanced lightweight materials for Automobiles: A review. Materials and Design 2022;221. https://doi.org/10.1016/j.matdes.2022.110994.

[4] Pu Y, Ma F, Zhang J, Yang M. Optimal Lightweight Material Selection for Automobile Applications Considering Multi-Perspective Indices. IEEE Access 2018;6:8591–8. https://doi.org/10.1109/ACCESS.2018.2804904.

[5] Jing S, Zhang H, Zhou J, Song G. Optimum weight design of functionally graded material gears. Chin J Mech Eng 2015;28:1186–93. https://doi.org/10.3901/CJME.2015.0930.118.

[6] Total production of crude steel. WorldsteelOrg n.d. https://worldsteel.org/steel-topics/statistics/annual-production-steel-data/?ind=P1_crude_steel_total_pub/WORLD_ALL (accessed February 20, 2023).

[7] Primary Aluminium Production. International Aluminium Institute n.d. https://international-aluminium.org/statistics/primary-aluminium-production/ (accessed February 20, 2023).

[8] Primary magnesium production worldwide 2021. Statista n.d. https://www.statista.com/statistics/569515/primary-magnesium-production-worldwide/ (accessed February 21, 2023).

[9] Jadav H, Badheka V, Upadhyay G, Mehta K. Dissimilar welding of magnesium alloy to aluminium alloy: a review. Advances in Materials and Processing Technologies 2022;8:3794–821. https://doi.org/10.1080/2374068X.2021.2016564.

[10] Isa MSM, Moghadasi K, Ariffin MA, Raja S, Muhamad MR bin, Yusof F, et al. Recent research progress in friction stir welding of aluminium and copper dissimilar joint: a review. Journal of Materials Research and Technology 2021;15:2735–80. https://doi.org/10.1016/j.jmrt.2021.09.037.

[11] Raja S, Muhamad MR, Yusof F, Jamaludin MF, Suga T, Liu H, et al. Friction stir alloying of AZ61 and mild steel with Al-CNT additive. Sci Technol Weld Joining 2022;27:533–40. https://doi.org/10.1080/13621718.2022.2080449.

[12] Simar A, Avettand-Fènoël M-N. State of the art about dissimilar metal friction stir welding. Science and Technology of Welding and Joining 2017;22:389–403. https://doi.org/10.1080/13621718.2016.1251712.

[13] Patterson T, Hochanadel J, Sutton S, Panton B, Lippold J. A review of high energy density beam processes for welding and additive manufacturing applications. Weld World 2021;65:1235–306. https://doi.org/10.1007/s40194-021-01116-0.

[14] Meng Y, Lu Y, Li Z, Zhao S, Gao M. Effects of beam oscillation on interface layer and mechanical properties of laser-arc hybrid lap welded Al/Mg dissimilar metals. Intermetallics 2021;133:107175. https://doi.org/10.1016/j.intermet.2021.107175.

[15] Kumar N, Yuan W, Mishra RS. Friction Stir Welding of Dissimilar Alloys and Materials, Elsevier; 2015. https://doi.org/10.1016/B978-0-12-802418-8.00001-1.

[16] Çam G. Prospects of producing aluminum parts by wire arc additive manufacturing (WAAM). Materials Today: Proceedings 2022;62:77–85. https://doi.org/10.1016/j.matpr.2022.02.137.

[17] İpekoğlu G, Çam G. Formation of weld defects in cold metal transfer arc welded 7075-T6 plates and its effect on joint performance. IOP Conf Ser: Mater Sci Eng 2019;629:012007. https://doi.org/10.1088/1757-899X/629/1/012007.

[18] Çam G, Ventzke V, Dos Santos JF, Koçak M, Jennequin G, Gonthier-Maurin P. Characterisation of electron beam welded aluminium alloys. Science and Technology of Welding and Joining 1999;4:317–23. https://doi.org/10.1179/136217199101537941.

[19] Eftekhar AH, Sadrossadat SM, Reihanian M. Effect of heat input on microstructure and mechanical properties of TIG-welded semisolid cast AXE622 Mg alloy. Materials Characterization 2022;184:111692. https://doi.org/10.1016/j.matchar.2021.111692.

[20] Kashaev N, Ventzke V, Çam G. Prospects of laser beam welding and friction stir welding processes for aluminum airframe structural applications. Journal of Manufacturing Processes 2018;36:571–600.

[21] Liu P, Li Y, Geng H, Wang J. Microstructure characteristics in TIG welded joint of Mg/Al dissimilar materials. Materials Letters 2007;61:1288–91. https://doi.org/10.1016/j.matlet.2006.07.010.

[22] Pouranvari M. Critical review on fusion welding of magnesium alloys: metallurgical challenges and opportunities. Science and Technology of Welding and Joining 2021;26:559–80. https://doi.org/10.1080/13621718.2021.1982339.

[23] Shang J, Wang K, Zhou Q, Zhang D, Huang J, Li G. Microstructure characteristics and mechanical properties of cold metal transfer welding Mg/Al dissimilar metals. Materials & Design 2012;34:559–65. https://doi.org/10.1016/j.matdes.2011.05.008.

[24] Liu F, Wang H, Liu L. Characterization of Mg/Al butt joints welded by gas tungsten arc filling with Zn–29.5Al–0.5Ti filler metal. Materials Characterization 2014;90:1–6. https://doi.org/10.1016/j.matchar.2014.01.010.

[25] Morishige T, Kawaguchi A, Tsujikawa M, Hino M, Hirata T, Higashi K. Dissimilar Welding of Al and Mg Alloys by FSW. Mater Trans 2008;49:1129–31. https://doi.org/10.2320/matertrans.MC200768.

[26] Çam G, İpekoğlu G. Recent developments in joining of aluminum alloys. Int J Adv Manuf Technol 2017;91:1851–66. https://doi.org/10.1007/s00170-016-9861-0.

[27] Ahmed MMZ, El-Sayed Seleman MM, Fydrych D, Çam G. Friction Stir Welding of Aluminum in the Aerospace Industry: The Current Progress and State-of-the-Art Review. Materials 2023;16:2971. https://doi.org/10.3390/ma16082971.

[28] İpekoğlu G, Erim S, Kıral B, Çam G. Investigation into the effect of temper condition on friction stir weldability of AA6061 Al-alloy plates. Kovove Materialy 2013;51:155–63. https://doi.org/10.4149/km-2013-3-155.

[29] Çam G, Güçlüer S, Çakan A, Serindag H t. Mechanical properties of friction stir butt-welded Al-5086 H32 plate. Materials Science and Engineering Technology 2009;40:638–42. https://doi.org/10.1002/mawe.200800455.

[30] Küçükömeroğlu T, Aktarer SM, Çam G. Investigation of mechanical and microstructural properties of friction stir welded dual phase (DP) steel. IOP Conf Ser: Mater Sci Eng 2019;629:012010. https://doi.org/10.1088/1757-899X/629/1/012010.

[31] Küçükömeroğlu T, Aktarer SM, İpekoğlu G, Çam G. Microstructure and mechanical properties of friction-stir welded St52 steel joints. Int J Miner Metall Mater 2018;25:1457–64. https://doi.org/10.1007/s12613-018-1700-x.

[32] Çam G, Mistikoglu S, Pakdil M. Microstructural and Mechanical Characterization of Friction Stir Butt Joint Welded 63%Cu-37%Zn Brass Plate. Welding Journal 2009;88:225s–32s.

[33] Çam G, Serindağ HT, Çakan A, Mistikoglu S, Yavuz H. The effect of weld parameters on friction stir welding of brass plates. Materials Science and

Engineering Technology 2008;39:394–9. https://doi.org/10.1002/mawe.200800314.

[34] Günen A, Kanca E, Demir M, Çavdar F, Mistikoglu S, Çam G. Microstructural and mechanical properties of friction stir welded pure lead. Indian Journal of Engineering and Materials Sciences 2018;25.

[35] Lambiase F, Derazkola HA, Simchi A. Friction Stir Welding and Friction Spot Stir Welding Processes of Polymers—State of the Art. Materials 2020;13:2291. https://doi.org/10.3390/ma13102291.

[36] Fan G, Tomków J, Abdullah ME, Derazkola HA. Investigation on polypropylene friction stir joint: effects of tool tilt angle on heat flux, material flow and defect formation. Journal of Materials Research and Technology 2023;23:715–29. https://doi.org/10.1016/j.jmrt.2023.01.028.

[37] Eyvazian A, Hamouda AM, Aghajani Derazkola H, Elyasi M. Study on the effects of tool tile angle, offset and plunge depth on friction stir welding of poly(methyl methacrylate) T-joint. Proceedings of the Institution of Mechanical Engineers, Part B: Journal of Engineering Manufacture 2020;234:773–87. https://doi.org/10.1177/0954405419889180.

[38] Khalaf HI, Al-Sabur R, Demiral M, Tomków J, Łabanowski J, Abdullah ME, et al. The Effects of Pin Profile on HDPE Thermomechanical Phenomena during FSW. Polymers 2022;14:4632. https://doi.org/10.3390/polym14214632.

[39] Küçükömeroğlu T, Aktarer SM, İpekoğlu G, Çam G. Mechanical properties of friction stir welded St 37 and St 44 steel joints. Materials Testing 2018;60:1163–70. https://doi.org/10.3139/120.111266.

[40] Fu H, Chai Z, Han S, Liu D, Chang Y, Chen Y, et al. Effect of post-weld heat treatment on a friction stir welded joint between 9Cr-ODS and CLF-1 steels. Materials Characterization 2022;187:111868. https://doi.org/10.1016/j.matchar.2022.111868.

[41] Trdan U, Klobčar D, Berthe L, Šturm R, Bergant Z. High-cycle fatigue enhancement of dissimilar 2017A-T451/7075-T651 Al alloy joint fabricated by a single pass FSW without any post-processing. Journal of Materials Research and Technology 2023;25:2333–52. https://doi.org/10.1016/j.jmrt.2023.06.096.

[42] Niu P, Li W, Yang C, Chen Y, Chen D. Low cycle fatigue properties of friction stir welded dissimilar 2024-to-7075 aluminum alloy joints. Materials Science and Engineering: A 2022;832:142423. https://doi.org/10.1016/j.msea.2021.142423.

[43] Zhang J, Zhang Y, Chen X, Li Z, Huang G, Pan F. Improving joint performance of friction stir welded AZ31/ AM60 dissimilar Mg alloys by double-sided welding. Materials Science and Engineering: A 2023;882:145444. https://doi.org/10.1016/j.msea.2023.145444.

[44] Zhang J, Chen X, Liu S, Huang G, Jiang B, Tang A, et al. Non-uniform deformation behavior of dissimilar friction stir welded AM60/AZ31 joint and its influence on fracture. Materials Science and Engineering: A 2021;800:140318. https://doi.org/10.1016/j.msea.2020.140318.

[45] Kar A, Malopheyev S, Mironov S, Kaibyshev R, Suwas S, Kailas SV. A new method to elucidate fracture mechanism and microstructure evolution in

titanium during dissimilar friction stir welding of aluminum and titanium. Materials Characterization 2021;171:110791. https://doi.org/10.1016/j.matchar.2020.110791.

[46] Zhang X, Shi L, Wu C, Yang C, Gao S. Multi-phase modelling of heat and mass transfer during Ti/Al dissimilar friction stir welding process. Journal of Manufacturing Processes 2023;94:240–54. https://doi.org/10.1016/j.jmapro.2023.03.037.

[47] Khajeh R, Jafarian HR, Seyedein SH, Jabraeili R, Eivani AR, Park N, et al. Microstructure, mechanical and electrical properties of dissimilar friction stir welded 2024 aluminum alloy and copper joints. Journal of Materials Research and Technology 2021;14:1945–57. https://doi.org/10.1016/j.jmrt.2021.07.058.

[48] Abd Elnabi MM, Osman TA, El Mokadem A, Elshalakany AB. Evaluation of the formation of intermetallic compounds at the intermixing lines and in the nugget of dissimilar steel/aluminum friction stir welds. Journal of Materials Research and Technology 2020;9:10209–22. https://doi.org/10.1016/j.jmrt.2020.07.027.

[49] Wang J, Ling X, Zhang W, Lu X, Chen C. Microstructures and mechanical properties of friction stir welded butt joints of 3003-H112 aluminum alloy to 304 stainless steel used in plate-fin heat exchanger. Journal of Materials Research and Technology 2022;21:3086–97. https://doi.org/10.1016/j.jmrt.2022.10.161.

[50] MirHashemi SM, Amadeh A, Khodabakhshi F. Effects of SiC nanoparticles on the dissimilar friction stir weldability of low-density polyethylene (LDPE) and AA7075 aluminum alloy. Journal of Materials Research and Technology 2021;13:449–62. https://doi.org/10.1016/j.jmrt.2021.04.094.

[51] Aghajani Derazkola H, Kordani N, Mohammadi Abokheili R. Investigation of joining mechanism of electrical-assist friction stir joining between polyethylene (PE) and 316 stainless steel. ArchivCivMechEng 2022;22:199. https://doi.org/10.1007/s43452-022-00524-3.

[52] Çam G, Javaheri V, Heidarzadeh A. Advances in FSW and FSSW of dissimilar Al-alloy plates. Journal of Adhesion Science and Technology 2023;37:162–94. https://doi.org/10.1080/01694243.2022.2028073.

[53] Küçükömeroğlu T, Şentürk E, Kara L, İpekoğlu G, Çam G. Microstructural and Mechanical Properties of Friction Stir Welded Nickel-Aluminum Bronze (NAB) Alloy. J of Materi Eng and Perform 2016;25:320–6. https://doi.org/10.1007/s11665-015-1838-x.

[54] Çam G. Friction stir welded structural materials: beyond Al-alloys. International Materials Reviews 2011;56:1–48.

[55] Abdullah ME, M. Rohim MN, Mohammed MM, Derazkola HA. Effects of Partial-Contact Tool Tilt Angle on Friction Stir Welded AA1050 Aluminum Joint Properties. Materials 2023;16:4091. https://doi.org/10.3390/ma16114091.

[56] Derazkola HA, Eyvazian A, Simchi A. Modeling and experimental validation of material flow during FSW of polycarbonate. Materials Today Communications 2020;22:100796. https://doi.org/10.1016/j.mtcomm.2019.100796.

[57] Khodabakhshi F, Derazkola HA, Gerlich AP. Monte Carlo simulation of grain refinement during friction stir processing. J Mater Sci 2020;55:13438–56. https://doi.org/10.1007/s10853-020-04963-2.

[58] Jain R, Pal SK, Singh SB. Numerical modeling methodologies for friction stir welding process. Computational Methods and Production Engineering, Elsevier; 2017, p. 125–69. https://doi.org/10.1016/B978-0-85709-481-0.00005-7.

[59] Memon S, Fydrych D, Fernandez AC, Derazkola HA, Derazkola HA. Effects of FSW Tool Plunge Depth on Properties of an Al-Mg-Si Alloy T-Joint: Thermomechanical Modeling and Experimental Evaluation. Materials 2021;14:4754. https://doi.org/10.3390/ma14164754.

[60] Heidarzadeh A, Mironov S, Kaibyshev R, Çam G, Simar A, Gerlich A, et al. Friction stir welding/processing of metals and alloys: A comprehensive review on microstructural evolution. Progress in Materials Science 2021;117:100752. https://doi.org/10.1016/j.pmatsci.2020.100752.

[61] Ambrosio D, Morisada Y, Ushioda K, Fujii H. Material flow in friction stir welding: A review. Journal of Materials Processing Technology 2023:118116. https://doi.org/10.1016/j.jmatprotec.2023.118116.

[62] Ji H, Deng YL, Xu HY, Yin X, Zhang T, Wang WQ, et al. Numerical modeling for the mechanism of shoulder and pin features affecting thermal and material flow behavior in friction stir welding. Journal of Materials Research and Technology 2022;21:662–78. https://doi.org/10.1016/j.jmrt.2022.09.070.

[63] Zhang G, Wu C, Gao J. Ultrasonic line source and its coupling with the tool induced heat generation and material flow in friction stir welding. Journal of Materials Research and Technology 2022;21:502–18. https://doi.org/10.1016/j.jmrt.2022.09.053.

[64] Zhai M, Wu C, Su H. Influence of tool tilt angle on heat transfer and material flow in friction stir welding. Journal of Manufacturing Processes 2020;59:98–112. https://doi.org/10.1016/j.jmapro.2020.09.038.

[65] Aghajani Derazkola H, Kordani N, Aghajani Derazkola H. Effects of friction stir welding tool tilt angle on properties of Al-Mg-Si alloy T-joint. CIRP Journal of Manufacturing Science and Technology 2021;33:264–76. https://doi.org/10.1016/j.cirpj.2021.03.015.

[66] Elyasi M, Taherian J, Hosseinzadeh M, Kubit A, Derazkola HA. The effect of pin thread on material flow and mechanical properties in friction stir welding of AA6068 and pure copper. Heliyon 2023;9. https://doi.org/10.1016/j.heliyon.2023.e14752.

[67] Xie L, Zhu X, Sun W, Jiang C, Wang P, Yang S, et al. Investigations on the material flow and the influence of the resulting texture on the tensile properties of dissimilar friction stir welded ZK60/Mg–Al–Sn–Zn joints. Journal of Materials Research and Technology 2022;17:1716–30. https://doi.org/10.1016/j.jmrt.2022.01.127.

[68] Zhang G, Gao J, Wu C. Revealing the acoustic effects on heat transfer and material flow in ultrasonic assisted friction stir welding of dissimilar Al/Mg alloys. Journal of Materials Research and Technology 2023;26:1882–902. https://doi.org/10.1016/j.jmrt.2023.08.028.

[69] Chaudry UM, Han S-C, Jun T-S. Effect of welding speed on the microstructure and texture development in the individual weld zone of friction stir welded

DP780 steel. Journal of Materials Research and Technology 2023;23:4976–89. https://doi.org/10.1016/j.jmrt.2023.02.122.

[70] Zhang C, Huang G, Zhang D, Sun Z, Liu Q. Microstructure and mechanical properties in dissimilar friction stir welded AA2024/7075 joints at high heat input: effect of post-weld heat treatment. Journal of Materials Research and Technology 2020;9:14771–82. https://doi.org/10.1016/j.jmrt.2020.10.053.

[71] Liu XC, Ye T, Li YZ, Pei XJ, Sun Z. Quasi-in-situ characterization of microstructure evolution in friction stir welding of aluminum alloy. Journal of Materials Research and Technology 2023;25:6380–94. https://doi.org/10.1016/j.jmrt.2023.07.101.

[72] Ghiasvand A, Ranjbarnodeh E, Mirsalehi E. The microstructure and mechanical properties of single-pass and double-pass lap joint of Al 5754H-11 and Mg AZ31-O alloys by friction stir welding. Journal of Materials Research and Technology 2023. https://doi.org/10.1016/j.jmrt.2023.02.222.

[73] Nandan R, Debroy T, Bhadeshia H. Recent advances in friction-stir welding – Process, weldment structure and properties. Progress in Materials Science 2008;53:980–1023. https://doi.org/10.1016/j.pmatsci.2008.05.001.

[74] Kadian AK, Biswas P. A Comparative Study of Material Flow Behavior in Friction Stir Welding Using Laminar and Turbulent Models. J of Materi Eng and Perform 2015;24:4119–27. https://doi.org/10.1007/s11665-015-1520-3.

[75] Fu B, Qin G, Li F, Meng X, Zhang J, Wu C. Friction stir welding process of dissimilar metals of 6061-T6 aluminum alloy to AZ31B magnesium alloy. Journal of Materials Processing Technology 2015;218:38–47. https://doi.org/10.1016/j.jmatprotec.2014.11.039.

[76] Liu H, Chen Y, Yao Z, Luo F. Effect of Tool Offset on the Microstructure and Properties of AA6061/AZ31B Friction Stir Welding Joints. Metals 2020;10:546. https://doi.org/10.3390/met10040546.

[77] Yamamoto N, Liao J, Watanabe S, Nakata K. Effect of intermetallic compound layer on tensile strength of dissimilar friction-stir weld of a high strength Mg alloy and Al alloy. Materials Transactions 2009;50:2833–8. https://doi.org/10.2320/matertrans.M2009289.

[78] Zhao J, Wu C, Su H. Acoustic effect on the tensile properties and metallurgical structures of dissimilar friction stir welding joints of Al/Mg alloys. Journal of Manufacturing Processes 2021;65:328–41. https://doi.org/10.1016/j.jmapro.2021.03.057.

[79] Chen ZW, Cui S. On the forming mechanism of banded structures in aluminium alloy friction stir welds. Scripta Materialia 2008;58:417–20. https://doi.org/10.1016/j.scriptamat.2007.10.026.

[80] Mishra RS, Mahoney MW. Friction Stir Welding and Processing. ASM International; 2007.

[81] Ahmed MMZ, I. A. Habba M, Jouini N, Alzahrani B, Seleman MME-S, El-Nikhaily A. Bobbin Tool Friction Stir Welding of Aluminum Using Different Tool Pin Geometries: Mathematical Models for the Heat Generation. Metals 2021;11:438. https://doi.org/10.3390/met11030438.

[82] Xu Y, Ke L, Ouyang S, Mao Y, Niu P. Precipitation behavior of intermetallic compounds and their effect on mechanical properties of thick plate friction stir welded Al/Mg joint. JOURNAL OF MANUFACTURING PROCESSES 2021;64:1059–69. https://doi.org/10.1016/j.jmapro.2020.12.068.

[83] McWilliams BA, Yu JH, Yen C-F. Numerical simulation and experimental characterization of friction stir welding on thick aluminum alloy AA2139-T8 plates. Materials Science and Engineering: A 2013;585:243–52. https://doi.org/10.1016/j.msea.2013.07.073.

[84] Xu Y, Ke L, Mao Y, Liu Q, Xie J, Zeng H. Formation Investigation of Intermetallic Compounds of Thick Plate Al/Mg Alloys Joint by Friction Stir Welding. MATERIALS 2019;12. https://doi.org/10.3390/ma12172661.

[85] Reynolds AP. Visualisation of material flow in autogenous friction stir welds. Science and Technology of Welding and Joining 2000;5:120–4. https://doi.org/10.1179/136217100101538119.

[86] Malarvizhi S, Balasubramanian V. Influences of tool shoulder diameter to plate thickness ratio (D/T) on stir zone formation and tensile properties of friction stir welded dissimilar joints of AA6061 aluminum–AZ31B magnesium alloys. Materials & Design 2012;40:453–60. https://doi.org/10.1016/j.matdes.2012.04.008.

[87] Jain VKS, Yazar KU, Muthukumaran S. Development and characterization of Al5083-CNTs/SiC composites via friction stir processing. Journal of Alloys and Compounds 2019;798:82–92. https://doi.org/10.1016/j.jallcom.2019.05.232.

[88] Mehta KP, Patel R. On FSW Keyhole Removal to Improve Volume Defect Using Pin Less Tool. Key Engineering Materials 2019;821:215–21. https://doi.org/10.4028/www.scientific.net/KEM.821.215.

[89] Yuan T, Kang S, Jiang X, Zhao P. Exit-hole repairing in 7475 aluminium alloy welded joints based on refill friction stir processing. Science and Technology of Welding and Joining 2023;0:1–10. https://doi.org/10.1080/13621718.2023.2235791.

[90] Kim S, Hong J, Joo Y, Kang M. Synergistic effect of SiC nano-reinforcement and vibrator assistance in micro-friction stir welding of dissimilar AA5052-H32/AA6061-T6. Journal of Manufacturing Processes 2022;82:860–9. https://doi.org/10.1016/j.jmapro.2022.08.023.

[91] Ni Y, Fu L, Chen HY. Effects of travel speed on mechanical properties of AA7075-T6 ultra-thin sheet joints fabricated by high rotational speed micro pinless friction stir welding. Journal of Materials Processing Technology 2019;265:63–70. https://doi.org/10.1016/j.jmatprotec.2018.10.006.

[92] Khalaf HI, Al-Sabur R, Derazkola HA. Effect of number of tool shoulders on the quality of steel to magnesium alloy dissimilar friction stir welds. ArchivCivMechEng 2023;23:125. https://doi.org/10.1007/s43452-023-00673-z.

[93] Bokov DO, Jawad MA, Suksatan W, Abdullah ME, Świerczyńska A, Fydrych D, et al. Effect of Pin Shape on Thermal History of Aluminum-Steel Friction Stir Welded Joint: Computational Fluid Dynamic Modeling and Validation. Materials 2021;14:7883. https://doi.org/10.3390/ma14247883.

[94] Kumar K, Kailas SV. The role of friction stir welding tool on material flow and weld formation. Materials Science and Engineering: A 2008;485:367–74. https://doi.org/10.1016/j.msea.2007.08.013.

[95] Sahu PK, Pal S, Pal SK, Jain R. Influence of plate position, tool offset and tool rotational speed on mechanical properties and microstructures of dissimilar Al/Cu friction stir welding joints. Journal of Materials Processing Technology 2016;235:55–67. https://doi.org/10.1016/j.jmatprotec.2016.04.014.

[96] Venkateswaran P, Reynolds AP. Factors affecting the properties of Friction Stir Welds between aluminum and magnesium alloys. Materials Science and Engineering: A 2012;545:26–37. https://doi.org/10.1016/j.msea.2012.02.069.

[97] Lohwasser D, Chen Z. Friction stir welding: From basics to applications. Cambridge: Woodhead Publishing Limited; 2010.

[98] Asl NS, Mirsalehi SE, Dehghani K. Effect of TiO2 nanoparticles addition on microstructure and mechanical properties of dissimilar friction stir welded AA6063-T4 aluminum alloy and AZ31B-O magnesium alloy. JOURNAL OF MANUFACTURING PROCESSES 2019;38:338–54. https://doi.org/10.1016/j.jmapro.2019.01.023.

[99] Pishevar MR, Omidvar H, Mohandesi JA, Safarkhanian MA. Effect of applying second-pass welding and welding parameters on the defects and mechanical properties in friction-stir lap-welded AA5456 sheets. Weld World 2016;60:497–506. https://doi.org/10.1007/s40194-016-0320-1.

[100] Salih OS, Ou H, Sun W. Heat generation, plastic deformation and residual stresses in friction stir welding of aluminium alloy. International Journal of Mechanical Sciences 2023;238:107827. https://doi.org/10.1016/j.ijmecsci.2022.107827.

[101] Fu X, Chen K, Zhang Q, Chen N, Wang M, Hua X. Interfacial intermetallic compound layer in friction stir welded Mg/Al joints: Relationship between thickness and the welding temperature history. Journal of Magnesium and Alloys 2023. https://doi.org/10.1016/j.jma.2023.01.010.

[102] Kah P, Rajan R, Martikainen J, Suoranta R. Investigation of weld defects in friction-stir welding and fusion welding of aluminium alloys. Int J Mech Mater Eng 2015;10:26. https://doi.org/10.1186/s40712-015-0053-8.

[103] Nie J-F. Precipitation and Hardening in Magnesium Alloys. Metall Mater Trans A 2012;43:3891–939. https://doi.org/10.1007/s11661-012-1217-2.

[104] Palanivel S, Mishra RS, Davis B, DeLorme R, Doherty KJ, Cho KC. Effect of Initial Microstructure on the Microstructural Evolution and Joint Efficiency of a We43 Alloy During Friction Stir Welding. In: Mishra R, Mahoney MW, Sato Y, Hovanski Y, Verma R, editors. Friction Stir Welding and Processing VII, Cham: Springer International Publishing; 2016, p. 253–61. https://doi.org/10.1007/978-3-319-48108-1_26.

[105] Gao L, Chen RS, Han EH. Effects of rare-earth elements Gd and Y on the solid solution strengthening of Mg alloys. Journal of Alloys and Compounds 2009;481:379–84. https://doi.org/10.1016/j.jallcom.2009.02.131.

[106] Qiu R, Iwamoto C, Satonaka S. The influence of reaction layer on the strength of aluminum/steel joint welded by resistance spot welding. Materials

Characterization 2009;60:156–9. https://doi.org/10.1016/j.matchar.2008.07.005.

[107] Song JL, Lin SB, Yang CL, Fan CL, Ma GC. Analysis of intermetallic layer in dissimilar TIG welding–brazing butt joint of aluminium alloy to stainless steel. Science and Technology of Welding and Joining 2010;15:213–8. https://doi.org/10.1179/136217110X12665048207610.

[108] Lv XQ, Wu CS, Padhy GK. Diminishing intermetallic compound layer in ultrasonic vibration enhanced friction stir welding of aluminum alloy to magnesium alloy. Materials Letters 2017;203:81–4. https://doi.org/10.1016/j.matlet.2017.05.090.

[109] Lv X, Wu C, Yang C, Padhy GK. Weld microstructure and mechanical properties in ultrasonic enhanced friction stir welding of Al alloy to Mg alloy. Journal of Materials Processing Technology 2018;254:145–57. https://doi.org/10.1016/j.jmatprotec.2017.11.031.

[110] Singh VP, Patel SK, Ranjan A, Kuriachen B. Recent research progress in solid state friction-stir welding of aluminium–magnesium alloys: a critical review. Journal of Materials Research and Technology 2020;9:6217–56. https://doi.org/10.1016/j.jmrt.2020.01.008.

[111] Shah LH, Othman NH, Gerlich A. Review of research progress on aluminium–magnesium dissimilar friction stir welding. Science and Technology of Welding and Joining 2018;23:256–70. https://doi.org/10.1080/13621718.2017.1370193.

[112] Sato YS, Park SHC, Michiuchi M, Kokawa H. Constitutional liquation during dissimilar friction stir welding of Al and Mg alloys. Scripta Materialia 2004;50:1233–6. https://doi.org/10.1016/j.scriptamat.2004.02.002.

[113] Yan J, Xu Z, Li Z, Li L, Yang S. Microstructure characteristics and performance of dissimilar welds between magnesium alloy and aluminum formed by friction stirring. Scripta Materialia 2005;53:585–9. https://doi.org/10.1016/j.scriptamat.2005.04.022.

[114] Zettler R, Da Silva AAM, Rodrigues S, Blanco A, Dos Santos JF. Dissimilar Al to Mg alloy friction stir welds. Advanced Engineering Materials 2006;8:415–21. https://doi.org/10.1002/adem.200600030.

[115] Khodir SA, Shibayanagi T. Dissimilar Friction Stir Welded Joints between 2024-T3 Aluminum Alloy and AZ31 Magnesium Alloy. Materials Transactions 2007;48:2501–5. https://doi.org/10.2320/matertrans.MRA2007093.

[116] Zhao Y, Lu Z, Yan K, Huang L. Microstructural characterizations and mechanical properties in underwater friction stir welding of aluminum and magnesium dissimilar alloys. Materials and Design 2015;65:675–81. https://doi.org/10.1016/j.matdes.2014.09.046.

[117] Abdollahzadeh A, Shokuhfar A, Cabrera JM, Zhilyaev AP, Omidvar H. The effect of changing chemical composition on dissimilar Mg/Al friction stir welded butt joints using zinc interlayer. JOURNAL OF MANUFACTURING PROCESSES 2018;34:18–30. https://doi.org/10.1016/j.jmapro.2018.05.029.

[118] Verma J, Taiwade RV, Reddy C, Khatirkar RK. Effect of friction stir welding process parameters on Mg-AZ31B/Al-AA6061 joints. MATERIALS AND

MANUFACTURING PROCESSES 2018;33:308–14. https://doi.org/10.1080/10426914.2017.1291957.

[119] Abdollahzadeh A, Shokuhfar A, Cabrera JM, Zhilyaev AP, Omidvar H. In-situ nanocomposite in friction stir welding of 6061-T6 aluminum alloy to AZ31 magnesium alloy. JOURNAL OF MATERIALS PROCESSING TECHNOLOGY 2019;263:296–307. https://doi.org/10.1016/j.jmatprotec.2018.08.025.

[120] McLean AA, Powell GLF, Brown IH, Linton VM. Friction stir welding of magnesium alloy AZ31B to aluminium alloy 5083. Science and Technology of Welding and Joining 2003;8:462–4. https://doi.org/10.1179/136217103225009134.

[121] Zheng B, Hu X, Lv Q, Zhao L, Cai D, Dong S. Study of self-reaction assisted friction stir welding of AZ31B Mg/5052 Al alloys. Materials Letters 2020;261:127138. https://doi.org/10.1016/j.matlet.2019.127138.

[122] Firouzdor V, Kou S. Al-to-Mg friction stir welding: Effect of material position, travel speed, and rotation speed. Metallurgical and Materials Transactions A: Physical Metallurgy and Materials Science 2010;41:2914–35. https://doi.org/10.1007/s11661-010-0340-1.

[123] Liu Z, Meng X, Ji S, Li Z, Wang L. Improving tensile properties of Al/Mg joint by smashing intermetallic compounds via ultrasonic-assisted stationary shoulder friction stir welding. JOURNAL OF MANUFACTURING PROCESSES 2018;31:552–9. https://doi.org/10.1016/j.jmapro.2017.12.022.

[124] Meng X, Jin Y, Ji S, Yan D. Improving friction stir weldability of Al/Mg alloys via ultrasonically diminishing pin adhesion. Journal of Materials Science & Technology 2018;34:1817–22. https://doi.org/10.1016/j.jmst.2018.02.022.

[125] Song Q, Wang H, Ji S, Ma Z, Jiang W, Chen M. Improving joint quality of hybrid friction stir welded Al/Mg dissimilar alloys by RBFNN-GWO system. Journal of Manufacturing Processes 2020;59:750–9. https://doi.org/10.1016/j.jmapro.2020.10.037.

[126] Kumar S, Wu C. Suppression of intermetallic reaction layer by ultrasonic assistance during friction stir welding of Al and Mg based alloys. Journal of Alloys and Compounds 2020;827:154343. https://doi.org/10.1016/j.jallcom.2020.154343.

[127] Hu W, Ma Z, Ji S, Song Q, Chen M, Jiang W. Improving the mechanical property of dissimilar Al/Mg hybrid friction stir welding joint by PIO-ANN. JOURNAL OF MATERIALS SCIENCE & TECHNOLOGY 2020;53:41–52. https://doi.org/10.1016/j.jmst.2020.01.069.

[128] Chen W, Wang W, Liu Z, Zhai X, Bian G, Zhang T, et al. Improvement in tensile strength of Mg/Al alloy dissimilar friction stir welding joints by reducing intermetallic compounds. JOURNAL OF ALLOYS AND COMPOUNDS 2021;861. https://doi.org/10.1016/j.jallcom.2020.157942.

[129] Wu C, Wang T, Su H. Material flow velocity, strain and strain rate in ultrasonic vibration enhanced friction stir welding of dissimilar Al/Mg alloys. Journal of Manufacturing Processes 2022;75:13–22. https://doi.org/10.1016/j.jmapro.2021.12.055.

[130] Zhao J, Wu C, Shi L. Effect of ultrasonic field on microstructure evolution in friction stir welding of dissimilar Al/Mg alloys. Journal of Materials Research and Technology 2022;17:1–21. https://doi.org/10.1016/j.jmrt.2021.12.133.

[131] Xiaoqing J, Yongyong L, Tao Y, Shujun C, Lei W, Wang J. Enhanced mechanical properties of dissimilar Al and Mg alloys fabricated by pulse current assisted friction stir welding. Journal of Manufacturing Processes 2022;76:123–37. https://doi.org/10.1016/j.jmapro.2022.02.007.

[132] Zhao J, Wu C, Shi L, Su H. Evolution of microstructures and intermetallic compounds at bonding interface in friction stir welding of dissimilar Al/Mg alloys with/without ultrasonic assistance. JOURNAL OF MATERIALS SCIENCE & TECHNOLOGY 2023;139:31–46. https://doi.org/10.1016/j.jmst.2022.08.025.

[133] Xu Y, Ke L, Mao Y, Sun J, Duan Y, Yu L. An innovative joint interface design for reducing intermetallic compounds and improving joint strength of thick plate friction stir welded Al/Mg joints. Journal of Magnesium and Alloys 2022. https://doi.org/10.1016/j.jma.2022.01.007.

[134] Tan M, Wu C, Shi L. Formation Mechanism of Thicker Intermetallic Compounds in Friction Stir Weld Joints of Dissimilar AA2024/AZ31B Alloys. MATERIALS 2023;16. https://doi.org/10.3390/ma16010051.

[135] Muhammad NA, Geng P, Wu C, Ma N. Unravelling the ultrasonic effect on residual stress and microstructure in dissimilar ultrasonic-assisted friction stir welding of Al/Mg alloys. International Journal of Machine Tools and Manufacture 2023;186:104004. https://doi.org/10.1016/j.ijmachtools.2023.104004.

[136] Mofid MA, Abdollah-zadeh A, Malek Ghaini F. The effect of water cooling during dissimilar friction stir welding of Al alloy to Mg alloy. Materials & Design (1980-2015) 2012;36:161–7. https://doi.org/10.1016/j.matdes.2011.11.004.

[137] Mofid MA, Abdollah-Zadeh A, Gür CH. Investigating the formation of intermetallic compounds during friction stir welding of magnesium alloy to aluminum alloy in air and under liquid nitrogen. International Journal of Advanced Manufacturing Technology 2014;71:1493–9. https://doi.org/10.1007/s00170-013-5565-x.

[138] Mofid MA, Loryaei E. Investigating microstructural evolution at the interface of friction stir weld and diffusion bond of Al and Mg alloys. JOURNAL OF MATERIALS RESEARCH AND TECHNOLOGY-JMR&T 2019;8:3872–7. https://doi.org/10.1016/j.jmrt.2019.06.049.

[139] Kumar M, Das A, Ballav R. Influence of the Zn interlayer on the mechanical strength, corrosion and microstructural behavior of friction stir-welded 6061-T6 aluminium alloy and AZ61 magnesium alloy dissimilar joints. Materials Today Communications 2023;35:105509. https://doi.org/10.1016/j.mtcomm.2023.105509.

[140] Prasad BL, Neelaiah G, Krishna MG, Ramana SVV, Prakash KS, Sarika G, et al. Joining of AZ91 Mg alloy and Al6063 alloy sheets by friction stir welding. JOURNAL OF MAGNESIUM AND ALLOYS 2018;6:71–6. https://doi.org/10.1016/j.jma.2017.12.004.

[141] Li P, You G, Wen H, Guo W, Tong X, Li S. Friction stir welding between the high-pressure die casting of AZ91 magnesium alloy and A383 aluminum alloy. J Mater Process Technol 2019;264:55–63. https://doi.org/10.1016/j.jmatprotec.2018.08.044.

[142] Sameer MD, Birru AK. Mechanical and metallurgical properties of friction stir welded dissimilar joints of AZ91 magnesium alloy and AA 6082-T6 aluminium alloy. JOURNAL OF MAGNESIUM AND ALLOYS 2019;7:264–71. https://doi.org/10.1016/j.jma.2018.09.004.

[143] Gester A, Thomae M, Wagner G, Strass B, Wolter B, Benfer S, et al. Hybrid joints of die-casted aluminum/magnesium by ultrasound enhanced friction stir welding (USE-FSW). WELDING IN THE WORLD 2019;63:1173–86. https://doi.org/10.1007/s40194-019-00767-4.

[144] Pourahmad P, Abbasi M. Materials flow and phase transformation in friction stir welding of Al 6013/Mg. Transactions of Nonferrous Metals Society of China (English Edition) 2013;23:1253–61. https://doi.org/10.1016/S1003-6326(13)62590-X.

[145] Shi H, Chen K, Liang Z, Dong F, Yu T, Dong X, et al. Intermetallic Compounds in the Banded Structure and Their Effect on Mechanical Properties of Al/Mg Dissimilar Friction Stir Welding Joints. J Mater Sci Technol 2017;33:359–66. https://doi.org/10.1016/j.jmst.2016.05.006.

[146] kumar U, Acharya U, Saha SC, Saha Roy B. Microstructure and mechanical property of friction stir welded Al-Mg joints by adopting modified joint configuration technique. Materials Today: Proceedings 2020;26:2083–8. https://doi.org/10.1016/j.matpr.2020.02.450.

[147] Ross K, Reza-E-Rabby Md, McDonnell M, Whalen SA. Advances in dissimilar metals joining through temperature control of friction stir welding. MRS Bull 2019;44:613–8. https://doi.org/10.1557/mrs.2019.181.

[148] Wang T, Sidhar H, Mishra RS, Hovanski Y, Upadhyay P, Carlson B. Evaluation of intermetallic compound layer at aluminum/steel interface joined by friction stir scribe technology. Materials & Design 2019;174:107795. https://doi.org/10.1016/j.matdes.2019.107795.

[149] Reza-E-Rabby Md, Ross K, Overman NR, Olszta MJ, McDonnell M, Whalen SA. Joining thick section aluminum to steel with suppressed FeAl intermetallic formation via friction stir dovetailing. Scripta Materialia 2018;148:63–7. https://doi.org/10.1016/j.scriptamat.2018.01.026.

[150] Mohammadi J, Behnamian Y, Mostafaei A, Izadi H, Saeid T, Kokabi AH, et al. Friction stir welding joint of dissimilar materials between AZ31B magnesium and 6061 aluminum alloys: Microstructure studies and mechanical characterizations. Materials Characterization 2015;101:189–207. https://doi.org/10.1016/j.matchar.2015.01.008.

[151] Steurer W. The Samson phase, β-Mg2Al3, revisited. Zeitschrift Für Kristallographie – Crystalline Materials 2007;222:259–88. https://doi.org/10.1524/zkri.2007.222.6.259.

[152] Halim SB, Bannour S, Abderrazak K, Kriaa W, Autric M. Numerical analysis of intermetallic compounds formed during laser welding of Aluminum-Magnesium

dissimilar couple. Thermal Science and Engineering Progress 2021;22:100838. https://doi.org/10.1016/j.tsep.2020.100838.

[153] Raghavan V. Al-Mg-Ni (Aluminum-Magnesium-Nickel). Journal of Phase Equilibria and Diffusion 2009;30:274–5. https://doi.org/10.1007/s11669-009-9519-9.

[154] Zhao J, Wu CS, Su H. Ultrasonic effect on thickness variations of intermetallic compound layers in friction stir welding of aluminium/magnesium alloys. Journal of Manufacturing Processes 2021;62:388–402. https://doi.org/10.1016/j.jmapro.2020.12.028.

[155] Kumar S, Wu C. Eliminating intermetallic compounds via Ni interlayer during friction stir welding of dissimilar Mg/Al alloys. Journal of Materials Research and Technology 2021;15:4353–69. https://doi.org/10.1016/j.jmrt.2021.10.065.

[156] Peng P, Wang K, Wang W, Yang T, Liu Q, Zhang T, et al. Intermetallic compounds: Formation mechanism and effects on the mechanical properties of friction stir lap welded dissimilar joints of magnesium and aluminum alloys. Materials Science and Engineering: A 2021;802:140554. https://doi.org/10.1016/j.msea.2020.140554.

[157] Huang T, Zhang Z, Liu J, Chen S, Xie Y, Meng X, et al. Interface Formation of Medium-Thick AA6061 Al/AZ31B Mg Dissimilar Submerged Friction Stir Welding Joints. Materials 2022;15. https://doi.org/10.3390/ma15165520.

[158] Sejani D, Li W, Patel V. Stationary shoulder friction stir welding–low heat input joining technique: a review in comparison with conventional FSW and bobbin tool FSW. Critical Reviews in Solid State and Materials Sciences 2021. https://doi.org/10.1080/10408436.2021.1935724.

[159] Zhao J, Wu C, Su H. Ultrasonic vibration-induced thinning of intermetallic compound layers in friction stir welding of dissimilar Al/Mg alloys. SCIENCE AND TECHNOLOGY OF WELDING AND JOINING 2022;27:621–8. https://doi.org/10.1080/13621718.2022.2096346.

[160] Eyvazian A, Hamouda A, Tarlochan F, Derazkola HA, Khodabakhshi F. Simulation and experimental study of underwater dissimilar friction-stir welding between aluminium and steel. Journal of Materials Research and Technology 2020;9:3767–81. https://doi.org/10.1016/j.jmrt.2020.02.003.

[161] Ji S, Cui X, Ma L, Liu H, Zuo Y, Zhang Z. Achieving High-Quality Aluminum to Copper Dissimilar Metals Joint via Friction Stir Double-Riveting Welding. Acta Metall Sin (Engl Lett) 2023;36:552–72. https://doi.org/10.1007/s40195-022-01512-5.

[162] Chen YC, Nakata K. Microstructural characterization and mechanical properties in friction stir welding of aluminum and titanium dissimilar alloys. Materials & Design 2009;30:469–74. https://doi.org/10.1016/j.matdes.2008.06.008.

[163] Wang Y, Prangnell PB. The significance of intermetallic compounds formed during interdiffusion in aluminum and magnesium dissimilar welds. Materials Characterization 2017;134:84–95. https://doi.org/10.1016/j.matchar.2017.09.040.

[164] Zhang M-X, Huang H, Spencer K, Shi Y-N. Nanomechanics of Mg–Al intermetallic compounds. Surface and Coatings Technology 2010;204:2118–22. https://doi.org/10.1016/j.surfcoat.2009.11.031.

[165] Venkateswaran P, Xu Z-H, Li X, Reynolds AP. Determination of mechanical properties of Al–Mg alloys dissimilar friction stir welded interface by indentation methods. J Mater Sci 2009;44:4140–7. https://doi.org/10.1007/s10853-009-3607-4.

[166] Chen B, Wang Y, Xiao C, Zhang M, Ni G, Li D. The formation mechanism of intermetallic compounds in Al/Mg friction-stir weld joint. MATERIALS SCIENCE AND TECHNOLOGY 2018;34:703–11. https://doi.org/10.1080/02670836.2017.1410926.

[167] Mofid MA, Abdollah-Zadeh A, Ghaini FM, Gür CH. Submerged Friction-Stir Welding (SFSW) Underwater and Under Liquid Nitrogen: An Improved Method to Join Al Alloys to Mg Alloys. Metall and Mat Trans A 2012;43:5106–14. https://doi.org/10.1007/s11661-012-1314-2.

[168] Rathod MJ, Kutsuna M. Joining of Aluminum Alloy 5052 and Low-Carbon Steel by Laser Roll Welding. Welding Journal 2004:16–26.

[169] Guo Y, Liu G, Jin H, Shi Z, Qiao G. Intermetallic phase formation in diffusion-bonded Cu/Al laminates. J Mater Sci 2011;46:2467–73. https://doi.org/10.1007/s10853-010-5093-0.

[170] Long L, Peng Y, Sun B, Liu W. Study on the interfacial bonding mechanism of Al/Mg gradient material. Mater Res Express 2020;7:016542. https://doi.org/10.1088/2053-1591/ab6536.

[171] Balluffi RW, Allen SM, Carter WC. Kinetics of materials. John Wiley & Sons; 2005.

[172] Baghdadi AH, Sajuri Z, Selamat NFM, Omar MZ, Miyashita Y, Kokabi AH. Effect of intermetallic compounds on the fracture behavior of dissimilar friction stir welding joints of Mg and Al alloys. INTERNATIONAL JOURNAL OF MINERALS METALLURGY AND MATERIALS 2019;26:1285–98. https://doi.org/10.1007/s12613-019-1834-5.

[173] Chen Y, Zhang R, He C, Liu F, Yang K, Wang C, et al. Effect of texture and banded structure on the crack initiation mechanism of a friction stir welded magnesium alloy joint in very high cycle fatigue regime. International Journal of Fatigue 2020;136:105617. https://doi.org/10.1016/j.ijfatigue.2020.105617.

[174] Kumar S, Wu C. Strengthening Effects of Tool-Mounted Ultrasonic Vibrations during Friction Stir Lap Welding of Al and Mg Alloys. METALLURGICAL AND MATERIALS TRANSACTIONS A-PHYSICAL METALLURGY AND MATERIALS SCIENCE 2021;52:2909–25. https://doi.org/10.1007/s11661-021-06282-w.

[175] Wang T, Wu C. Effect of ultrasonic on friction stir welding formation of aluminum/ magnesium dissimilar alloys. Journal of Materials Engineering 2022;50:20–34. https://doi.org/10.11868/j.issn.1001-4381.2021.000597.

[176] Ji S, Meng X, Liu Z, Huang R, Li Z. Dissimilar friction stir welding of 6061 aluminum alloy and AZ31 magnesium alloy assisted with ultrasonic. Mater Lett 2017;201:173–6. https://doi.org/10.1016/j.matlet.2017.05.011.

[177] Liu Z, Ji S, Meng X. Improving Joint Formation and Tensile Properties of Dissimilar Friction Stir Welding of Aluminum and Magnesium Alloys by Solving the Pin Adhesion Problem. JOURNAL OF MATERIALS ENGINEERING AND PERFORMANCE 2018;27:1404–13. https://doi.org/10.1007/s11665-018-3216-y.

[178] Hou W, Ahmad Shah LH, Huang G, Shen Y, Gerlich A. The role of tool offset on the microstructure and mechanical properties of Al/Cu friction stir welded joints. Journal of Alloys and Compounds 2020;825:154045. https://doi.org/10.1016/j.jallcom.2020.154045.

[179] Chen Y, Cai Z, Ding H, Zhang F. The Evolution of the Nugget Zone for Dissimilar AA6061/AA7075 Joints Fabricated via Multiple-Pass Friction Stir Welding. Metals 2021;11:1506. https://doi.org/10.3390/met11101506.

[180] Dewangan SK, Tripathi MK, Manoj MK. Material Flow Behavior and Mechanical Properties of Dissimilar Friction Stir Welded Al 7075 and Mg AZ31 Alloys Using Cd Interlayer. METALS AND MATERIALS INTERNATIONAL 2022;28:1169–83. https://doi.org/10.1007/s12540-021-00980-1.

[181] Ji S, Li Z, Zhang L, Zhou Z, Chai P. Effect of lap configuration on magnesium to aluminum friction stir lap welding assisted by external stationary shoulder. Materials & Design 2016;103:160–70. https://doi.org/10.1016/j.matdes.2016.04.066.

[182] Yue Y, Li Z, Ji S, Huang Y, Zhou Z. Effect of Reverse-threaded Pin on Mechanical Properties of Friction Stir Lap Welded Alclad 2024 Aluminum Alloy. Journal of Materials Science & Technology 2016;32:671–5. https://doi.org/10.1016/j.jmst.2016.03.005.

[183] Niu S, Ji S, Yan D, Meng X, Xiong X. AZ31B/7075-T6 alloys friction stir lap welding with a zinc interlayer. Journal of Materials Processing Technology 2019;263:82–90. https://doi.org/10.1016/j.jmatprotec.2018.08.009.

[184] Ji S, Niu S, Liu J. Dissimilar Al/Mg alloys friction stir lap welding with Zn foil assisted by ultrasonic. Journal of Materials Science & Technology 2019;35:1712–8. https://doi.org/10.1016/j.jmst.2019.03.033.

[185] Zhong X, Zhao Y, Pu J, Yan K, Liang H, Song S. Microstructure Characterization and Mechanical Properties of Mg/Al Dissimilar Joints by Friction Stir Welding with Zn Interlayer. PHYSICS OF METALS AND METALLOGRAPHY 2020;121:1309–18. https://doi.org/10.1134/S0031918X20130190.

[186] Wu B, Liu J, Song Q, Lv Z, Bai W. Controllability of joint integrity and mechanical properties of friction stir welded 6061-T6 aluminum and AZ31B magnesium alloys based on stationary shoulder. HIGH TEMPERATURE MATERIALS AND PROCESSES 2019;38:557–66. https://doi.org/10.1515/htmp-2019-0001.

[187] Mehta KP, Carlone P, Astarita A, Scherillo F, Rubino F, Vora P. Conventional and cooling assisted friction stir welding of AA6061 and AZ31B alloys. MATERIALS SCIENCE AND ENGINEERING A-STRUCTURAL MATERIALS PROPERTIES MICROSTRUCTURE AND PROCESSING 2019;759:252–61. https://doi.org/10.1016/j.msea.2019.04.120.

[188] Shi L, Wu CS, Liu XC. Modeling the effects of ultrasonic vibration on friction stir welding. Journal of Materials Processing Technology 2015;222:91–102. https://doi.org/10.1016/j.jmatprotec.2015.03.002.

[189] He C, Wang T, Zhang Z, Qiu C. Coupling effect of axial ultrasonic vibration and tool thread on the microstructure and properties of the friction stir lap welding joint of Al/Mg dissimilar alloys. JOURNAL OF MANUFACTURING PROCESSES 2022;80:95–107. https://doi.org/10.1016/j.jmapro.2022.05.008.

[190] Tan M, Wu C, Su H. Ultrasonic effects on microstructures and mechanical properties of friction stir weld joints of dissimilar AA2024/AZ31B alloys. WELDING IN THE WORLD 2023;67:373–84. https://doi.org/10.1007/s40194-022-01429-8.

[191] Hu Y, Liu H, Fujii H, Ushioda K. Effect of ultrasound on microstructure evolution of friction stir welded aluminum alloys. Journal of Manufacturing Processes 2020;56:362–71. https://doi.org/10.1016/j.jmapro.2020.05.005.

[192] Bai Y, Su H, Wu C. Enhancement of the Al/Mg Dissimilar Friction Stir Welding Joint Strength with the Assistance of Ultrasonic Vibration. METALS 2021;11. https://doi.org/10.3390/met11071113.

[193] Zhao J, Su H, Shi L, Wu C. Effect of Exterted Ultrasonic Power on Microstructure and Properties of Dissimilar Al/Mg Alloys UVeFSW Joints. Journal of Mechanical Engineering 2020;56:24–32. https://doi.org/10.3901/JME.2020.06.024.

[194] Sajed M, Guerrero JWG, Derazkola HA. A Literature Survey on Electrical-Current-Assisted Friction Stir Welding. Applied Sciences 2023;13:1563. https://doi.org/10.3390/app13031563.

[195] Stolyarov V, Calliari I, Gennari C. Features of the interaction of plastic deformation and pulse current in various materials. Materials Letters 2021;299:130049. https://doi.org/10.1016/j.matlet.2021.130049.

[196] Chen S, Wang L, Jiang X, Yuan T, Jiang W, Liu Y. Microstructure and mechanical properties of AZ31B Mg alloy fabricated by friction stir welding with pulse current. JOURNAL OF MANUFACTURING PROCESSES 2021;71:317–28. https://doi.org/10.1016/j.jmapro.2021.09.031.

[197] Paidar M, Kazemi A, Mehrez S, Oladimeji Ojo O, Matyuso Nasution MK, Mironov SN. Investigation of modified friction stir clinching-brazing process of AA2024 Al/AZ31 Mg: metallurgical and mechanical properties. Arch Civ Mech Eng 2021;21. https://doi.org/10.1007/s43452-021-00267-7.

[198] Wang Y, Al-Zubaidy B, Prangnell PB. The Effectiveness of Al-Si Coatings for Preventing Interfacial Reaction in Al-Mg Dissimilar Metal Welding. Metall Mat Trans A Phys Metall Mat Sci 2018;49:162–76. https://doi.org/10.1007/s11661-017-4341-1.

[199] Zheng B, Zhao L, Lv Q, Wan G, Cai D, Dong S, et al. Effect of Sn interlayer on mechanical properties and microstructure in Al/Mg friction stir lap welding with different rotational speeds. MATERIALS RESEARCH EXPRESS 2020;7. https://doi.org/10.1088/2053-1591/ab9fbb.

[200] Dong S, Lin S, Zhu H, Wang C, Cao Z. Effect of Ni interlayer on microstructure and mechanical properties of Al/Mg dissimilar friction stir welding joints.

SCIENCE AND TECHNOLOGY OF WELDING AND JOINING 2022;27:103–13. https://doi.org/10.1080/13621718.2021.2014742.

[201] Shah LH, Gerlich A, Zhou Y. Design guideline for intermetallic compound mitigation in Al-Mg dissimilar welding through addition of interlayer. Int J Adv Manuf Technol 2018;94:2667–78. https://doi.org/10.1007/s00170-017-1038-y.

Mr. Usman Abdul Khaliq is a research scholar in the Department of Mechanical Engineering, Faculty of Engineering, University of Malaya, Kuala Lumpur, Malaysia. He has completed his B.Sc. (2007) and M.Sc. in Metallurgical and Materials Engineering (2009) from the University of Engineering and Technology (UET), Lahore, Pakistan. At present, he is pursuing a Ph.D. from the University of Malaya. His research areas are high energy density welding process, laser-arc hybrid welding, friction stir welding, and additive manufacturing.

Dr Mohd Ridha Muhamad is a Senior Lecturer in the Department of Mechanical Engineering and is jointly a member of the Center of Advanced Manufacturing and Materials Processing at the University of Malaya. He obtained his Ph.D. degree from Utsunomiya University Japan in 2015, specializing in magnetic abrasive finishing for the finishing of the internal tube surface. Currently, he is working on a magnetic manufacturing method for various applications in heat exchangers and surface finishing. In a separate project, he collaborates with Japan Welding Research Institute to optimize the friction stir welding process in a sustainable way to be implemented in the manufacturing industry in Malaysia.

Dr. Farazila Binti Yusof is an Associate Professor in the Department of Mechanical Engineering and is jointly a Head of the Center of Advanced Manufacturing and Materials Processing at the University of Malaya. She received her PhD degree from the Nagaoka University of Technology, Japan. She is currently holding the position of Deputy Dean of Higher Degree in the Faculty of Engineering, University of Malaya. Her research interest is in advanced materials joining (laser welding, friction stir welding, soldering, brazing), powder metallurgy, and additive manufacturing. She has to her credit many research publications in international refereed journals and conferences.

Dr. Suriani Ibrahim is a Senior Lecturer in the Department of Mechanical Engineering and is jointly a member of the Center of Advanced Manufacturing and Materials Processing at the University of Malaya. She obtained her PhD degree from Chulalongkorn University, Thailand in 2016. Her research interests include biosensors, biocatalysts, polymer electrolytes, protein engineering, and nanomaterials. She has to her credit many research publications including book chapters.

Mr. Mohammad Syahid Mohd Isa is a research scholar in the Department of Mechanical engineering, University of Malaya. Previously he completed his MSc in Material Science from Eötvös Loránd University, Hungary and a B.Eng in Mechanical Engineering from Auckland University of Technology, New Zealand. His interests include welding, joining, and nanomaterials. He is currently working on the optimization of friction stir welding for battery application manufacturing.

Professor Dr. Zhan Chen received his BE (materials engineering) degree from Central South University in China in 1982 and completed his ME in 1985 and Ph.D. research in 1989 at the University of Auckland. In 2000 he joined the Department of Mechanical Engineering at AUT and is associated with teaching activities in engineering materials, manufacturing technologies, and failure analysis. His area of expertise includes biomaterials, manufacturing engineering, machine tools, manufacturing processes and technologies, materials engineering, metals and alloy materials, and tribology. His contributions include more than 100 highly cited publications. His publications have been cited more than 2850 times (Google Scholar (2023), h-index = 30). His book, Friction Stir Welding: From Basics to Applications, is a well-known contribution to researchers working in the field of friction stir welding.

Professor Dr. Gürel Çam is currently a full professor at the Department of Mechanical Engineering of Iskenderun Technical University, İskenderun-Hatay, Turkey. He earned his PhD degree in Materials Science from the Imperial College of Science, Technology, and Medicine, University of London, U.K., in 1990. He has contributed to 143 research publications (ResearchGate-2023) and his publications have been cited more than 6550 times (Google Scholar (2023), h-index = 43). His research interests include welding technologies including friction stir welding, diffusion bonding, electron beam welding, laser beam welding, characterization of welded joints, and low transformation temperature (LTT) filler materials. He is a member of AWS (American Welding Society), USA, and DVS (Deutsche Verband für Schweisstechnik), Germany. He is also a member of the General Board, Institute of Turkish Welding Technologies, İstanbul, Turkey.

Declaration of interests

☒ The authors declare that they have no known competing financial interests or personal relationships that could have appeared to influence the work reported in this paper.

☐ The authors declare the following financial interests/personal relationships which may be considered as potential competing interests: